

1. Report No. FHWA-RD-75-18		2. Government Accession No.		3. Recipient's Catalog No. PB 244 134	
4. Title and Subtitle VEHICLE DETECTION - Phase I: SPVD Development				5. Report Date January 1975	
				6. Performing Organization Code	
7. Author(s) D. O. Wick and R. A. Lubke				8. Performing Organization Report No.	
9. Performing Organization Name and Address Honeywell Inc. 2600 Ridgway Parkway Minneapolis, Minnesota 55413				10. Work Unit No. (TRAI) FCP 82B5262	
				11. Contract or Grant No. DOT-FH-11-8149	
12. Sponsoring Agency Name and Address Federal Highway Administration Offices of Research and Development Washington, D.C. 20590				13. Type of Report and Period Covered Final Report	
				14. Sponsoring Agency Code T-0115	
15. Supplementary Notes Contract Manager: Frank J. Mammano					
16. Abstract <p>Vehicle detectors are key components of all street and freeway traffic control and surveillance systems. Detector requirements for these applications include: low cost, accurate detection, minimum installation time and cost, reliable under all environmental conditions, low maintenance and calibration requirements, and ability to detect all vehicles on any standard roadway surface.</p> <p>An advanced vehicle detector concept called the Self-Powered Vehicle Detector (SPVD) was examined by this project. The SPVD is a new traffic detector consisting of a magnetometer sensor, RF communication link, and self-contained battery source. It is packaged into a small cylinder designed to be placed in roadway bore holes, completely under the roadway surface. Vehicles are detected and this information is transmitted by RF communication to a receiver in a traffic control enclosure up to 500 feet distant. SPVD operational life-time is at least one year. The SPVD is an advanced new approach to reducing installation cost. Its feasibility was proven using three SPVD Engineering models in this project.</p>					
17. Key Words Low cost, advanced vehicle detection concept, self powered, accurate vehicle counter.			18. Distribution Statement No restrictions. This document is available to the public through the National Technical Information Service, Springfield, Virginia 22161. PRICES SUBJECT TO CHANGE		
19. Security Classif. (of this report) Unclassified		20. Security Classif. (of this page) Unclassified		21. No. of Pages	22. Price

i-b

TABLE OF CONTENTS

<u>Section</u>	<u>Page</u>
I INTRODUCTION	1
II SUMMARY	2
III PROJECT OBJECTIVE	5
IV TECHNICAL DISCUSSION	6
System Technical Objectives	6
Power Source	7
RF Link	7
Sensor	7
System Technical Approach	7
Power Source	8
RF Link	8
Sensor	8
Progress and Results	8
Power Source	8
Communication Link Overview	11
Communication Link	12
Communication Link Performance	17
Communication Link Roadside Unit	18
Multi-detector Installations	21
Tone Decoder	21
Tone Decoder Performance	24
Sensor	25
Sensor Technical Requirements	25
Signature Collection and Analysis	25
Magnetometer Design Approach	31
Magnetometer Operation	31
Sensor Performance	43
Other System Parameters	46
SPVD Temperature Extremes	46
Physical Dimensions	46
Reliability Estimate	47
SPVD Selling Price Estimate	49
Conclusions	50
Recommendations	51

Preceding page blank

TABLE OF CONTENTS (continued)

<u>Section</u>		<u>Page</u>
Appendix A	DETAILED POWER SOURCE ANALYSIS, SPVD	53
Appendix B	SPVD TRANSMITTER FREQUENCY TRADEOFF ANALYSIS	71
Appendix C	PASSIVE VEHICLE DETECTOR ANALYSIS	87
Appendix D	SPVD Production Drawings	92

LIST OF FIGURES

<u>Figure</u>		<u>Page</u>
1	SPVD vehicle signatures	2
2	SPVD engineering model components	3
3	SPVD transmitter block diagram	13
4	Typical tone generator	13
5	Modulator, crystal oscillator, and doubler	14
6	Class C buffer	15
7	Typical power amplifier stage	15
8	Typical one-shot timer	16
9	Antenna matching network	17
10	Tone decoder	21
11	Buffer/highpass filter	22
12	Typical tone decoder	22
13	Vehicle presence flip flop	23
14	Threshold detector	23
15	Typical 3-axis magnetic signature	26
16	Volkswagen signature (W-E), 4 ft off centerline	27
17	Full size car signature (E-W), 4 ft off centerline	29
18	Volkswagen signature (E-W), 4 ft off centerline	30
19	SPVD sensor block diagram	31
20	Magnetometer operation	32
21	Toroidal core coil assembly	33
22	Unicoil magnetometer operation	34
23	Block diagram of SPVD sensor	35
24	Voltage controlled oscillator and transducer driver	36
25	Demodulator/amplifier	36
26	Feedback and hold circuits	37
27	Full wave rectifier	38
28	Threshold detector with hysteresis	38
29	Anti-chatter circuit	39
30	Leading edge detector	39
31	Trailing edge detector	40
32	Stopped vehicle rejection logic	41
33	Sample control logic	41
34	Low voltage detector	42
35	+4 volt regulator	42
36	Static detection zone, VW Beetle, 10 mph	44
37	Static detection zone, VW Beetle, 10 mph	44
38	Static detection zone, Ford Torino, 10 mph	45
39	Static detection zone, Ford Torino, 10 mph	45
40	Temperature extremes extrapolated from test data	47

LIST OF FIGURES (continued)

<u>Figure</u>		<u>Page</u>
41	SPVD prototype development plan	51
42	Battery test circuit for self powered vehicle detector	55
43	Groundwave propagation losses	76
44	Field strength versus distance 26.6 MHz, 4"x4" loop in asphalt, 5 db/div.	81
45	Near-field vehicle nulls, range = 200 ft, orthogonal 26.6 MHz loops, asphalt roadway, Ford station wagon, 10 db/div.	83
46	Near-field vehicle nulls, range = 500 ft, asphalt roadway, 10 db/div.	84
47	Near-field vehicle nulls, range = 495 ft, reinforced concrete, 10 db/div.	85
48	Experimental layout	86
49	Harmonic resonator sensing concept	87
50	Passive roadway unit - sensor circuit (simplified schematic)	87
51	Second harmonic conversion efficiency	90

LIST OF TABLES

<u>Table</u>		<u>Page</u>
1	Battery types tested	9
2	SPVD received field strength	17
3	Comparative field strengths	18
4	Receiver specifications	19
5	Vehicle minimum signals (excluding nulls) during detection as defined by requirements	28
6	SPVD reliability prediction	48
7	Battery capacity	53
8	Results of battery tests	57
9	Battery identification	64
10	First data: no battery capacity removed	65
11	Data taken after 0.8 ampere hour discharging at 0.400 A/Hr. rate	67
12	Data taken after 1.5 ampere hours removed at 0.4 A/Hr. rate	67
13	Data taken after = 8.0 ampere hours removed	68
14	Data taken during battery capacity removal	68
15	Test data at -20°F	70
16	Summary of frequency tradeoffs	80

SECTION I
INTRODUCTION

This final report covers Phase I of the vehicle detection project. The vehicle detection project, contract number DOT-FH-11-8149, is a contract between Honeywell Inc. and the Federal Highway Administration. The Phase I portion of this contract is entitled "Self-Powered Vehicle Detection (SPVD)" and was conducted from 1 July 1973 through 31 December 1974. E. H. Schmidt was project manager.

Other key personnel assigned to the Phase I portion of this project were:

D. C. Wick	-	Principal Investigator
R. A. Lubke	-	Senior Development Engineer
J. C. Ravis	-	Principal Development Engineer
L. E. Koehler	-	Principal Research Engineer
D. Wertman	-	Senior Staff Engineer

The following section contains a summary of project activities. Details on the project objectives and scope, technical approach and results, and conclusions and recommendations then follow.

SECTION II
SUMMARY

This report presents the results of a technology development project for the development and feasibility demonstrations of an advanced concept called a self-powered vehicle detector (SPVD).

The project began 1 July 1973 and continued through 31 December 1974.

The long-range objective of the SPVD program is to supply a vehicle detector having lower procurement, installation, maintenance, and operating costs than currently operational vehicle detectors. The SPVD satisfies this objective. It reduces the cost of installing the vehicle detection transducer and eliminates the need for conduits and wiring between the transducer and roadside junction box. Because the SPVD is a self-contained unit, it can be installed in the roadway by a simple hole-boring procedure, dropping the SPVD in the resulting hole, and then covering the hole with an environmental seal. As shown in Figure 1 vehicles passing over the SPVD are detected by a two-axis magnetometer type vehicle sensor. The

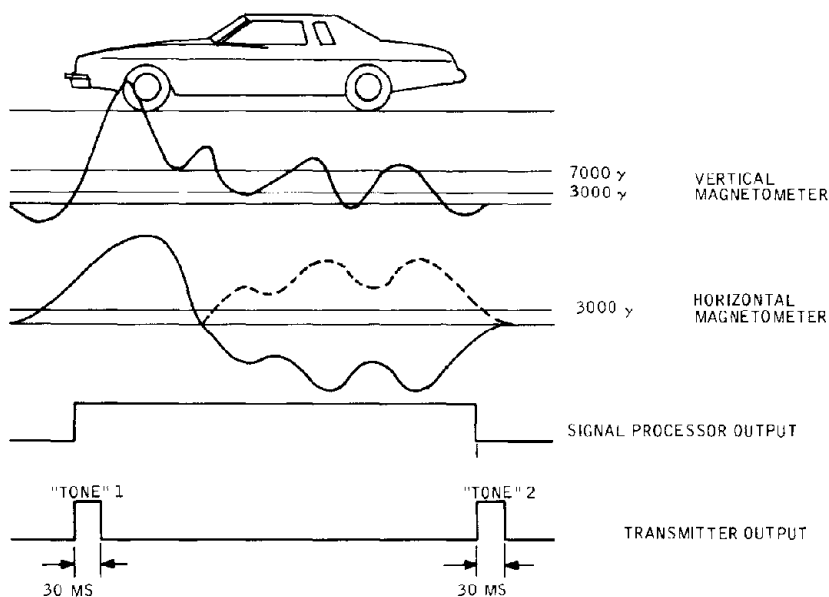


Figure 1. SPVD vehicle signatures

vehicle's leading edge is detected when a vertically oriented magnetometer detects a change of more than 7000γ . The vehicle trailing edge is detected when both the vertical and horizontal (N-S) oriented magnetometers fall below 3000γ . This detection information is transmitted to a roadside receiver by a pulsed RF communications link. Detection information transmitted by the communications link consists of the vehicle leading-edge tone pulse, the vehicle trailing-edge tone pulse, and a separate tone pulse representing low power supply voltage. The communication link tone pulses frequency modulate a 35 MHz carrier frequency. The roadside receiver, located up to 500 feet from the SPVD, decodes the three transmitted tone pulses and operates relays in a method similar to standard vehicle detection receiver electronics. Because of a one-year operational lifetime goal, the SPVD was developed using advanced low-power design techniques.

Three engineering models of the SPVD were designed, built, and tested during this project. Figure 2 is a photograph of one of the engineering model SPVD, receiver, and traffic control interface.

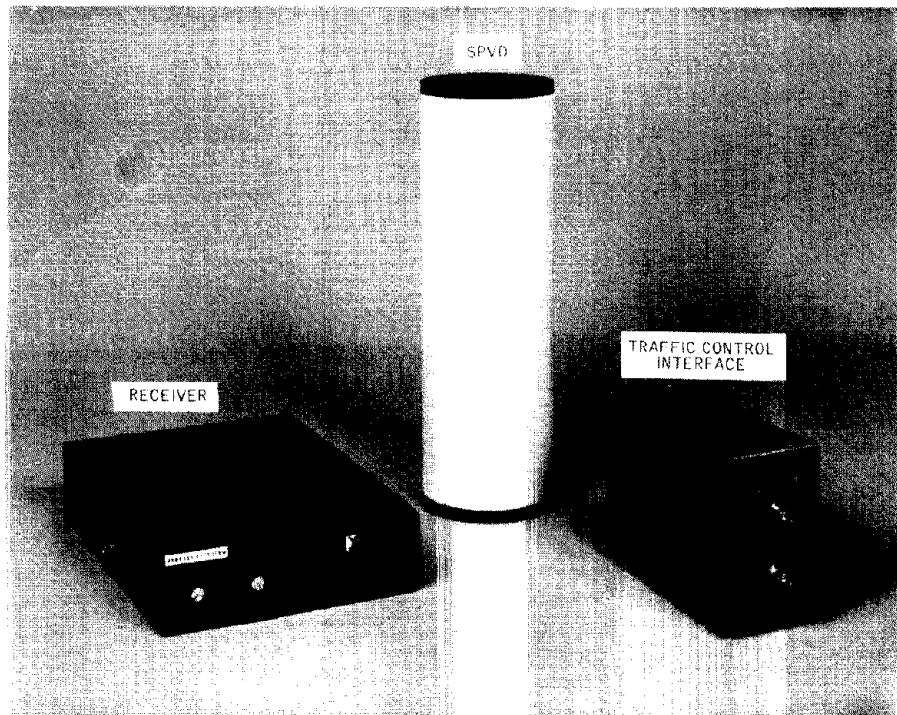


Figure 2. SPVD engineering model components

Testing in a typical roadway environment revealed satisfactory attainment of nearly all design goals set forth early in the project. The SPVD detected vehicles, from motorcycles to semi-trailer trucks, and from a momentary stop to legal highway speed. The SPVD magnetometer vehicle detection transducer was designed to operate with d-c response using low-power electronic circuitry.

The SPVD communication link operated successfully over the full design goal range of 500 feet under worst-case conditions of transmission from steel-reinforced paving material. The SPVD communication link was designed using a low-power 30-MHz to 35-MHz RF transmitter, time sequentially feeding orthogonal magnetic dipole antennas. The antennas were located at the bottom of the SPVD unit, surrounding the battery power source. The three tones modulating the RF carrier (a vehicle leading edge, a vehicle trailing edge, and a (power source) low-voltage warning tone) were received at the roadside receiver and input to tone decoders. The tone decoders, their respective logic, and relays at the roadway receiver permitted integration of the SPVD-generated tones into typical traffic control logic.

The SPVD design goals were that it must operate, unattended, for one year, with maximum vehicle counts of 20,000 per day, and at any location in the continental United States. The environmental temperature extremes at the 6-inch burial depth of the SPVD may vary between -20°F to $+140^{\circ}\text{F}$. As discussed in the technical portion of this report, it was experimentally proven that a standard LeClanche (carbon-zinc) lantern battery will provide the necessary power for the SPVD.

The SPVD package size design goal was three inches diameter by six inches long. Other package shapes could be considered if there was not an excessive effect on installation costs. SPVD models developed in this project were engineering models; consequently, they did not satisfy the package size design goal. They are approximately 4-1/2 inches diameter by 14 inches long because of the six-volt lantern battery and the need to maximize antenna size and efficiency. It is anticipated that a prototype SPVD could be reduced to four inches diameter by nine inches long. This size will not increase installation costs because current pavement core drills used with State Highway Departments are usually four to five inches diameter.

SECTION III

PROJECT OBJECTIVE

The objective of the Phase I portion of this project was to design, develop, and evaluate a self-powered vehicle detector for use with local intersection controllers and computer-controlled traffic systems.

This objective was satisfied by the development, test, and delivery to the Federal Highway Administration of three SPVD models. One of the SPVD models was an experimental breadboard model configuration and the other two were engineering model configurations.

SECTION IV
TECHNICAL DISCUSSION

The Self-Powered Vehicle Detector (SPVD) is a new concept of vehicle detection. This concept comprises two major components: the roadway unit and the roadside unit.

The roadway unit contains a vehicle sensor, RF transmitter, and a self-contained power source. Vehicle presence is transmitted to the roadside unit via a RF communication link precluding external wires. Installation is accomplished by boring a circular hole in the roadway, inserting the unit, and then covering the hole.

The roadside unit consists of an RF receiver and a tone decoder. Vehicle presence information, transmitted by the roadway unit, is received and then processed by the tone decoder which provides a relay closure to indicate vehicle presence.

System Technical Objectives

The system objectives and design goals for the SPVD are:

- | | |
|-------------------------------|---|
| ● Physical Dimensions | 3 inches diameter x 6 inches long |
| ● Operating Temperature Range | -30°F to +170°F |
| ● Number of Vehicles/Day | 20, 000 |
| ● Vehicle Speed | 0-80 mph |
| ● Power Source Monitor | Transmission of low-battery indication to roadside unit |
| ● Operational Lifetime | One year |

An additional objective of the SPVD project was to determine the feasibility of a completely passive roadway unit. This concept described in Appendix C, was analyzed in parallel with development of the SPVD. The passive roadway concept was rapidly found to be impractical because of the high RF power levels required. Since the SPVD was found to be a practical concept, the passive roadway concept was not developed further in the project.

Power Source

Specific objectives for the power source were to:

- Provide a battery with physical dimensions consistent with the overall system package.
- Provide a power capacity sufficient to meet the system lifetime.
- Determine a cost versus size and lifetime tradeoff.

RF Link

The objectives for the RF link were:

- Transmission range of 500 feet.
- Transmitter radiated power of less than 100 mw.
- Receiver signal-to-noise ratio of 10 db, or greater.
- Encode vehicle presence information into the RF transmission.
- Operate with a buried transmitter antenna.
- FCC license not required.

Sensor

The primary objective was to design a vehicle sensor having a detection capability of ± 4 feet for cars and trucks and ± 2 feet for motorcycles. The sensor had to accomplish this objective while buried beneath the roadway. In addition, this objective had to be accomplished with low-power circuitry for long battery lifetime.

System Technical Approach

The technical approach to attain the system objectives was to:

- Assign maximum allowable physical dimensions to the power source and RF-link antenna.
- Assign temperature stability requirements to the roadway and road-side subsystem components.
- Determine the bandwidth needed of the sensor to meet the vehicle speed objective by analysis of vehicle signatures.
- Develop a power source monitor to signal the RF link of a low-power condition for transmission to the roadside unit.
- Meet lifetime and vehicles/day objective by estimating the number of ampere-hours available from the power source, by parceling available power between the RF transmitter and sensor, and by using pulsed RF transmissions.
- Keep production cost low by using integrated circuits and by designing for production.

- Operating Temperature -20°F to +140°F
- Size Within SPVD package
- Availability Standard commercial
- Cost Low

Reviews of these SPVD requirements were discussed with representatives of Union Carbide, Mallory, and Ray-O-Vac. Both alkaline cells and lithium cells are considered by the battery manufacturers to be the most likely candidates for the SPVD application. (All companies considered the temperature extremes to be the major problem area. There was no test data, however, based upon the expected operating conditions for the SPVD.)

In this group, Mallory was the only manufacturer that made a lithium cell. Mallory's data, and that of other lithium cell manufacturers, indicated that this cell might also be appropriate for the SPVD.

Another possible power source was the six-volt lantern battery, which contains four LeClanche size "F" cells. Each "F" cell is the same diameter as a "D" cell and about 1-1/4 inches longer. Since this provides a larger cell area and cell capacity, it was thought that it may compensate, at the SPVD load, for the normal degradation in performance of the LeClanche cell at temperatures below 0°F. The advantage of this battery is that four cells are interconnected and potted in a container, thus providing a convenient and reliable package. This type of battery is a standard power source for barricade flasher units, and its price was likely to be lower than the other kinds of batteries being considered. The disadvantages of the lantern battery could be poorer performance at low temperature, and the need for increasing the length of the SPVD unit.

Samples of manufacturer-recommended battery types and performance tests (see Appendix A) were conducted, Table 1.

Table 1. Battery types tested

Manufacturer	Type	Quantity	Nominal Voltage (V)
Union Carbide	E95 Alkaline Energizer (D Size)	3	1.5
	No. 609 Super 99 Lantern Battery	3	6.0
Mallory	MN 1300 Alkaline Duracell (D Size)	3	1.5
	LO-26 Lithium Cell (D Size)	2	2.8
Ray-O-Vac	No. 813 Alkaline Energy Cell (D Size)	3	1.5

The batteries underwent a continuous load of 500 microamperes (simulating the maximum load excluding the transmitter) plus pulses of three magnitudes: 20, 30 or 35 milliamperes (simulating the estimated range of current required for transmitter operation). For each current level, pulse duration was 10 milliseconds. These pulses were applied in a sequence providing a delay of 250 msec. between the first and second pulse and of 1.0 second between the second and third pulse. The cycle repeated as long as desired. This sequence simulated a succession of cars traveling at about 60 miles per hour over the SPVD.

Each of the batteries, in the condition received from the manufacturers, was tested at the following temperatures: -30°F , -20°F , -10°F , 0°F , 70°F , $+120^{\circ}\text{F}$, and $+140^{\circ}\text{F}$. Shortly after the temperature chamber was raised to $+160^{\circ}\text{F}$ for the final-planned temperature level, one of the two lithium cells blew its safety vent plug and released its sulfur dioxide depolarizer and some of the electrolyte liquid into the environmental chamber. The 160°F test was abandoned. It should be noted that the lithium cell manufacturers claim the capability of operation at 160°F .

On the basis of a minimum acceptable voltage of 4.8 volts required for the transmitter, the performance of the fresh batteries in initial tests was as follows:

- Alkaline cell - Operation satisfactory at all test loads and temperatures. The minimum voltage (at -30°F) under the pulse load was the equivalent of 5.9 volts for a 4-cell battery. All cells were remarkably similar in performance.
- Lithium cell - Performance was unsatisfactory until the battery was at 0°F and the minimum current load of 20 ma. At higher test temperatures, performance was satisfactory under all three levels of current.
- Lantern battery - At -30°F , performance was satisfactory only under the 20 ma load. At all higher test temperatures, performance was satisfactory under all three loads.

After these initial tests, some of the alkaline and lantern batteries were discharged at high rates to determine their performance when their capacities were reduced (simulating several successive stages in the required operating life of one year). These results were as follows:

1. After the first capacity withdrawal from the lantern battery, it was able to operate satisfactorily at -30°F under all three current levels, and it continued to demonstrate this capability after further discharge of capacity.

2. The lithium cell continued to demonstrate unsatisfactory performance at -30°F . After 3.5 days under a continuous load of 500 micro-amperes, performance under the pulse load continued to remain unsatisfactory. Subsequently, the safety vent began to release sulfur dioxide gas, but the vent plug did not eject from the cell. This cell was therefore removed from the test program.
3. The alkaline cells continued to operate in a satisfactory manner. All operating tests were conducted at low temperature, either -30°F or -20°F .

In summary:

1. All alkaline cells met the full performance requirements at all temperature levels.
2. The lantern batteries were marginal at -30°F when fresh, but met the full requirements at all temperature levels after some capacity had been withdrawn from the batteries.
3. The lithium cells were unsatisfactory at temperatures below 0°F . The safety vents in both cells released sulfur dioxide from the electrolyte under conditions that should not have caused such venting. The batteries were inoperative after the venting. The sulfur dioxide gas, combining with water vapor, could harm SPVD components.

The excellent performance of the heavy-duty lantern batteries at low temperatures was unexpected by Union Carbide engineers. Two of the lantern batteries were sent to Union Carbide's laboratories for examination. Union Carbide engineers reported to Honeywell that these No. 609 Super 99 Lantern Batteries were made according to the basic 609 specification and were not of any special design. They did say, however, that their line of batteries is always subject to change and improvement. As a result of these tests, the Union Carbide No. 609 Super 99 Lantern Battery was selected as the SPVD power source.

Communication Link Overview

From the beginning of the program, it was obvious for a number of reasons that the greatest influence on the transmitter design would be the selected operating frequency. For instance, since the roadway unit had to be a "low power consumption" device to meet the one-year lifetime, the transmitter circuit efficiencies, which depend upon frequency, had to be maximized. Secondly, the chosen frequency had to minimize propagation losses through the Earth and thus reduce antenna power as the SPVD employs a buried antenna. Thirdly, the operating frequency affected the size of the transmitting antenna and its efficiency which, in turn, affected overall package size of the roadway unit. After a detailed frequency analysis tradeoff was conducted (see Appendix B), the 27 MHz-50 MHz range was selected.

The next tradeoff considered was what kind of modulation to use to place the vehicle presence information on the RF carrier. Noise measurements in the 2-200 MHz band revealed that impulse noise from vehicle ignition systems will be the greatest source of RF noise at frequencies of 25 MHz or greater.^{1, 2}

Frequency modulation was used rather than amplitude modulation because it offers better performance in the presence of impulse noise, requires almost no modulator power, and provides a constant-amplitude.³

To complete the building blocks of the RF link, the receiver section of a 30-MHz mobile FM transceiver was selected because of its commercial availability. In addition, these units are designed for the same operational environment as the SPVD receiver, and therefore, meet the necessary specifications on temperature, sensitivity and spurious response rejection.

Communication Link

Roadway Unit -- A block diagram of the transmitter is contained in Figure 3. (See also schematics.) Basically, the transmitter consists of a crystal oscillator which is frequency modulated by one of three tone generators, two RF power amplifier stages, two orthogonal loop antennas and timing and control circuits.

The tone generators (Figure 4) which receive an enable pulse from the magnetometer sensor are used to signify vehicle leading edge, vehicle trailing edge, or under-voltage (low-power source) condition. The crystal oscillator (Figure 5) which operates at $1/2 f_0$ is frequency modulated with a varicap diode. The collector tank circuit doubles the crystal frequency to the final operating frequency (f_0).

¹Skomal, E. N., "An Analysis of Metropolitan Incidental Radio Noise Data," IEEE Trans. Electromagnetic Compatibility, EMC-15, p. 45, May 1973.

²Dietz, et al., "Man-Made Noise," Report to FCC Technical Committee of the Advisory Committee for Land Mobile Radio Services, June 1966.

³Buesing, R. T., "Modulation Methods and Channel Separation in the Land Mobile Service", IEEE Trans. Vehicular Technology, VT-19, p. 187, May 1970.

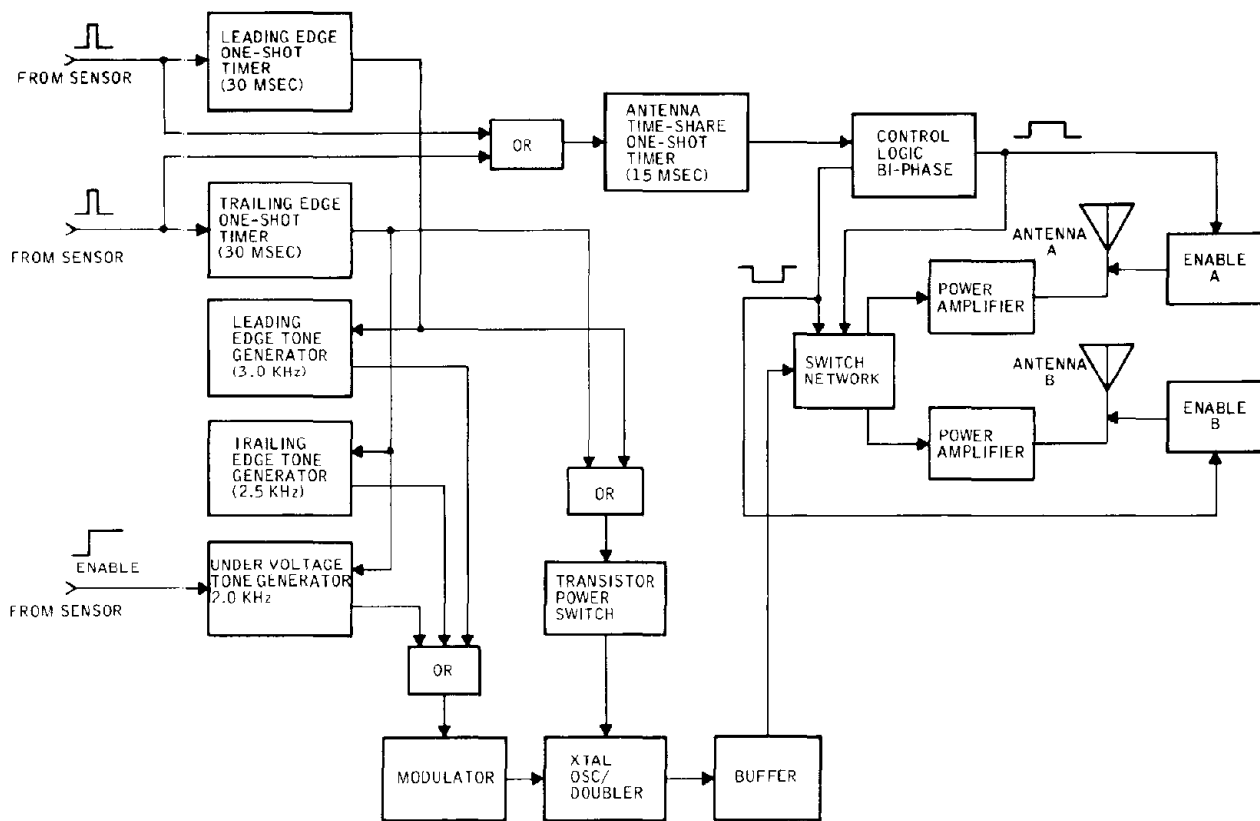


Figure 3. SPVD transmitter block diagram

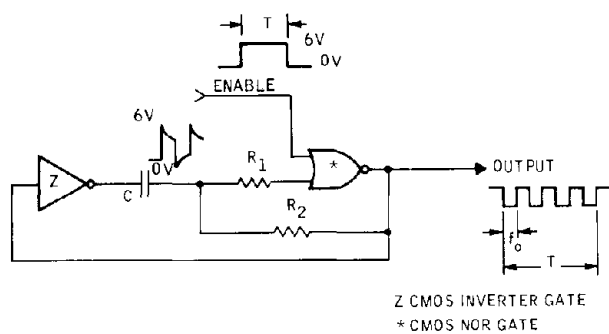


Figure 4. Typical tone generator

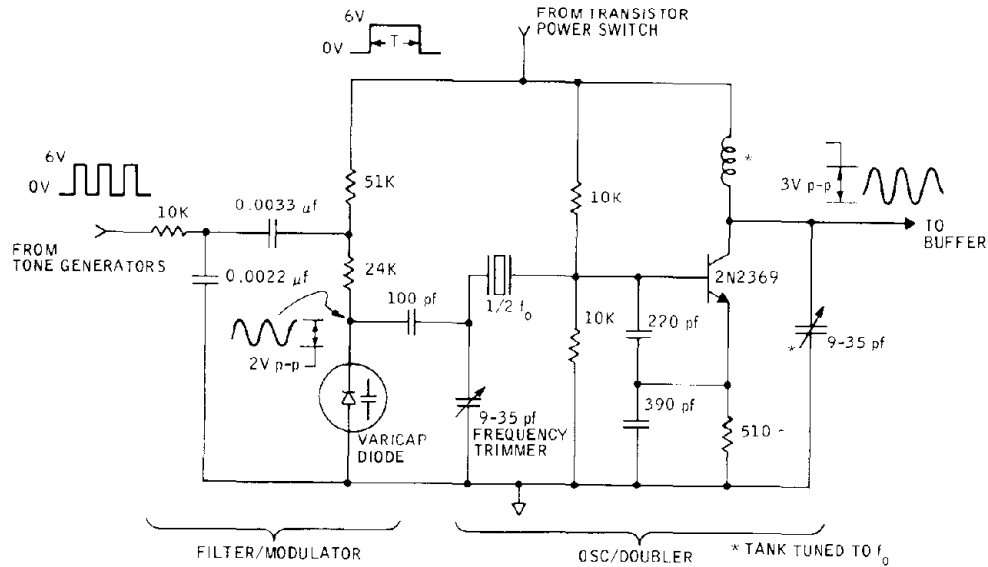


Figure 5. Modulator, crystal oscillator, and doubler

After the buffer stage, Figure 6, the signal goes through a diode switch network which steers the signal to each power amplifier on a time-shared basis (Figure 7).

Even though the antennas are positioned orthogonally, they interact with each other during transmission. The enable circuits on each antenna detune the inactive one to minimize interaction.

The control circuits perform two functions: First, they generate the 30-millisecond timing pulse (Figure 8) which enables the tone generators and applies power, via the power switch, to the oscillator. Secondly, they generate the 15-millisecond timing control for the time-sharing circuits in the power amplifier. When the transmitter oscillator is keyed on, the appropriate tone-generating multivibrator 2.0 kHz, 2.5 kHz, 3.0 kHz is enabled during the entire 30-millisecond transmission time. When the undervoltage sensor output indicates that the battery voltage has dropped below 4.8 volts, the normal trailing edge tone is replaced by another tone to signify undervoltage.

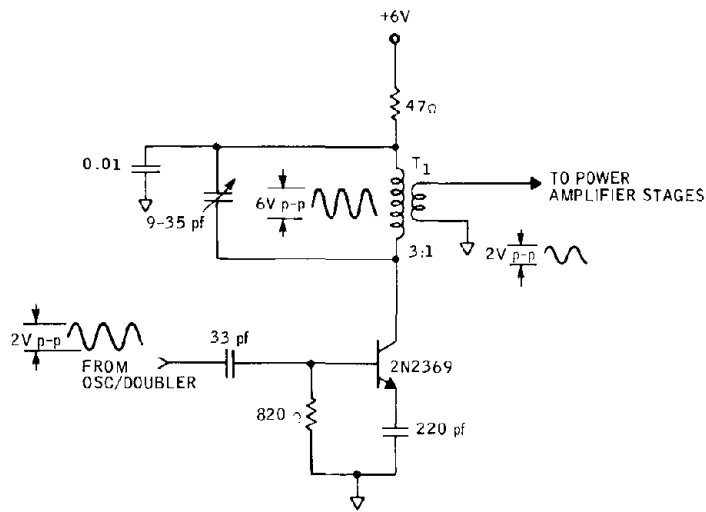


Figure 6. Class C buffer

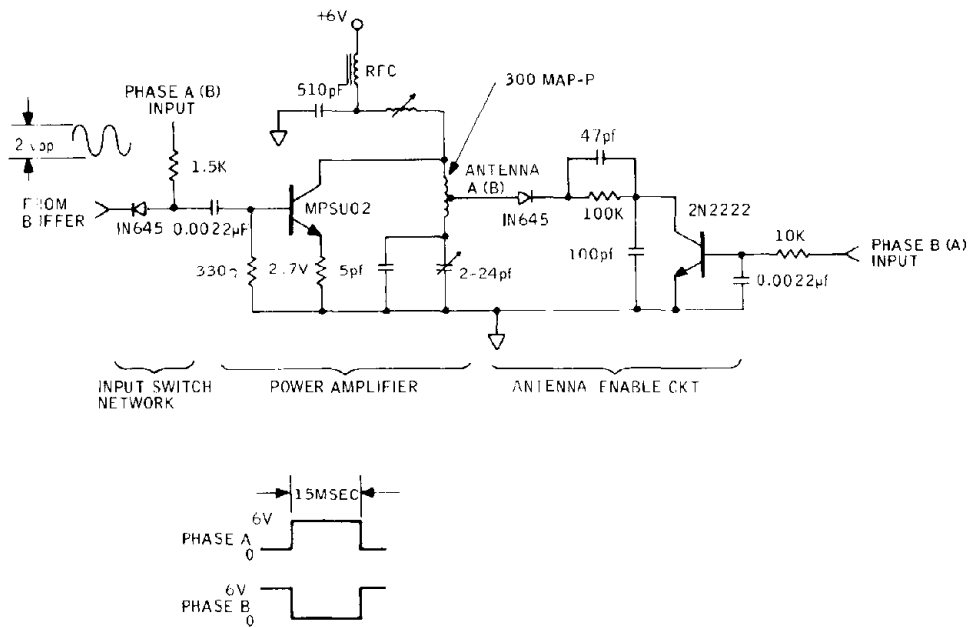


Figure 7. Typical power amplifier stage

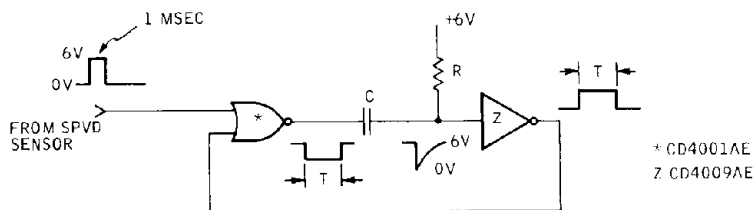


Figure 8. Typical one-shot timer

Each RF amplifier has a 4 x 6 inch, two-turn loop antenna in its collector circuit. The two antennas are mounted orthogonally and enclose the 6-volt lantern battery that powers the SPVD. The effect of conducting bodies within the enclosed area of a loop antenna was determined experimentally with a 26.6-MHz transmitter and a 4 x 6 inch loop on an open form. A 6-volt lantern battery was placed within the loop. Field-strength measurements were made at 200 and 500 feet with the transmitter installed in asphalt test holes. The radiation efficiency of the "loaded" loop decreased in direct proportion to the reduction in unobstructed area. A more serious degradation had been anticipated in efficiency because of increased circuit losses in addition to the reduction in area, but this is not the case. The radiation efficiency of a 4 x 6 inch loop with a lantern battery exposed is almost identical to that of a 4 x 4 inch "open" loop.

The antenna construction utilizes No. 14 solid, tinned copper wire attached to a fiberglass rectangular form. The antenna Q equals 160 with the battery inside the loop.

During the course of the final design of the antenna and its power amplifier, the discovery was made that to achieve a low power supply drain in this stage, and thus meet the SPVD lifetime goals while providing the RF power output needed to achieve the 500-foot transmission range, the antenna would have to be matched to the power amplifier. The network in Figure 9 was found to accomplish this essential task. Without this network the power amplifier consumed over twice the present current drain of 30 ma. Circuit values were empirically determined.

The entire transmitter electronics are mounted on one circular printed circuit board of approximately 3-3/4 inches in diameter.

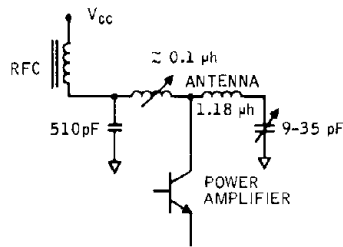


Figure 9. Antenna matching network

Communication Link Performance -- Transmitter power output decreases approximately 3.5 db when the battery voltage is lowered from 6 volts to 4.8 volts. Over the temperature range from -30°F to $+160^{\circ}\text{F}$, RF output is within 2 db of the room temperature value. Frequency stability over this temperature range is ± 0.002 percent.

Power input to the final amplifier stage of the transmitter is approximately 120 mw with a 6-volt supply. The entire transmitter circuit, including the control logic and switching, draws about 45 ma at 6 volts, decreasing to 35 ma at 4.8 volts.

Typical transmission performance is as listed in Tables 2 and 3.

Table 2. SPVD received field strength

Distance (feet)	Field Strength (db) (SPVD Battery Voltage 5.7V)
30	-32
100	-46
200	-54
300	-61
400	-66
500	-68

Table 3. Comparative field strengths

Field Strength (db)	Condition
-64	Transmitter sitting alongside the installation hole.
-68	Transmitter in asphalt at same distance as above.

Excellent receiver quieting was achieved at 500 feet. The transmitter was also tested in a reinforced concrete roadway. Since testing was done in a small, uncompleted area of I35W, it was most convenient to place the receiver antenna in a Honeywell parking lot. There was no power available in this location for the spectrum analyzer; consequently, receiver quieting was the only observation made. The receiver antenna height was approximately six feet above the transmitter. Typically, 10 dbm of field strength is lost in this medium. Here again, however, excellent receiver quieting was observed at distances estimated at over 500 feet.

Communication Link Roadside Unit

The design of the roadside unit encompassed two subsystem components – receiver and tone decoder. It was necessary to use a receiver with enough sensitivity to operate with the input signal strengths obtained from the roadway transmitter. The tone decoder is necessary to extract the vehicle presence information from the received audio signal.

Receiver -- The selected receiver is the receiver section of an E. F. Johnson Model 507 FM Mobile Communications Transceiver. Specifications for this device are contained in Table 4. Of particular interest is the quieting sensitivity (better than -90 dbm) and the audio frequency bandwidth (<3 kHz). This audio bandwidth produced an undesirable restriction on the performance of the communication link, as will be shown later. However, due to the schedule and cost constraints of the program, it was felt that buying a commercial receiver was preferable to designing one.

An inductively loaded mobile whip antenna was selected in an operational SPVD system, this antenna could be protected by a fiberglass housing. Although the antenna was intended for 27-MHz Citizens Band usage, it was felt that it would suffice for the SPVD operating at 30-35 MHz. This, in fact, proved to be the case in field tests.

Table 4. Receiver specifications

<u>General</u>	
FCC Type Acceptance Filing Number	Johnson 842-0507
Compliance	Type Accepted, FCC Rules Parts 21, 89, 91 and 93 Type Accepted, Canadian DOC Specification RSS-139
Frequency Ranges	VHF-FM, 30 to 50 MHz
Channels	1, 2 Pretuned, crystal- controlled
Input Power	12 VDC nominal, negative ground
Dimensions	6.4 cm high x 20.3 cm wide x 29.2 cm deep (2-1/2" high x 8" wide x 11-1/2" deep)
Transceiver Weight	3.2 Kg (7.0 pounds)
Microphone	Hand-held ceramic with coil cord
Circuitry	All solid-state
<u>Receiver</u>	
Antenna Impedance	50 ohms, nominal
Frequency Range	30.0 to 50.0 MHz
Intermediate Frequencies	10.7 MHz and 455 KHz
Frequency Stability	±0.0020% or better, -30° to +60°C
Usable Sensitivity (for 12 db SINAD)	0.4 microvolt, or better
Quieting Sensitivity (for 20 db Quieting)	0.4 microvolt, or better
Squelch Sensitivity	0.30 microvolt, maximum squelch range 8 db ±2 db
Modulation Acceptance Bandwidth	± 6.5 kHz
Selectivity Adjacent Channel Rejection	65 db (20 kHz spacing)
Intermodulation Rejection	60 db (50 db w/noise blanker)

All specifications subject to change without notice.

Table 4. Receiver specifications (continued)

<u>Receiver (continued)</u>	
Spurious and Image Rejection	85 db
Audio Output Power	3 W with less than 5% distortion
Audio Frequency Response	+2, -8 db of a 6 db per octave de-emphasis characteristic; 300 - 3000 Hz
Hum and Noise Ratio	60 db, or better
Speaker Impedance	3.2 ohms
<u>Transmitter</u>	
Antenna Impedance	50 ohms, nominal
Power Output	25 watts, minimum
Frequency Range	30.0 to 50.0 MHz
Frequency Stability	$\pm 0.0020\%$ or better, -30° to +60°C
Emission	16F3 (phase modulation, ± 5 kHz)
Modulation Limiting	± 5 kHz
Spurious and Harmonic Attenuation	60 db, or better
Hum and Noise Ratio	60 db, or better
Audio Frequency Distortion	10% or better
Audio Frequency Response	+1, -3 db of a 6 db per octave pre-emphasis characteristics, 300 - 3000 Hz
<u>Power Requirements</u>	
Input Power Source	12 VDC nominal (13.8 VDC actual), negative ground, from a battery generator source

Table 4. Receiver specifications (continued)

<u>Power Requirements (continued)</u>	
Battery Drain -	
Standby:	Squelched 0.2 A
	Unsquelched, 3W Output 0.6 A
Transmit:	Maximum 6.0 A
Rated Duty Cycle	EIA Intermittent Duty
Circuit Protection	Fused input cable and reverse polarity protection circuit

All specifications subject to change without notice.

Multi-detector Installations -- During the course of this program, the conclusion was reached that each roadway unit within a 500-foot radius of the roadside unit would have to operate on a separate frequency. Otherwise, the roadside unit could not determine which roadway unit detected a vehicle. Due to program time and funding limitations, a separate receiver was purchased for each roadway unit rather than attempting to develop a single, multichannel receiver. At present, the separate receivers may share a single, common antenna.

Tone Decoder -- A block diagram of the tone decoder is shown in Figure 10. (See also schematic.) The decoder uses two signals from the receiver, audio and squelch level.

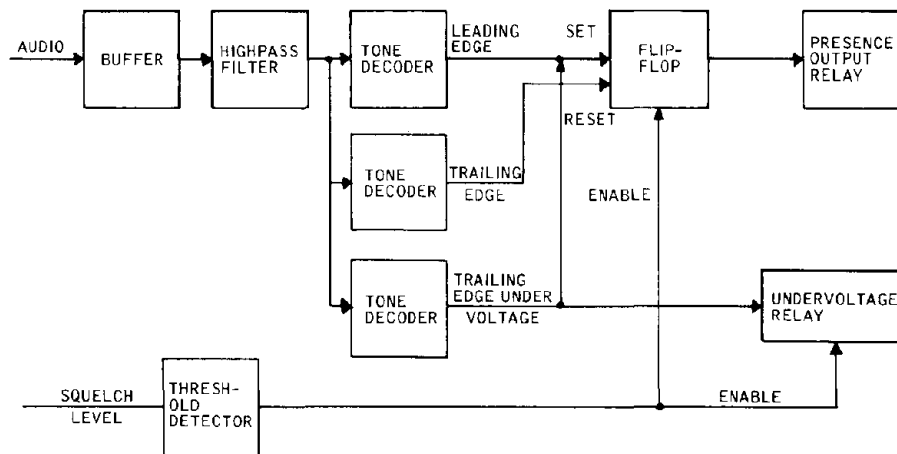


Figure 10. Tone decoder

The audio signal is first applied to a buffer stage (Figure 11) where the signal level can be adjusted, and from there it is applied to a two-pole, high-pass active filter. The signal then goes to three tone-decoder

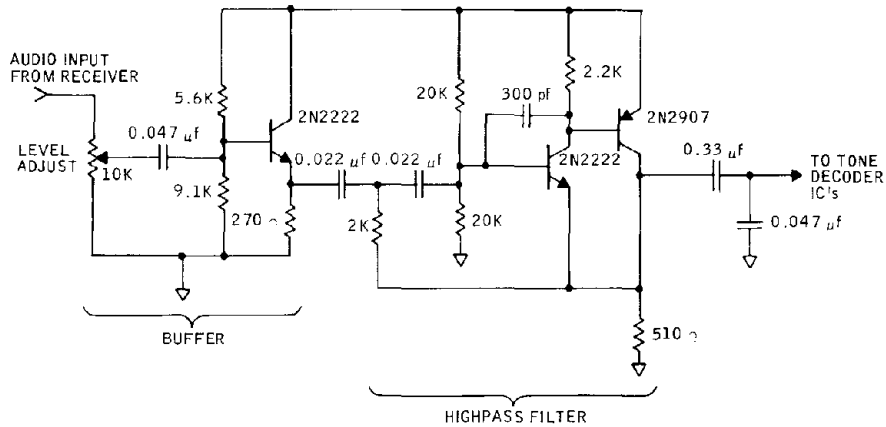


Figure 11. Buffer/highpass filter

integrated circuits (TDIC) (Figure 12) whose inputs are connected in parallel: one for vehicle leading edge, one for vehicle trailing edge, and one for power source undervoltage. The outputs of the decoders are used to set and reset flip-flops (Figure 13) and drive the appropriate relays.

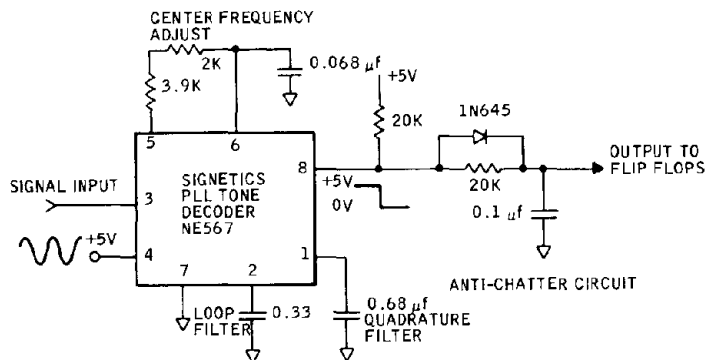


Figure 12. Typical tone decoder

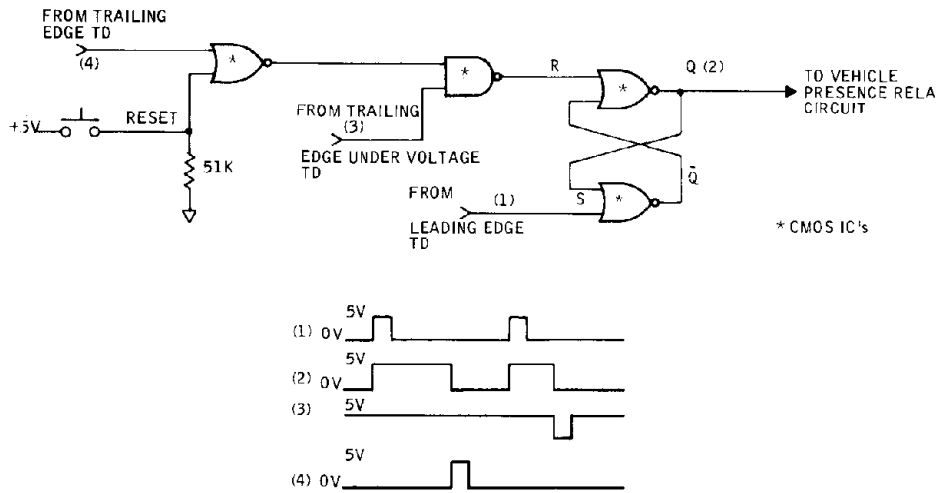


Figure 13. Vehicle presence flip flop

The squelch signal, which indicates the presence of an RF signal, from the receiver is threshold detected (Figure 14) and used to enable the flip-flops mentioned above to be set or reset during the 30-millisecond transmit period.

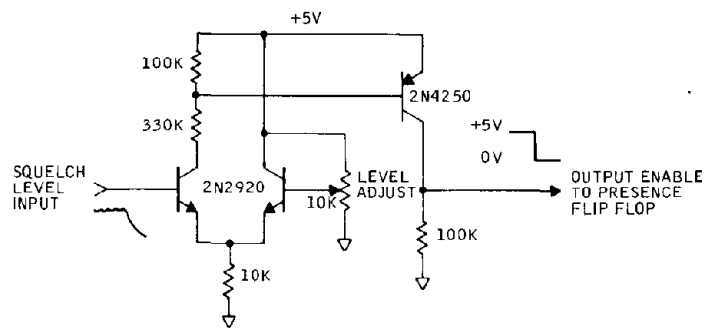


Figure 14. Threshold detector

Tone Decoder Performance -- Tone decoder performance was reasonable for a feasibility model. However, it did suffer from the upper audio bandpass limit of 3 kHz imposed by the receiver. The two areas of weak performance were:

- Limited rejection of random noise from the receiver's FM discriminator with no incoming RF signal.
- Limited rejection of voice transmissions on the same frequency as SPVD.

As is typical of FM receivers, the absence of an input RF signal causes the FM discriminator to produce random audio noise. This noise amplitude is sufficiently high to cause the audio amplifiers to swing their full limits. Often the noise will be clipped, increasing the harmonic frequency content of the signal. If precautionary measures are not taken, the TDIC's which are phase-locked loops, will respond to this noise, thus producing a false vehicle indication. Two steps were taken to overcome this problem. One was the highpass filter addition, described above; the other was the threshold detector which used the squelch level from the receiver. The filter reduced the amount of clipped (low frequency) audio reaching the TDIC's. The most effective step was the addition of the threshold detector on squelch level. These two steps were an effective, if not elegant, solution.

The limited rejection of voice frequency transmissions, and in some cases, music, on the same operating frequency as SPVD continue to plague SPVD. Of course, the most obvious solution is to obtain a "clear channel". Short of that, a more elegant solution of encoding vehicle presence information on the RF carrier must be found. The situation can be improved by reducing the response time of the TDIC's at the expense of increasing the transmit pulse duration from 30 milliseconds (15 milliseconds per antenna) to some greater value. But this increases power consumption and thereby decreases the lifetime of the roadway unit. Alternative solutions are to obtain a receiver with wider audio bandwidth. This approach would allow higher tone frequencies and narrower TDIC bandwidth to be used, thus allowing the response time to be decreased. A worst-case lockup time of about 15 or 10 cycles is typical of a phase-locked-loop tone decoder with 10 percent bandwidth. A tone frequency of 2 kHz or higher is necessary to achieve 10-millisecond response times. This is not a peculiar fault of phase-locked decoders; the same fundamental limitations on response time and bandwidth apply to any decoding technique. Or, one might be able to use a two-tone encoding scheme for vehicle presence information.

Sensor

Sensor Technical Requirements -- The following technical requirements were generated for the purposes of evaluating the sensor design.

- Detection Speed Range 0 mph to 80 mph
- Detection Type Pulse out at leading edge and trailing edge of vehicle
- Detection Range (Lateral) Cars: ±4 feet
 Trucks: ±4 feet
 Buses: ±4 feet
 Motorcycles: ±2 feet
- Power Drain Less than 300 μ amperes at 6.0 volts
- Temperature -20°F to +160°F

Signature Collection and Analysis -- The selected sensor concept was formulated from examination of three-axis magnetic signatures acquired from several vehicle types. The signature data was acquired under controlled conditions from a Ford four-door sedan, Vega station wagon, Volkswagen Beetle, 40-foot trans-type bus, semi-trailer truck, and a motorcycle. All data acquired in the signature acquisition effort are contained in report number FHWA-RD-7522.

These signatures were examined at length to develop a signal processing scheme compatible with the detection requirements. This signature examination lead to the conclusion that more than one axis of sensing was required to meet the detection specification. This conclusion was a result of signal nulls being present in the signal from any single axis. One such typical signature is shown in Figure 15.

To determine the levels which would give proper detection, the minimum signals from each axis for various vehicles were tabulated and are shown in Table 5. (The "along axis" is the axis in which the vehicle is traveling.)

During examination of the values generated in Table 5, it was found that in the across axis the signal was stronger at a 4-foot offset than at a 0-foot offset for a Volkswagen and a full-sized auto. (See Figure 16.)

Since it is desired to have a decreasing signal at four feet, it appeared that the across axis would be unsatisfactory. However, one more sensor requirement, which is implicit, is that the sensor should not produce double vehicle counts for a single vehicle. To achieve this, the signatures were observed for nulls. Figures 17 and 18 show that to avoid coincident nulls, the vertical and N-S axes should be used.

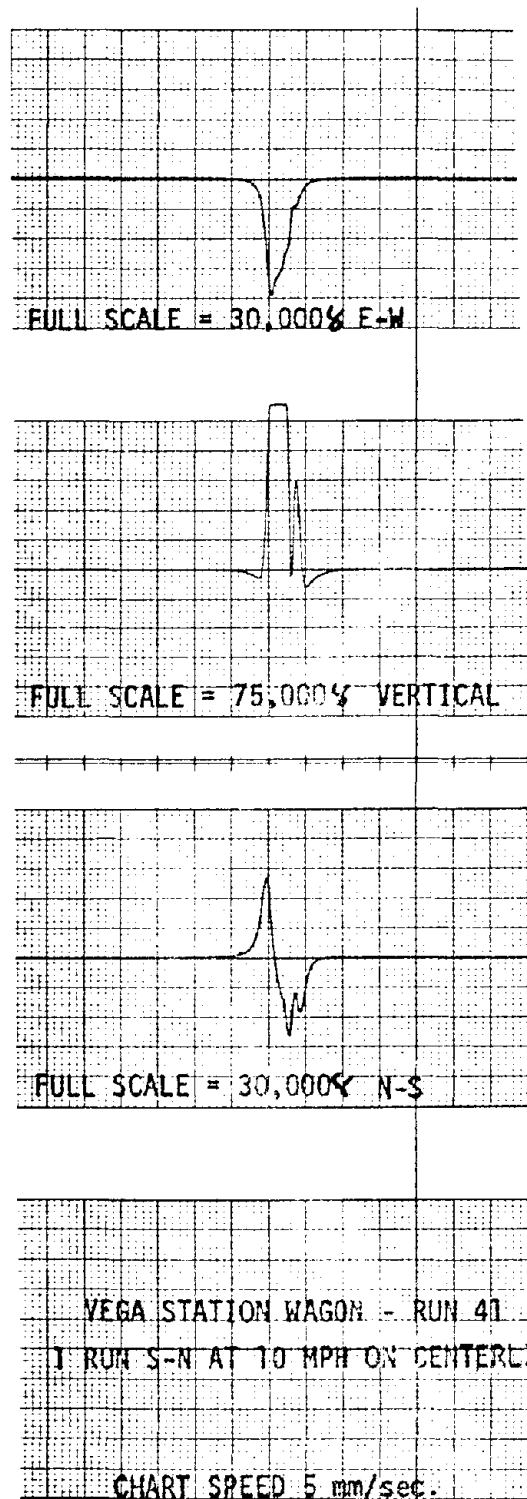


Figure 15. Typical 3-axis magnetic signature

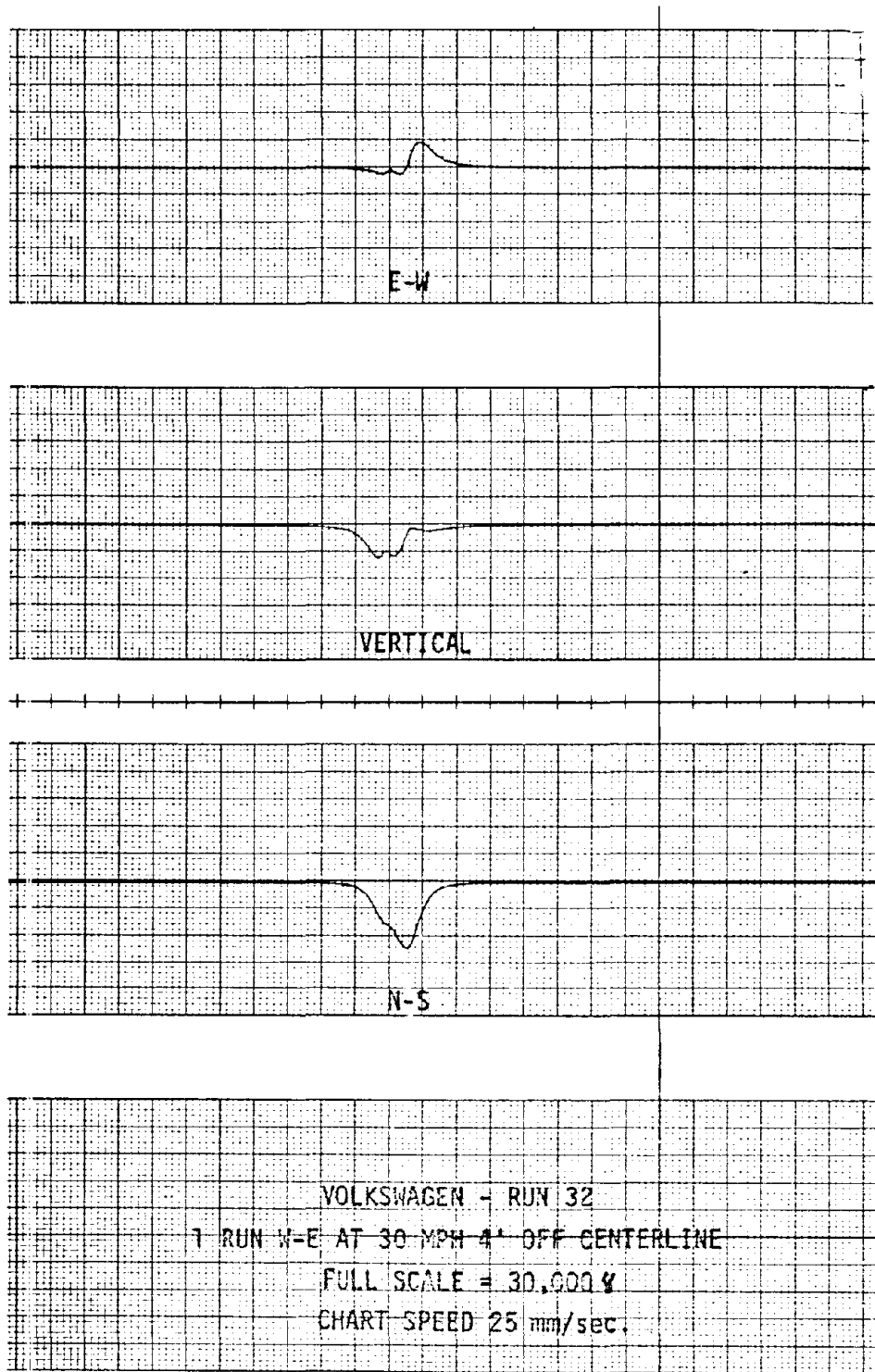


Figure 16. Volkswagen signature (W-E), 4 ft off centerline

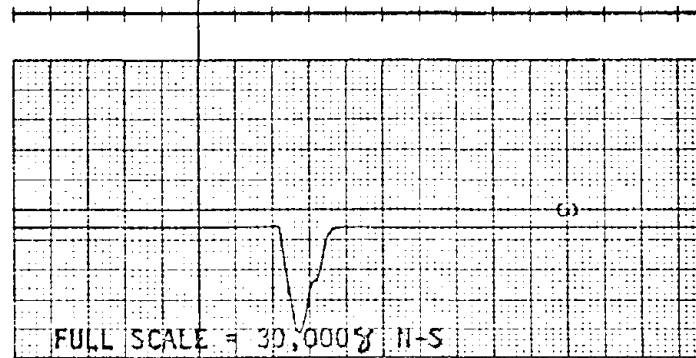
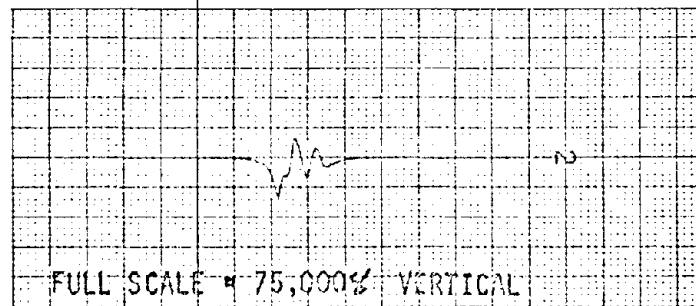
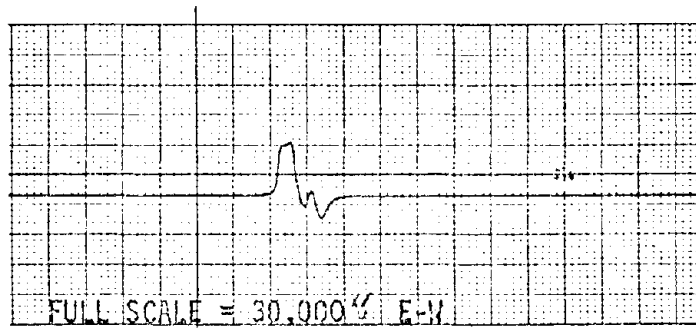
Table 5. Vehicle minimum signals
(excluding nulls) during detection
as defined by requirements

Vehicle	Offset Distance (feet)	Minimum Magnetic Signal (γ) With Respect To Vehicle Motion		
		Along Axis γ	Across Axis γ	Vertical γ
Motorcycle	0	2,000	2,000	7,500
Motorcycle	4	1,500	1,000	2,000
Truck	0	15,000	18,000	20,000
Truck	4	4,000	7,000	6,000
Bus	0	7,500	3,000	12,000
Bus	4	3,000	2,000	3,000
Volkswagen	0	7,000	3,000	7,000
Volkswagen	4	3,000	7,000	2,000
Sedan	0	9,000	4,000	15,000
Sedan	4	2,400	8,000	2,000

A further examination of the vertical signal indicates initial detection for all vehicles is more consistent in the vertical axis. It also indicates that an initial detection requirement of 7000 γ peak is sufficient for all vehicles considered. However, to maintain the detection during vehicle coincidence, the along-axis signal must be considered. This leads to a requirement of maintaining detection during vehicle coincidence which is achieved by holding the detection as long as either axis signal is greater than 3000 γ .

In summary, the detection requirement should be achievable by the following signal processing criteria.

- Initial detection is when a signal of greater than 7000 γ peak is present in the vertical axis.
- The detection is continued as long as the signal is greater than 3000 γ in either the N-S or vertical axis.



BRUSH ACCUCHART

FORD 4 DR SEDAN FULL SIZE CAR - RUN 47
 1-RUN E-W AT 10 MPH 4' OFF CENTERLINE
 CHART SPEED 5 mm/sec

Figure 17. Full size car signature (E-W), 4 ft off centerline

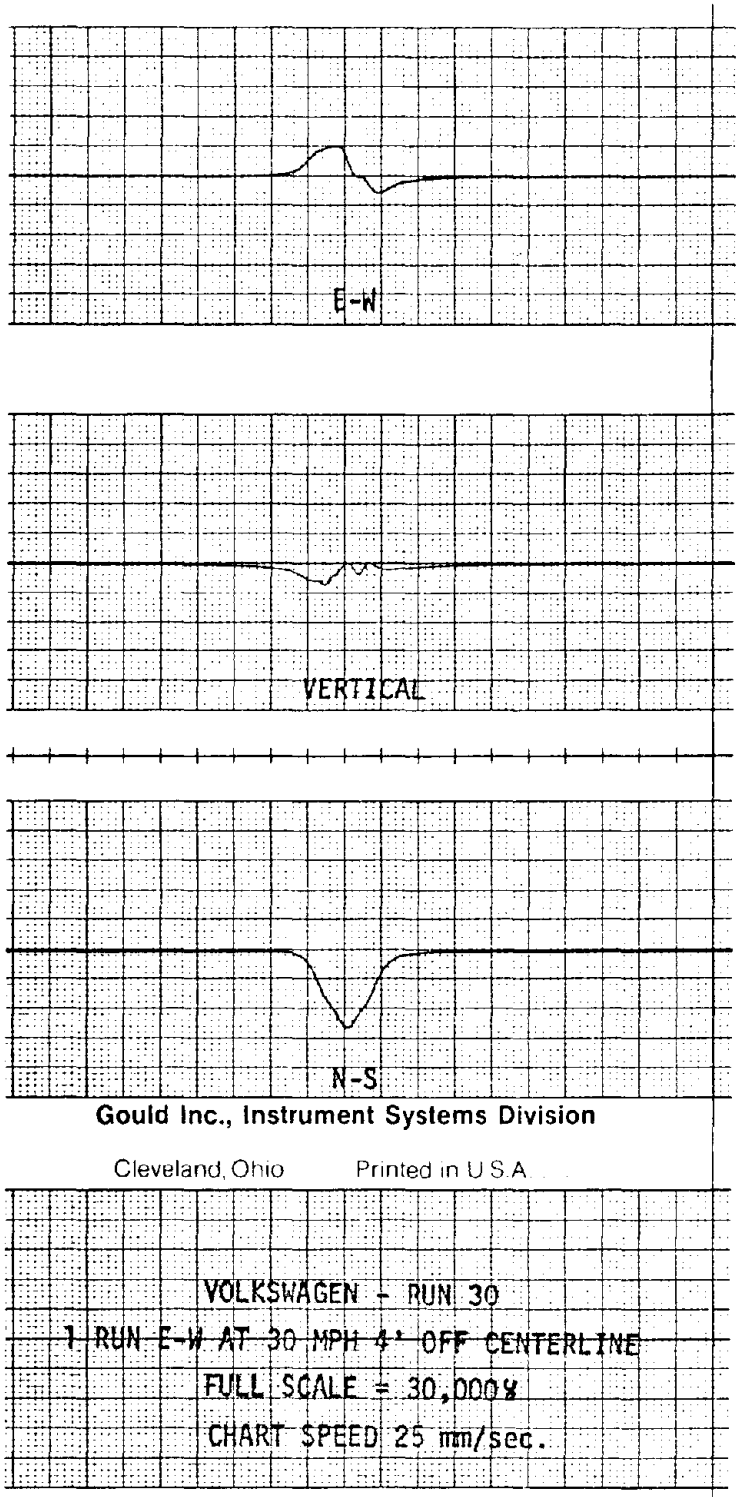


Figure 18. Volkswagen signature (E-W), 4 ft off centerline

The following magnetometer requirements are assumed in the development of the aforementioned signal processing concept:

- Frequency response (0 Hz to 20 Hz)
- D-C offset (less than ± 50 millivolts)
- Sensitivity (capable of 2 volt output for a 7000 γ peak signal while meeting the D-C offset requirement).
- Magnetic bias field (must be capable of meeting sensitivity and offset requirements in magnetic bias fields from +0.6 Oer. to -0.6 Oer.).

Magnetometer Design Approach -- The basic configuration of the magnetic sensor for the SPVD consists of a pulse-driven toroidal core transducer, demodulating circuit, signal processing circuit, and an autostabilization loop, as depicted in the block diagram of Figure 19. Honeywell has successfully developed a small, low-cost, self-powered magnetic sensor using this circuitry for both military and nonmilitary applications.

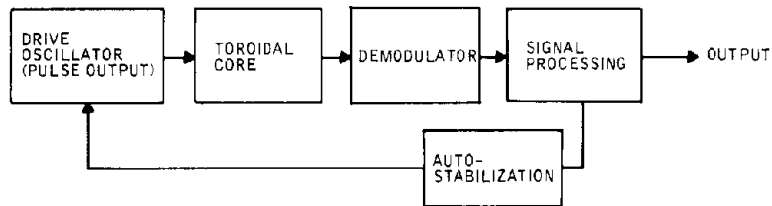


Figure 19. SPVD sensor block diagram

Magnetometer Operation -- Conceptually, the magnetic sensor functions as follows. A pulse oscillator applies drive pulses to the toroidal core at a fixed rate and amplitude (Figure 20). The output of the coil (that is, the voltage generated in a sensing winding) is a similar pulse train, amplitude modulated by the external magnetic field impressed upon the toroidal core. The demodulator circuit extracts this modulating signal, producing a voltage proportional to the imposed magnetic field. (Subsequent paragraphs will discuss the elimination of one core winding.)

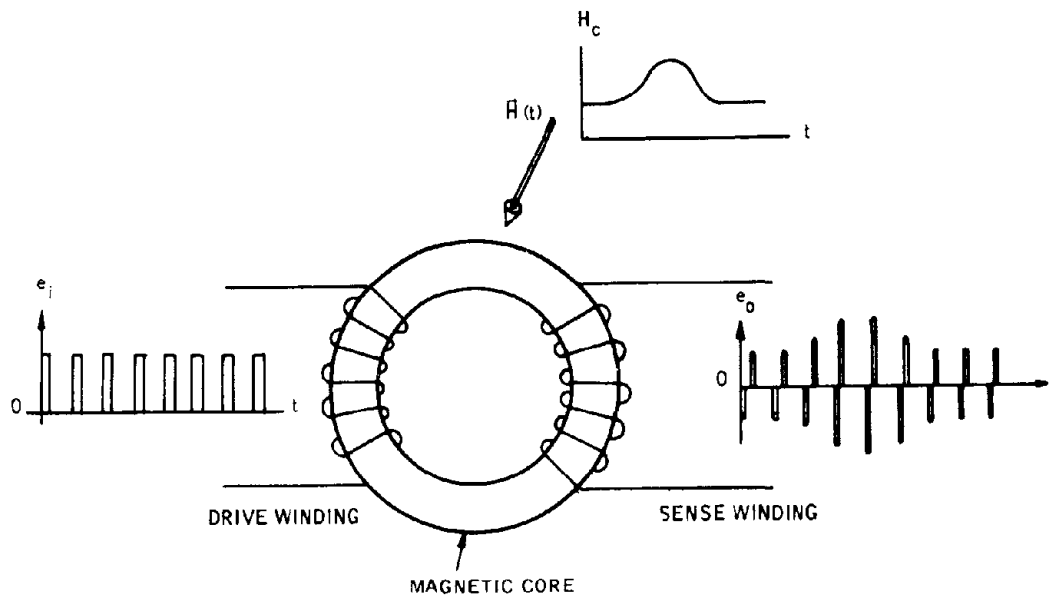


Figure 20. Magnetometer operation

The sense coil output is processed through analog and digital circuits to detect the presence of a vehicle over the sensor. The processing includes full wave rectification, momentary null rejection, stopped vehicle detection, and control signal derivation for the servo-stabilization circuits. The auto-stabilization circuit, providing a feedback path around the magnetometer, is necessary to compensate for long-term drift possibilities, and to make the sensor fully self-calibrating.

Magnetometer Design -- The Honeywell magnetometer core design, Figure 21, features a high permeability core with a single coil wound through it. The core itself consists of several layers of thin, high permeability tape wound on a stainless steel bobbin. The end of the tape is welded to provide a continuous magnetic path. A covering protects the core and completes the assembly. Since the core can be purchased as a finished component, the magnetic material is not handled, and possibly damaged, after the fabrication process.

The core is driven by a unipolar pulse into a saturated state (Figure 22). After each drive pulse, the magnetic field in the coil collapses, causing the polarity of the voltage across the drive coil terminal to reverse; the coil, then becoming a generator, produces a voltage proportional to the flux in the core.

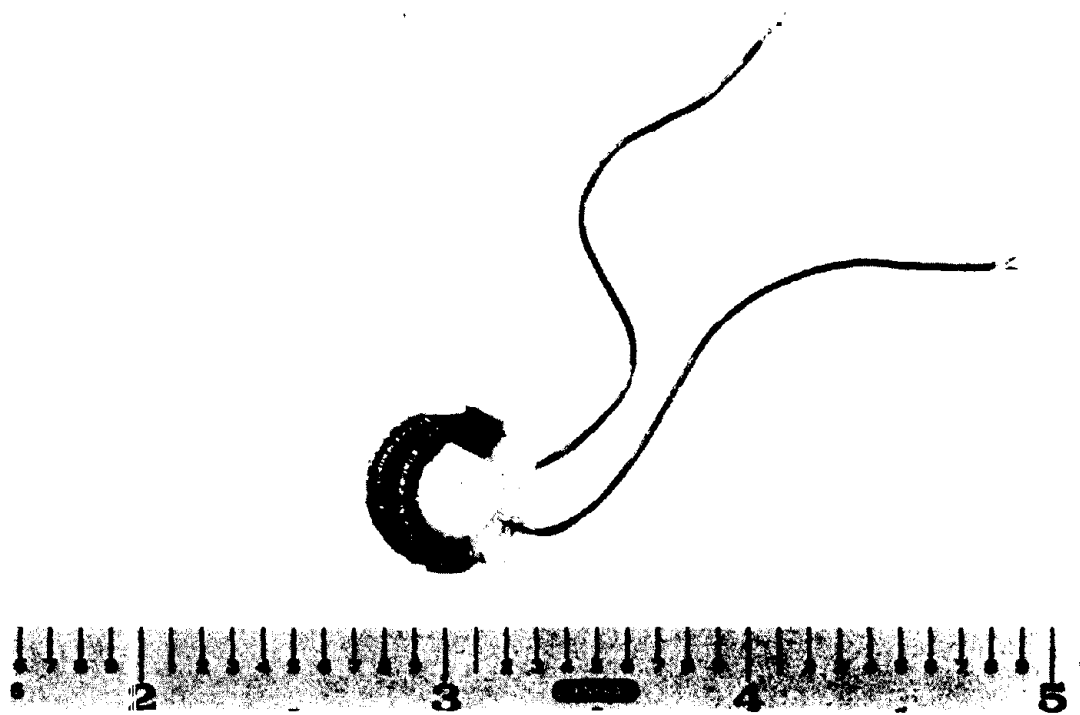
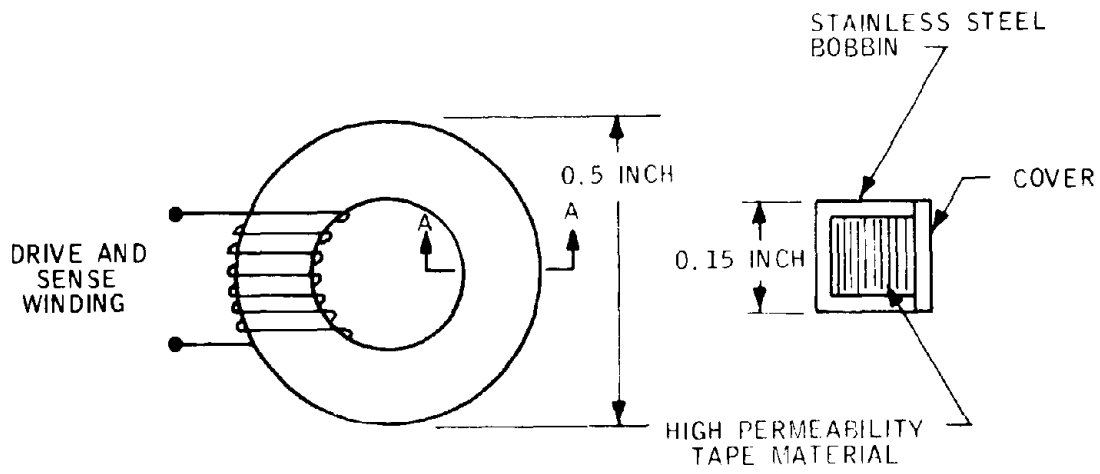


Figure 21. Toroidal core coil assembly

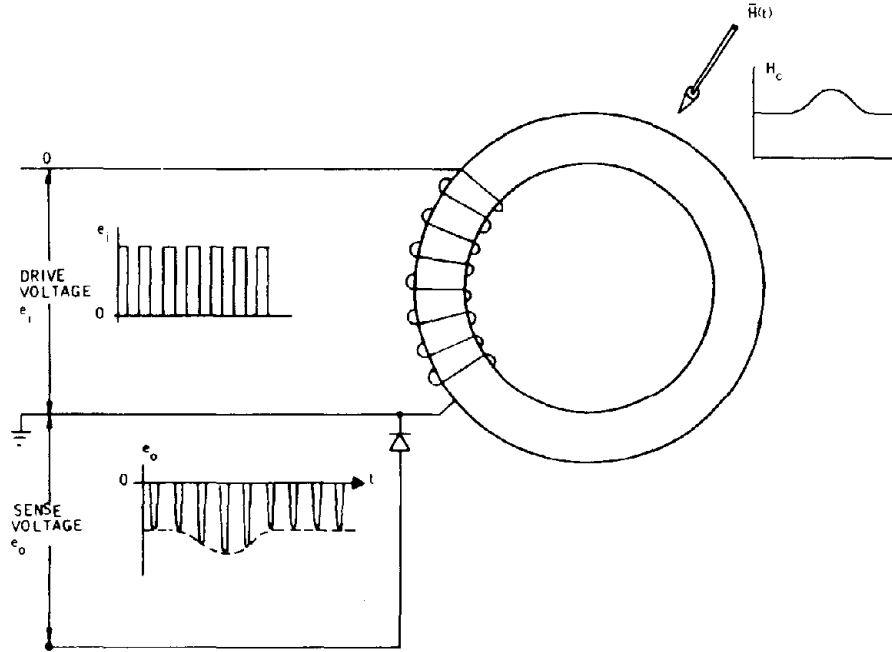


Figure 22. Unicoil magnetometer operation

Any time-varying external magnetic field within range of the magnetometer will cause a flux change in the core proportional to its magnitude. The flux introduced by the time-varying external field will be summed with the flux in the core, which is produced by the drive pulse and the earth's magnetic field. The net result is a changing flyback voltage developed when the drive pulse terminates. This changing voltage is detected and used for vehicle detection.

Sensor Design -- Figure 23 contains the block diagram of the sensor. The magnetic transducer and associated electronics, consisting of a voltage controlled oscillator (VCO), demodulator/amplifier, hold circuit, and feedback network, comprise the magnetometer. The hold circuit and feedback network provide the magnetometer with a d-c response capability which is necessary for long presence detection times; i. e., stopped vehicle. The sensor is implemented with two magnetic axes.

The signal processing hardware consists of two full-wave rectifiers, level detector, anti-chatter circuit, and circuits to generate leading and trailing edge pulses.

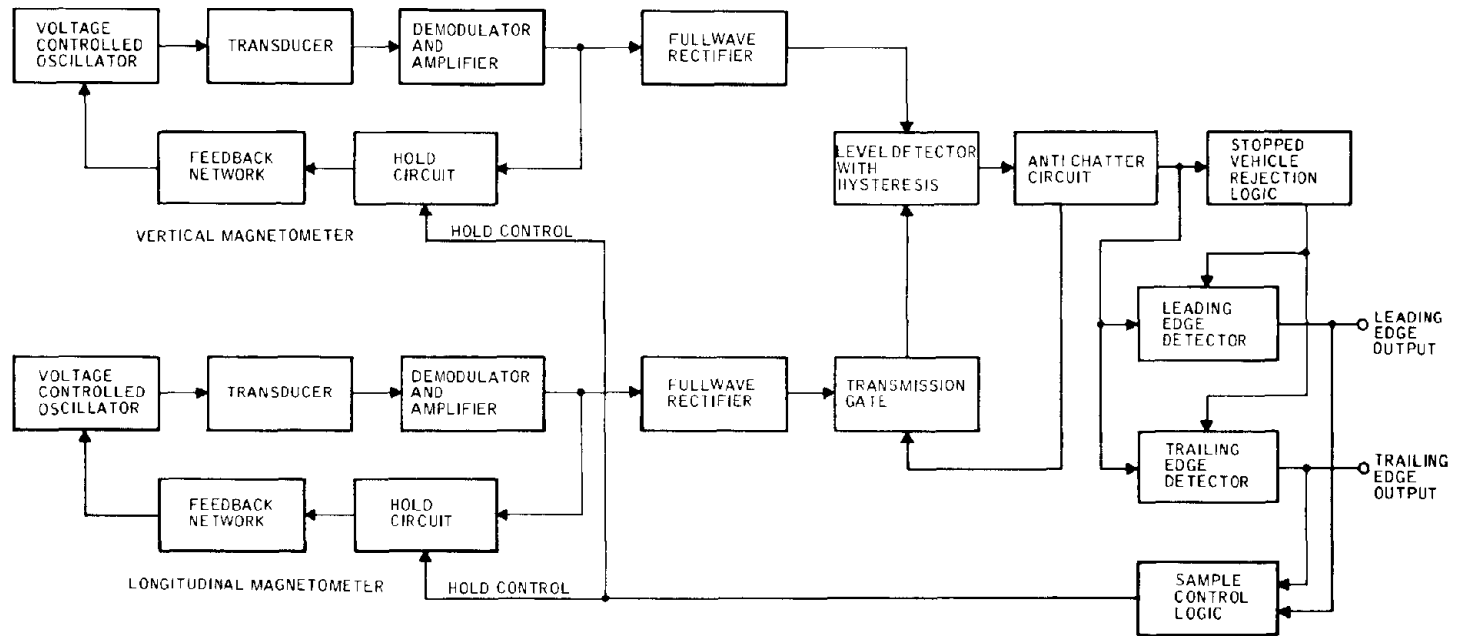


Figure 23. Block diagram of SPVD sensor

The VCO and driver used to drive the magnetic core into saturation is shown in Figure 24. The driver for this application has a repetition rate of 1000 Hz and a pulse width of 25-35 microseconds. A pulsed drive yields a significant reduction in current drain in the driver and magnetometer combination. The basic part of the driver circuitry is a standard, commercially available, integrated circuit.

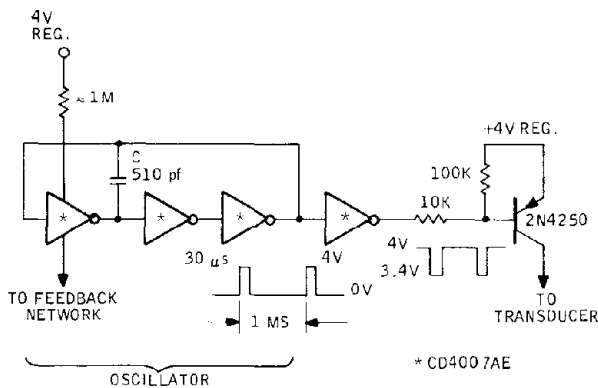


Figure 24. Voltage controlled oscillator and transducer driver

The flyback voltage produced by the collapsing field is integrated by a diode-capacitor circuit (Figure 25). The diode prevents the drive pulses from charging the detection capacitor, while allowing the negative flyback voltage to charge it. The capacitor charges to a d-c level proportional to the flux in the core under static conditions. As the flux in the core changes under influence of vehicle presence, voltage across the capacitor changes, and the change is coupled into the amplifier. The RC time constants are selected to reject all frequencies above 30 Hz, and the output signal is direct coupled to ensure a d-c response.

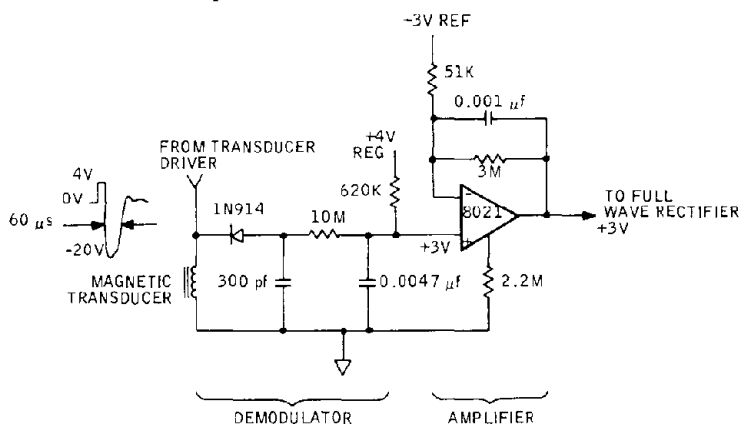


Figure 25. Demodulator/amplifier

The level detector output is fed through an anti-chatter circuit (Figure 29) to assure proper operation when the input is in a region close to the threshold. The output of the anti-chatter circuit is fed into the leading and trailing edge pulse generators and into a transmission gate. The output of the anti-chatter pulse circuit enables the horizontal axis channel when the level detector is initiated to permit either channel to hold the level detector on. The level detector will then stay on as long as either channel is above 3000 γ .

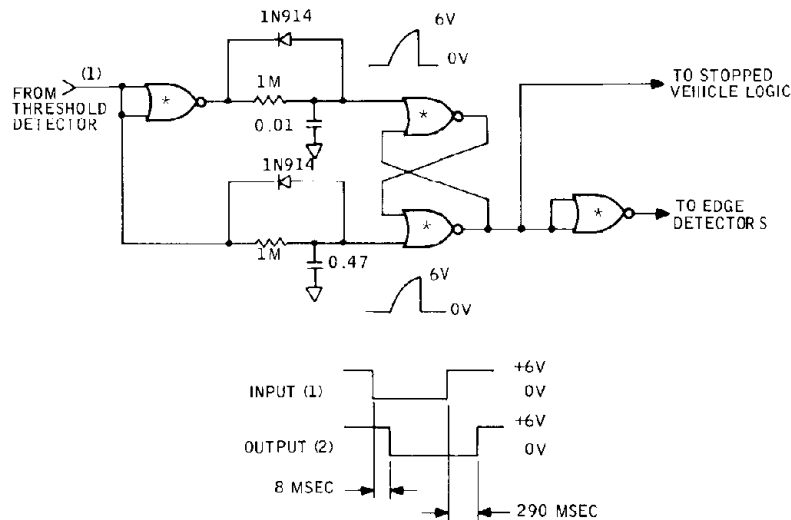


Figure 29. Anti-chatter circuit

The leading and trailing edge detectors, Figures 30 and 31, indicate the leading and trailing edges of the vehicle are used directly to key the RF transmitter.

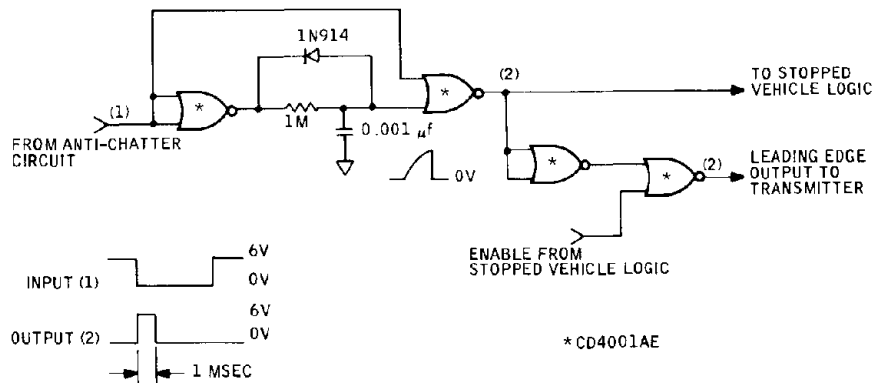


Figure 30. Leading edge detector

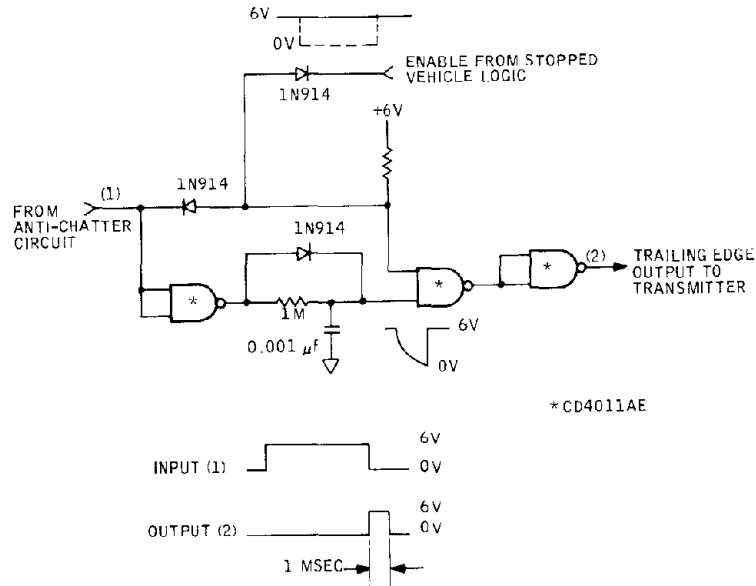


Figure 31. Trailing edge detector

Because the hold circuit is locked out during vehicle presence by the sample control logic and the magnetometer section does not have an infinite presence time (see page 43) the amplifier will drift during long stopped vehicle times. To avoid this, the stopped vehicle rejection logic (Figure 32) will cause the sample control logic (Figure 33) to enable the hold circuits and renull the magnetometers. In addition, the stopped vehicle rejection logic is designed to prevent a trailing edge pulse from occurring during the renulling process and prevents a leading edge pulse from occurring when the stopped vehicle initially moves away.

The low voltage detector (Figure 34) is merely a comparator circuit which compares the attenuated battery voltage to the +4 v regulated supply. When the battery voltage falls below +4.8 v, the circuit signals the transmitter to relay this information the next time a vehicle is detected.

A 4.0 volt regulator, Figure 35, is included for use by the sensitive magnetometer circuits and others where a stable reference is needed. The circuit is a straightforward voltage regulator. As with any regulator which derives its reference voltage via the output, the regulator might not turn on when the line voltage is first applied. Therefore, a startup circuit is included. S1 is a transmission gate (CD4016) which is connected as a start-up switch.

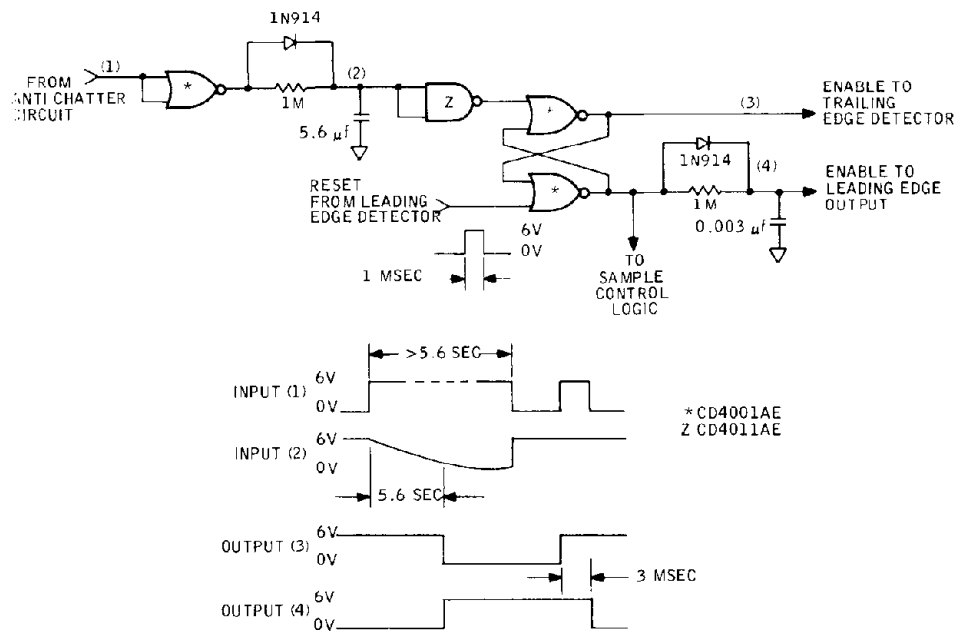


Figure 32. Stopped vehicle rejection logic

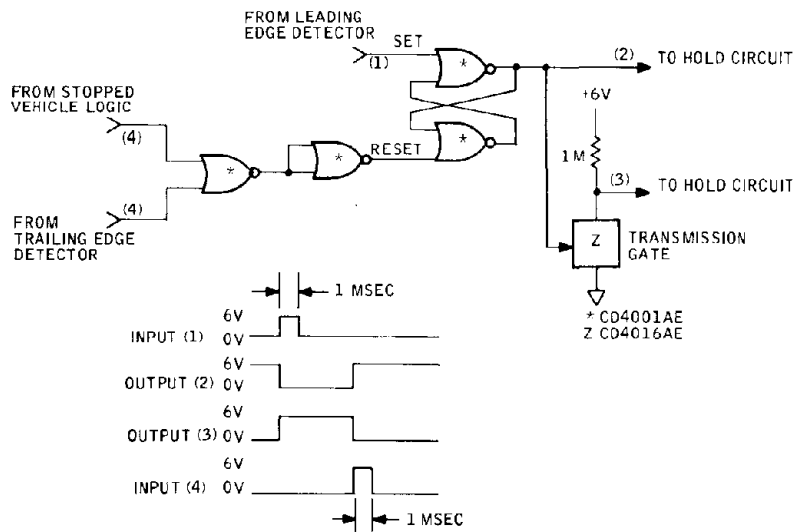


Figure 33. Sample control logic

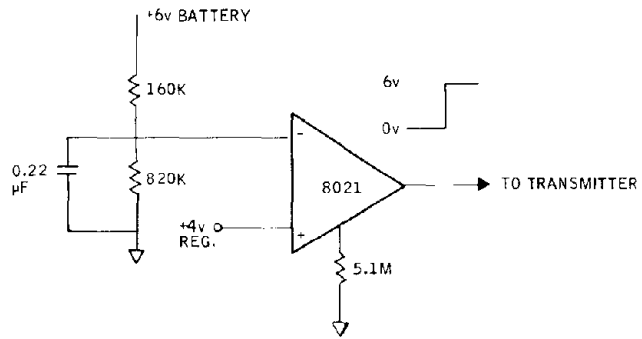


Figure 34. Low voltage detector

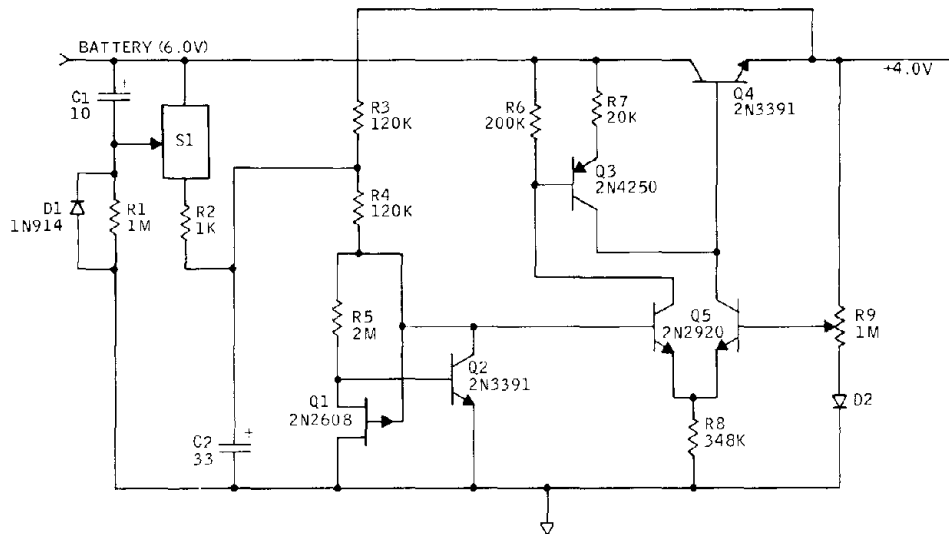


Figure 35. +4 volt regulator

Sensor Performance -- Figures 36 to 39 are the results of the static detection zone tests. As is noted in Figures 36 and 38, one zone was not tested due to weather conditions on the day all the data runs were made. In view of the remaining program tasks which had to be done, the effort required to gather (and the amount of useful information to be gained) these few extra data points, this zone was not rescheduled for testing. (From observation of Figures 37 and 39, and considering the declination of the ambient magnetic field, one would expect a nearly symmetrical pattern in Figures 36 and 38).

Due to the limitation of the vehicle test pad locations, vehicle speeds were limited to 30 mph maximum during this program. Therefore, the 80-mph detection capability was not experimentally verified. However, based upon the frequency content of the vehicle signatures, and the amplifier frequency response cutoff of 48 Hz, the sensor should be capable of detection at high speeds. The transducer is not speed sensitive, which means that the amplifier is the response-determining component.

One source of improper operation of the sensor remains with regard to stopped vehicle detection. The symptoms of the operation of stopped vehicle detection are that the trailing edge of the stopped vehicle and the leading edge of next vehicle may not always be properly processed by the sensor. What often happens is that when the stopped vehicle moves away, a trailing edge is not generated and, in addition, a leading edge pulse is not generated for the next vehicle. Thus these two events are not always transmitted to the roadside receiver. The source of this improper action is the long zeroing time of the magnetometer feedback loop. If the vehicle stops over the sensor in such a position that the magnetometer is experiencing a very large input signal, the rezeroing time of the feedback loop, which can be on the order of 23 seconds, exceeds the stopped vehicle detector time of 5.6 seconds. This action fools the detector into thinking it saw another stopped vehicle which results in inhibiting the trailing and next leading edges. The solution to this problem is to design and incorporate a digital feedback scheme to replace the analog feedback network and hold circuit scheme in the magnetometer. Due to program time and funding considerations, this solution was not pursued.

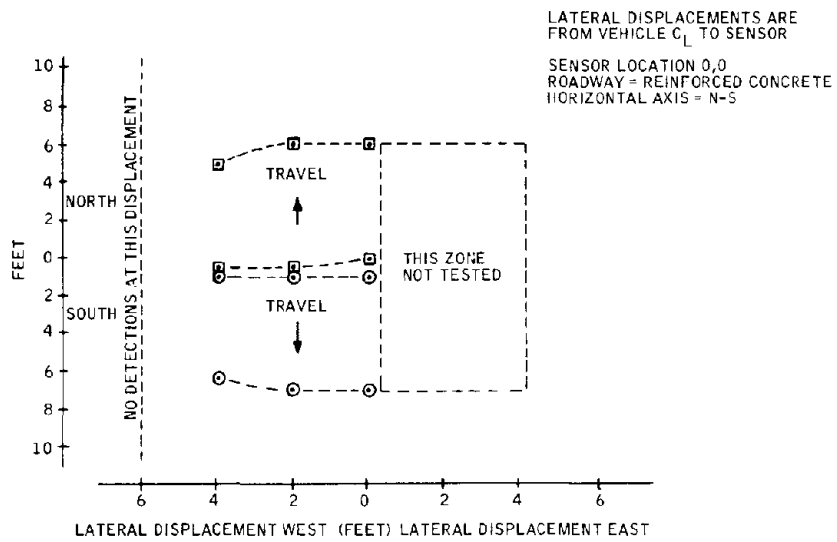


Figure 36. Static detection zone, VW Beetle, 10 mph

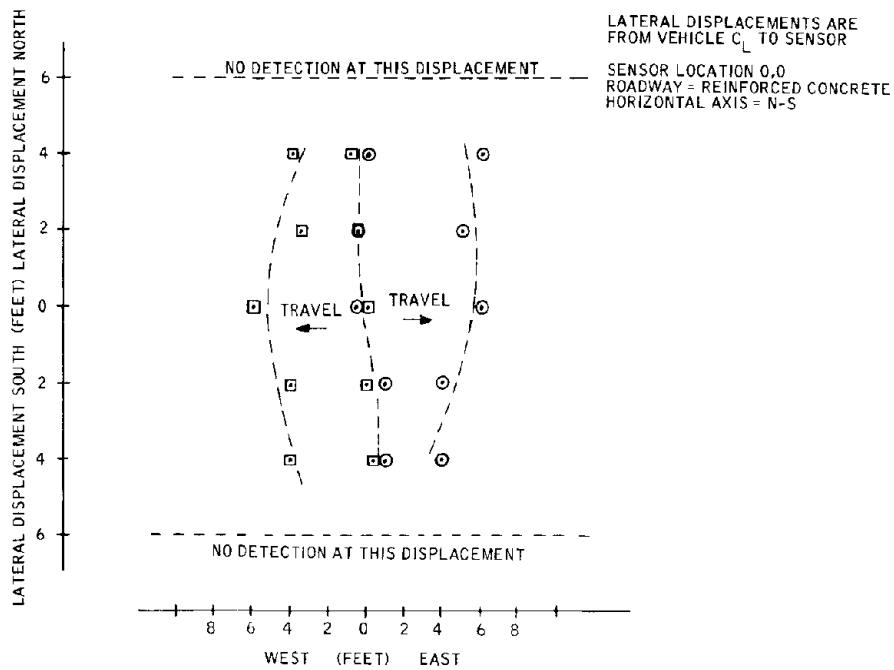


Figure 37. Static detection zone, VW Beetle, 10 mph

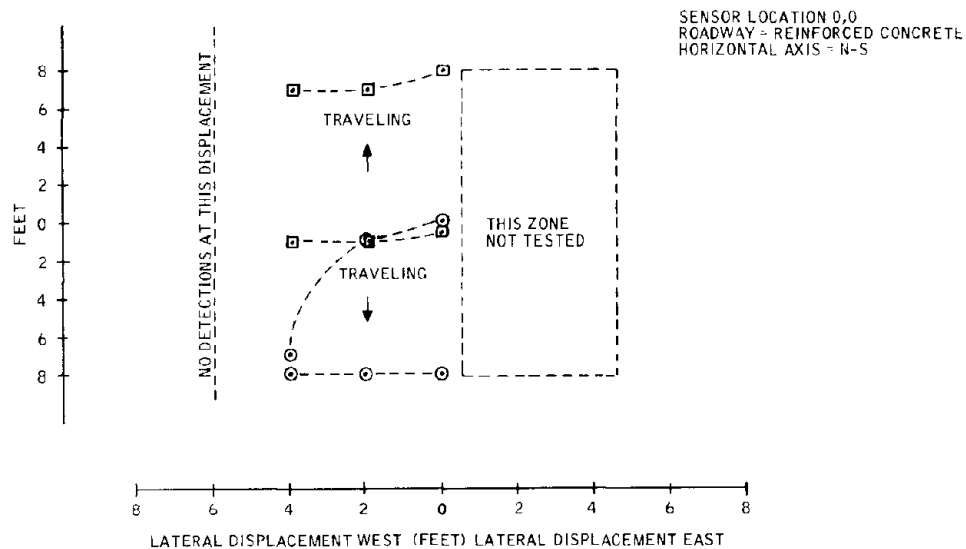


Figure 38. Static detection zone, Ford Torino, 10 mph

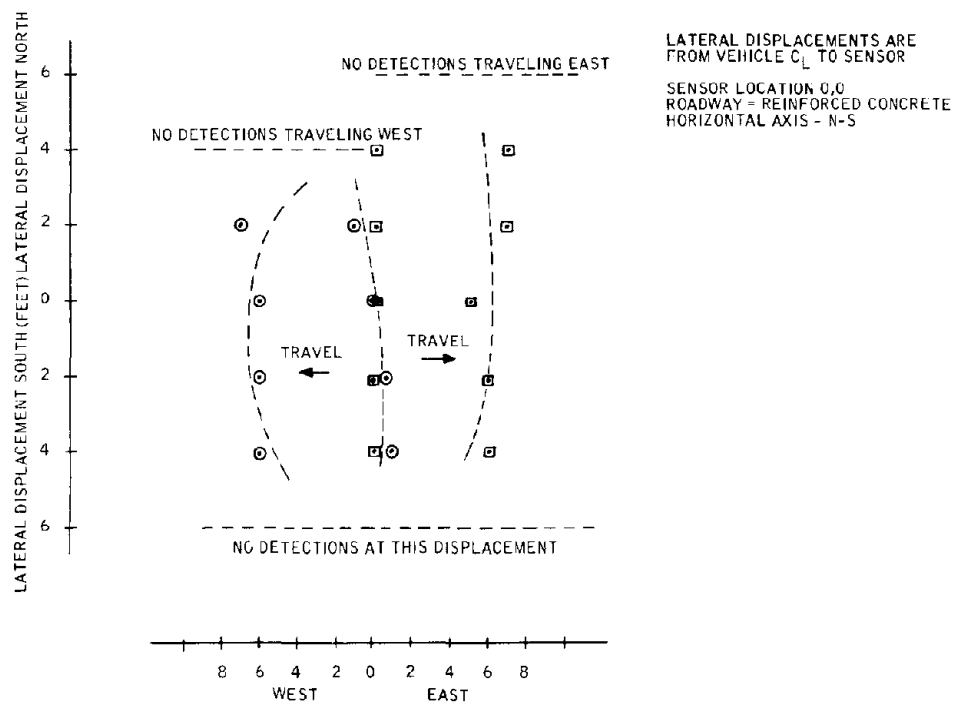


Figure 39. Static detection zone, Ford Torino, 10 mph

Other System Parameters

SPVD Temperature Extremes -- Early in the SPVD program, the power source analysis indicated that the -30°F to $+170^{\circ}\text{F}$ temperature goal would be very difficult to meet. Therefore, an analysis was conducted to investigate the temperature extremes existing in bituminous and concrete highways throughout the continental USA. The investigation was conducted to determine whether the 170°F to -30°F SPVD temperature extremes were realistic or whether there was justification to change the SPVD specification to reflect a lower maximum and a higher minimum temperature. To obtain literature on the subject, the following contacts were made:

Minnesota Highway Department/Both Concrete and Engineering
Specialists
University of Minnesota Civil Engineering Department
Portland Cement Association/Local Office
Highway Research Board/National Academy of Sciences/Washington,
D. C.

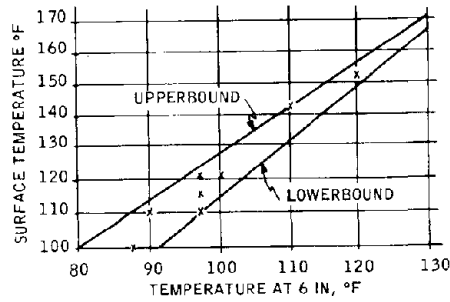
Although the references to the literature were obtained from all of these sources, the actual documents were obtained from the University of Minnesota Engineering Library.

Temperature extremes extrapolated from test data taken throughout the United States (Minnesota to Arizona) are shown in Figure 40. As can be observed in the figure, if the extremes of $+170^{\circ}\text{F}$ and -30°F are assumed to be surface extremes. Then they correspond to extremes at 6 inches of $+130^{\circ}\text{F}$ and -20°F .

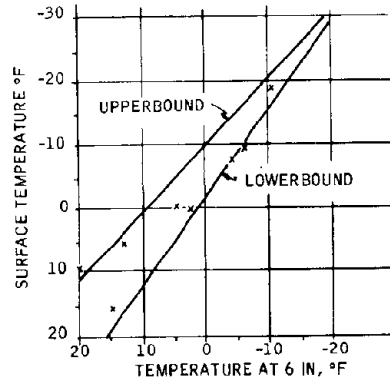
As a result, the reduced temperature range was adopted for the power source, sensor, and transmitter sections of the roadway unit.

Physical Dimensions -- During the design of the sensor and RF-link transmitter, it was determined that additional battery capacity would be required to meet the operational lifetime goal of one year. This requirement made the "C" size cells unacceptable; i. e., a larger capacity source was needed. As the power source analysis (AppendixA) pointed out, the favored battery was the lantern battery. However, this battery has a diagonal dimension of about 3-1/8 inches.

The transmitter antenna, too, it was found, could achieve greater efficiencies if it had a larger diameter. Further, it was learned from the Minnesota Highway Department that the minimum size core drill in their operation is 4 inches in diameter (resulting in a 4.5-inch hole). As a result, the maximum diameter of the SPVD was allowed to increase to 4.5 inches.



GRAPH 1. HIGH TEMPERATURE DATA



GRAPH 2. LOW TEMPERATURE DATA

Figure 40. Temperature extremes extrapolated from test data

Because of program funding limitations, custom printed circuit boards were not used for the sensor. As a result, the length of SPVD exceeded the design goal of 6 inches. Use of custom LSIC's and custom printed circuit boards could significantly reduce the present length of 14.5 inches.

The final environmental package concept is as follows: The main body consists of Schedule 40, PVC tubing; O.D. is 4.5 inches, wall thickness is .225 inches. On the top end is an aluminum plate secured by machine screws and sealed with epoxy. The bottom end of the package is secured with machine screws and has an O-ring seal. The bottom plate is also aluminum. Total package length is about 14.5 inches.

Reliability Estimate

An important factor in the development of vehicle detectors is system reliability. A preliminary reliability analysis of a projected SPVD design was conducted to evaluate compliance with two primary reliability parameters, namely:

- As a design goal, the self-contained energy source shall power the SPVD roadway unit for at least a one-year life.
- The required mean-time-between failure (MTBF) of the SPVD is one year.

Preliminary analysis shows that the power source requirement can be achieved.

A reliability analysis of the SPVD roadway and roadside units shows these units to have a MTBF of approximately 1.5 years, exclusive of the energy source which is assumed to be replaced at the time of its useful life limitation. This analysis shows the predicted SPVD MTBF to be well above the one-year MTBF requirement. The preliminary reliability analysis is presented in Table 6.

Honeywell's approach to assuring compliance with contractual reliability requirements is initiated during the proposal phase with a preliminary reliability assessment which is then iterated as the design progresses to the delivered production hardware. Depending on the contractual requirements, the reliability requirements may then be demonstrated by a formal testing program conducted on the production prototype and/or production systems. Recognizing the uncertain nature of all predictive processes, Honeywell has developed a standardized reliability prediction technique using parts type count and adjusted weighting factors (part failure rates) with both the general technique of the military's MIL-HBK-217A, as a basic guide, and specialized methods tailored precisely to Honeywell hardware. This approach to MTBF prediction has proven itself to yield results superior to other known methods as applied to Honeywell systems. Typically, Honeywell predictions fall within the range of 2/3 to 3/2 of the field-measured MTBFs on the mature system.

Table 6. SPVD reliability prediction

Part Type	Part Failure Rate, λ (%/1000 Hours)	Roadway Unit		Roadside Unit	
		N	$N\lambda$	N	$N\lambda$
Capacitor	0.005	59	0.295	33	0.165
Diode	0.074	11	0.814	10	0.74
Inductor	0.02	14	0.280	11	0.22
Integrated Circuit	0.07	11	0.77	11	0.77
Resistor	0.008	66	0.52	45	0.36
Transistor	0.02	17	0.34	9	0.18
Power Supply	2.0		---	1	2.0
	Subtotals =		3.027		4.435
Total SPVD Failure Rate = 3.027 + 4.435 = 7.462%/1000 Hours					
SPVD MTBF = $\frac{10^5}{7.462}$ = 13,401 hours = 1.5 years					

The success of this prediction system is attributable to control of reliability through several factors, all under continuing improvement: standardized processes and practices in design; standard and consistent procurement and production methods that relate one generation of equipment to the next; standard piece-part design margins and derating criteria universally applied; and standard weighting factors (failure rates) controlled by a central reliability organization and periodically adjusted to reflect feedbacks.

Referring to Table 6, part failure rates are assigned to each generic part type which is to be used in the proposed or actual hardware design. These failure rates, expressed in "%/hours" (which is equivalent to failures per 10^5 part operating hours) are based on field experience of Honeywell designed and built systems. To obtain the device and system failure rate, the projected or actual quantity of each generic part type is multiplied by the part failure rate--the summation of the part failure rate--part quantity is the total device or system failure rate. The system MTBF is then computed as the reciprocal of the system failure rate.

A review of the SPVD reliability requirements indicates that a minimum of 3.5 SPVD unit-years of testing would be required to demonstrate the one-year MTBF to a 90 percent confidence, assuming the occurrence of no failures during this test time. A test program of this magnitude appears to be prohibitive during a design and development program from the standpoint of calendar time and quantity of available hardware for reliability testing. Experience also shows that reliability of developmental hardware is not indicative of the mature production equipment, to which the reliability requirements pertain. Honeywell found that it is typical to experience a factor of 10 to 100 difference between system reliability measured on developmental hardware and that measured on the mature production systems. Honeywell therefore recommends that updated analytical reliability assessments be performed during the design and development phase and that the reliability demonstration test be conducted on a sample of production prototype or production hardware.

As an integral part of a SPVD design and development program, Honeywell would implement a reliability program to assure that the production hardware complies with the specified reliability goals and requirements. A reliability engineer would assist the design group in various configuration analyses to arrive at an optimum design.

SPVD Selling Price Estimate -- The estimate of the SPVD selling price is not based on the actual costs for the feasibility models developed in this project. The selling price estimate is based on a prototype model where it is anticipated that a significant portion of the feasibility model circuitry would be reduced into custom integrated circuits. This is a more realistic treatment of objectively estimating the actual selling price.

The estimated single unit selling price, in 1975 dollars, for a complete OEM produced, distributed and supported SPVD system, including a Roadway Unit and a Roadside Unit, is as follows:

100 Production Run Lot

\$ 535/system

1000 Production Run Lot

\$390/system

These prices are contingent on the assumption that all SPVD components needed for production are purchased in quantity lots of 10 times the production run lot and that non-recurring costs are amortized over a mature ten-year product need.

Conclusions

Although this project investigated an entirely new concept, the models performed very well against the design goals. Only three of the seven design goals were not met. But more importantly, there is very high confidence that with further development, these three goals can also be achieved.

The performance against stopped vehicles and over temperature, two of the goals which were not entirely met, could be greatly improved with work on the feedback network and hold circuit; specifically, the incorporation of a digital scheme based upon low-power CMOS IC's. Program funding would not allow a full-scale investigation of this scheme.

The third remaining goal, size of the roadway unit, could be approached by using custom integrated circuits. It is felt that the design goal length of six inches is perhaps unrealistic. However, the present length of 14.5 inches could certainly be reduced by three inches or more by integrating the sensor electronics.

The RF link performed well. The major obstacle anticipated was the 500-foot transmission design goal, and this was achieved. Granted, the security of the link against voice and music transmissions on the same frequency could be improved, but this improvement is not seen as being an insurmountable or extremely difficult problem. Many solutions could be evaluated.

Another extremely important design goal, which we feel was met, was the one-year operational lifetime. In fact, this goal was met with a good deal of margin! With future power source improvements, an operational lifetime goal of two years might be approachable.

Recommendations

As detailed in previous paragraphs, the SPVD project has met with considerable success. Based on this success it is recommended that the SPVD be carried into a prototype model development project.

The objective of this new SPVD project would be to design, fabricate, and evaluate production prototype models of the SPVD. This new project would enable a logical and effective method of continuing, without disruption, SPVD development already carried through feasibility proof and delivery of engineering models.

Figure 41 is a recommended project plan for development of a prototype SPVD. The first activity would be development and feasibility proof of a digital magnetometer sensor having improved performance over the current SPVD analog magnetometer sensor. Specific areas of improvement are cited in stalled vehicle detection, operational temperature range extension, and reduction in the longitudinal static detection zone. When this activity is complete, prototype development of nine SPVD models

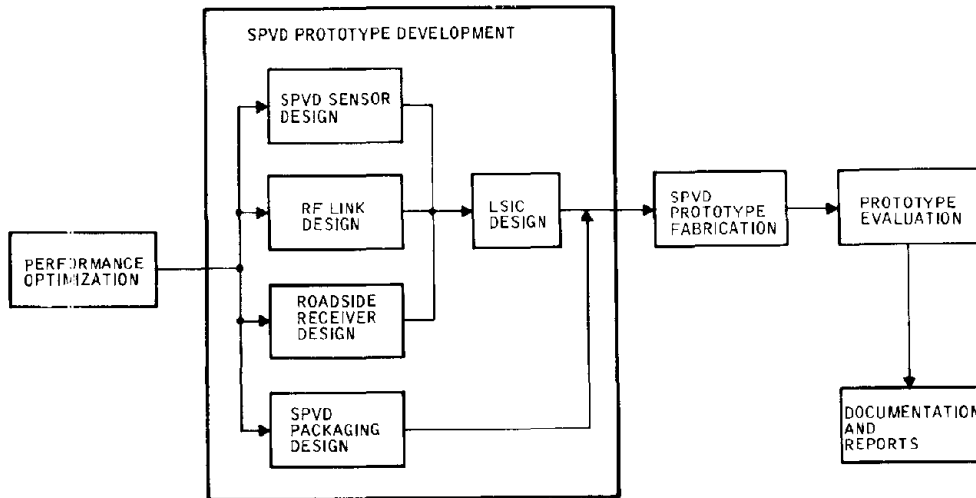


Figure 41. SPVD prototype development plan

would be initiated. This development would reduce the sensor transmitter and roadside units to producible designs, stressing low cost and reliable operation. A major part of this activity would be resolution of the RF link security; whether the solution is an allocated clear RF channel or special coding technique. The magnetometer sensor, certain parts of the RF link, and control circuitry would be subjected to a Large Scale Integrated Circuit (LSIC) design resulting in one or more LSIC chips comprising the SPVD. An engineering model SPVD would then be fabricated and demonstrated to the Federal Highway Administration. Concurrent with developing the SPVD prototype design, a packaging design would be conducted to develop a suitable enclosure for the SPVD. Part of the packaging design would investigate methods of installation and environmental protection to the SPVD while in a roadway environment. The next activities in the recommended SPVD project would result in nine SPVD prototype units. These prototype units would be subsequently delivered to the Federal Highway Administration for evaluation.

APPENDIX A
 DETAILED POWER SOURCE ANALYSIS, SPVD⁴

Using the design approaches for the Sensor and RF Link and preliminary power drain estimates, the required operating parameters are determined to be as follows:

- Voltage 6.0+ V to 4.8 V
- Current 0.30 mA continuous
35 mA pulses, 10 msec duration,
40,000 pulses per day
- Operating Temperature -20°F to +130°F

Table 7 contains the required battery capacity for a one-year operation.

Table 7. Battery capacity

	Battery Current (Milliamperes)	Hours (One-Year Operation)	Ampere- Hours
Continuous Loads			
Sensor + Transmitter Switch + Low-Voltage Detector	0.30	8,760	2.63
Pulse Loads			
Sensor	0.20	648	.13
Transmitter	35.00	40.5	1.42
Random Loads			
Sensor (Stopped Vehicles)	0.20	1,314	.26
			4.44

The battery will require additional capacity to compensate for losses occurring during storage and also resulting from exposure to high temperatures during the one year of operation in the SPVD. It was estimated that

⁴ The current and pulse durations were based upon early estimates of RF link requirements. Later facts dictated increased values. See the Addendum at the end of this appendix.

this will not exceed 10 percent of the battery capacity down to 4.8 volts, or about 0.60 ampere-hours. The total required capacity will then be about 5.0 ampere-hours. Union-Carbide, Mallory and Ray-O-Vac were given information on the above requirements. They recommended the D-size alkaline and lithium cells as likely candidates for this application. The lantern batteries were not thought to be suitable at very low temperatures, but were added to the test program since they would provide a low-cost, fully assembled and potted, four-cell (F-size) battery which might be able to deliver the short-duration current pulses.

Test Procedure and Results

Initial Tests

The loads applied to the cells or batteries consisted of a continuous load of 500 microamperes (simulating the estimated maximum load excluding the transmitter) plus pulses of three magnitudes; 20, 30, or 35 milliamperes, simulating the estimated range of current required for transmitter operation. For each level of current, the pulse duration was 10 milliseconds. The pulses were applied in a sequence providing a delay of 250 milliseconds between the first and second pulse, and a delay of 1.0 second between the second and third pulse. This cycle could be repeated as long as desired, simulating a succession of cars traveling at about 60 miles per hour over the SPVD. This test procedure was accomplished by use of the test circuit shown in Figure 42.

Each of the batteries, in the condition received from the manufacturers, was tested at the following temperatures; -30°F, -20°F, -10°F, 0°F, RT, +120°F, and +140°F. It had been planned to conduct a test at +160°F, but shortly after the temperature chamber was raised to this level, one of the two lithium cells blew its safety vent plug and released its sulfur dioxide depolarizer and some of the electrolyte liquid into the environmental chamber. The +160°F test was abandoned.

In this series of tests, the results in the following subparagraphs were observed:

Alkaline Cells -- The cells made by the three vendors were remarkably similar in performance. All operated satisfactorily at each test load and temperature, remaining above 1.2 volts (1/4 x 4.8 volts during the pulse loads. The minimum voltage observed under the pulse load of 35 mA at -30°F was 1.47 volts.

The voltage under the 500 microampere load alone varied from 1.58 volts to 1.51 volts over the temperature range of -30°F to +140°F, with some of the higher values occurring at the lower temperatures. The

As stated earlier, one of the two lithium cells became inoperative when its safety vent blew out after a short time at +160°F under no load. This vent is intended to prevent an explosion of the cell due to excessive internal pressure of the sulfur dioxide depolarizer. Such high pressure could be caused by shorting of the cell and/or high ambient temperatures. The manufacturer's specifications for the lithium cell claims the capability of operation at +160°F. The reason for the release of the safety vent in this instance is unknown.

Based upon discussions with Honeywell battery chemists and the Mallory Battery Company Technical Sales Manager, it is considered that the poor performance of the lithium cells at low temperatures is caused by a combination of the following factors:

- A reduction in the open circuit voltage as the temperature is reduced. This is typical of most batteries.
- An increase in the cell internal impedance as the temperature is reduced. This is typical of all batteries.
- A passivating film on the surface of the lithium anode caused by reaction of the lithium with sulfur dioxide. This film is a major factor in obtaining the storage capabilities of the cell. The film is eliminated when sufficient current is delivered by the cell for an adequate period. This phenomenon is called "voltage delay" and is also found in some other types of cells as, for example, the magnesium cell.

It is apparent that the combination of the 500-microampere continuous load and the pulse loads applied during the initial testing of the lithium cells did not "burn off" the passivating film. Satisfactory operation occurred only when the temperature had increased sufficiently to raise the cell open circuit voltage and decrease the cell internal impedance to a level which would support the pulse loads at the required voltage of 2.4 volts or higher.

Lantern Battery -- The heavy-duty lantern batteries were below the minimum voltage at -30°F and pulse loads of 30 and 35 microamperes. Under all other test conditions of load and temperature, their performance was satisfactory. The voltage of these batteries under the 500-microampere load alone varied from 6.3 volts at -30°F to 6.5 volts at +120°F. The voltage drop caused by the largest current pulse (this varied from 35 to 44 microamperes) was 0.1 volt at +140°F, increasing to 0.8 volt at -20°F, and 2.4 volts at -30°F. Although these voltage dips are about four times greater than would be obtained with a four-cell alkaline (D-size) battery (excluding the -30°F readings from the lantern battery), the performance of these batteries is considered to be very good. A one-minute sequence of the test pulse schedule indicated no apparent change in voltage readings.

Accelerated Life Test

After the above initial tests, some of the alkaline cells and lantern batteries were discharged at high rates to determine their performance when their capacities were reduced, thus simulating several successive stages in the required operating life of one year. All discharges were made with the batteries at room temperature, but the operating tests were conducted at -30°F. The first discharge occurred in a two-hour period with a 3.0-ohm load across the alkaline cells and a 13.2-ohm load across the lantern battery. The capacity removed from each unit was about 0.84 ampere-hours, or one-sixth of the estimated capacity required for one year of operation.

The simulated load tests showed that the batteries had declined to a lower voltage level, but the minimum voltage under the pulse load was adequately above the 1.2 volt per cell level. For the alkaline cells, the minimum was 1.31 volt and for the lantern battery it was 5.55 volts (equivalent to 1.39 volt per cell) at -30°F and 35-microampere current.

Further capacity withdrawals were made at current levels not exceeding 0.5 ampere and durations varying from about one hour to three and a half hours. After each stage, the load test was repeated. Occasionally, as the voltage continued its downward trend, a three minute sequence of the test pulse schedule was applied. This would be equivalent to about 150 cars passing over the detector in succession. The comparison of minimum voltage under the pulse load (35 to 40 microamperes between the first pulse and the pulse at the end of three minutes indicated a minor droop in voltage level (0.01 volt to 0.04 volt for the alkaline cells and 0.07 volt for the lantern battery).

At one stage in the above sequence, a 500-microfarad capacity was connected in parallel with each of the cells or batteries under test. There was no apparent change in voltage levels under the pulse loads resulting from the use of the capacitor.

Table 8 contains the final test measurement results.

Table 8. Results of battery tests

	Alkaline Cells	Lantern Battery
Total Capacity Withdrawn (ampere-hours)	8.17	6.7
Percent of Estimated Required Capacity	163	134
Voltage under 500-Microampere Load	1.27	5.4
Voltage under 35-microampere Load	1.24	--
Voltage under 40-microampere Load	--	5.25
Test Temperature (°F)	-20	-20

These data indicate an adequate margin in performance remaining in these batteries at the conclusion of the test.

Lithium Cell Final Test

As indicated in Table 8, the lithium cell passivation film is considered a contributing factor to its unacceptable performance under the SPVD required loads and temperatures. It was not considered to be appropriate to attempt to burn off this film with a heavy load since in the intended use there could be periods of minimum activity and the passivation film could re-form. As an alternative approach, a 5,600-ohm load (approximately 500-micro-amperes current, simulating the maximum detector load, excluding the transmitter) was connected to the remaining lithium cell. This load was applied for a period of 3.5 days. The pulse load cycle test was subsequently conducted at -30°F, there was no improvement in performance.

This lithium cell had remained in the environmental chamber while the alkaline cells and lantern batteries were being cycled between room temperature (for capacity discharge) and -30°F (for load operating tests). After a few days of such cycling, the lithium cell began to leak sulfur dioxide. The safety vent did not blow out, but apparently the temperature cycling may have affected the rubberlike seal used in the safety vent and permitted a slow release of the gas. This lithium cell was considered to have failed at this point.

Comments

In addition to the performance capabilities comparisons, other factors to consider in selecting the optimum battery for the SPVD application are:

Battery Package

The lantern battery is completely packaged in a convenient form for immediate use in an SPVD. Several standard types of terminals are available; coil springs, sockets, knurled nut and screw and fahnestock clips.

The alkaline D-cells are not available in a standard commercially available four-cell package. The only standard six-volt alkaline battery contains four G-size cells in series and is about 5.5 x 4.75 x 2.75 inches in size. It would require a 5.5-inch-diameter by 5.5-inch-long envelope and is too large for the planned diameter of the SPVD.

To provide a reliable power source, it is considered desirable to hard wire the batteries in series, preferably with welded connections to each cell, and then put the assembly into a package similar to the LeClanche lantern battery. The potting, in addition to providing a rugged support for the cells, will aid in reducing the leakage of electrolyte from the cells. This arrangement should decrease the internal capacity losses in the power sources, both before and during its use in the SPVD.

When packaged as discussed above, the alkaline "D" cell battery is expected to be about 1.25 inches shorter than the lantern battery, and will fit in the same diameter space.

Availability

The D-size alkaline cells are produced by Union Carbide, Mallory, Ray-O-Vac, Burgess, Marathon and Bright Star. All of these manufacturers should be capable of assembling these cells into a four-cell potted package at a reasonable additional cost. In addition, there are other companies that make battery packs, for applications such as communications equipment, by purchasing the cells from the manufacturers and assembling them into a suitable multi-cell package.

Heavy duty lantern batteries are made by Union Carbide (No. 609) and by Ray-O-Vac (No. 944). Only the Union Carbide battery was tested in this program. Their engineers were surprised by the excellent low-temperature performance obtained in these SPVD load tests. They have requested the return of two batteries for analysis in their Cleveland laboratories. Apparently, these batteries have been available only for the past few years and they occasionally make a limited quantity with some special improvements. It is possible that the samples obtained for the SPVD testing may contain an improvement which will become part of their standard production in the near future.

Ray-O-Vac has informed Honeywell that their heavy-duty lantern cell contains only zinc chloride as the electrolyte salt. The standard LeClanche cell contains a mixture of zinc chloride and ammonium chloride as electrolyte salts.

Mallory has informed Honeywell that they plan to have a heavy-duty lantern battery in production by the first quarter of 1974.

Until it can be determined that the Union Carbide lantern battery which was used in the above tests is similar to the Ray-O-Vac and the Mallory heavy-duty lantern batteries, it will not be possible to merely specify "heavy-duty lantern battery" as a suitable SPVD power source. This matter will be followed up with the manufacturers.

Cost

Relative cost data, both present and projected, obtained from the manufacturers are as follows

	<u>Four Alkaline D Cells*</u>	<u>Two Lithium D Cells*</u>	<u>Six Volt LeClanche Lantern Battery</u>
Small Quantities	\$4.00	\$23.00	\$.80
Large Quantities	\$1.20	\$ 6.80	\$.65

*Does not include cost of wiring and potting.

It is considered that the costs of alkaline and lantern batteries are fairly well stabilized. Because of higher costs of materials and facilities (such as dry-rooms), it is expected that lithium cells will remain more costly than the other two types. However, it is probable that the cost indicated in the above table for the lithium cells may eventually be reduced, to some extent, if the total quantities manufactured approach those for the alkaline cells.

Another factor to be considered is the battery replacement costs; that is, the removal of the SPVD from the roadway and insertion of a new power source. If this cost per SPVD is significant, then a more costly but higher energy capacity battery, may result in a lower total cost of ownership. The lithium cell may eventually provide this type of advantage.

For example, the Mallory lithium cell has about twice the energy density of the alkaline cell. If the power source is assembled as two parallel groups of two series-connected cells (total of four lithium cells) then it may be possible to obtain two years of SPVD operation with one power source.

As noted previously, the present Mallory lithium cells do not meet the performance requirements at low temperatures, partly because of the voltage delay characteristic. Honeywell has been informed by Mallory that a large scale effort is underway at the Mallory Research Laboratories to eliminate this voltage delay phenomenon. Furthermore, there are other lithium electrochemical systems available which do not exhibit any voltage delay. One or more of these improvements may be available in future lithium cells for use in the SPVD. These improvement could, at a later date, be incorporated in the SPVD since the voltage levels of two lithium cells in series would be compatible with the 4.8 volts to 6.0 volts design of the SPVD electronic circuits.

We requested Union Carbide to provide a more accurate estimate of battery capacity losses incurred during storage and high-temperature roadway environment. They provided the following estimates of capacity loss for the E95 alkaline cells and the No. 609 lantern battery.

After a one-year storage at 70°F, the percent capacity remaining is:

E95	95%
No. 609	90%

After exposure to high temperature for various periods of time the service life is:

<u>Storage Time</u>	<u>E95 Storage Temp.</u>		<u>No. 609 Storage Temp.</u>	
	<u>113°F</u>	<u>130°F</u>	<u>113°F</u>	<u>130°F</u>
1 Day	100%	100%	100%	100%
1 Week	98%	95%	97%	95%
1 Month	90%	85%	90%	65%
3 Months	85%	65%	85%	60%

It is estimated that during the one-year operating life of the SPVD, the duration of high temperatures to which the battery will be exposed will be as follows:

<u>Temperature °F</u>	<u>Hours</u>	<u>Cumulative Hours</u>
130	8	8
125	20	28
120	90	118
115	120	238
110	160	398
105	190	588
100	230	818

This adds up to slightly more than one month above 100°F. As a conservative estimate, the loss caused by one month at 113°F (10% loss for both the E95 and No. 609) can be used to calculate the required battery capacity.

If we assume that a battery may be stored at 70°F for one year and then operated one year in the SPVD, the service life expected, as a percentage of the fresh battery capacity, will be:

E95	95 x 90 = 85.5%
No. 609	90 x 90 = 81%

Battery Test Results

The following subparagraphs describes battery tests conducted in November of 1973 by Honeywell's Development and Evaluation Laboratory.

Units Tested

Three Alkaline "D" cells and three heavy duty six volt LeClanche batteries manufactured by Union Carbide Corp.

Three Alkaline "D" cells and two lithium "D" cells manufactured by Mallory.

Three Alkaline "D" cells manufactured by Ray-O-Vac.

Object of Test

Determine capability of batteries to sustain pulse loads at temperature extremes. Test at temperature range of -30°F to +160°F.

Documentation

The following listed data was taken during the test.

1. Battery Identification.
2. First Data: No Battery Capacity Removed.
3. Data Taken After 0.8 Ampere Hours Removed.
4. Data Taken After 1.5 Ampere Hours Removed.
5. Data Taken After Approximately 8.0 Ampere Hours Removed.
6. Data Taken During Battery Capacity Removal.
7. Battery Load Device With Traffic Simulator Timer.

Procedure

Performance tests were conducted on the batteries previously listed by applying a 500 microampere continuous load to the battery being tested and also applying pulse loads which would simulate traffic. These pulse loads were 35, 30, and 20 milliamperes. The traffic simulator applied the load for a 10 millisecond duration. The sequence of these pulses allowe a 250 msec. delay between the first and second pulse and a delay of one second between the second and third pulse. This sequence was continued for up to three minutes in some instances which simulated traffic over the SPVD traveling at about 60 miles per hour.

Each of the batteries was tested at the following temperatures: -30°F, -20°F, -10°F, 0°F, room temperature, +120°F and 140°F. A temperature test was also planned at 160°F and shortly after the temperature chamber was set to condition the batteries at this temperature, battery number 10, a Lithium cell, blew its safety vent plug. Sulphur dioxide depolarizer and some liquid electrolyte was released into the environmental chamber. The 160°F test was immediately abandoned.

After these initial tests, battery capacity was reduced in increments shown in Table 9 of Documentation. Load data was taken at several stages in the capacity removal phase. Voltages were so similar on the "D" cells that they were averaged when recording the capacity removal data.

The second Lithium battery started leaking gas although the safety vent plug did not eject. This battery was removed from test at this time.

Battery capacity was removed at room temperature in all instances and at the rates shown in Tables 10 through 14 of Documentation. Capacity was removed until the battery voltages were at 1.2 volts per cell during 35 milliamp pulse loads and conditioned at -20°F.

The test was complete at this time as 1.2 volts per cell, under simulated load, and at -20°F is the minimum acceptable performance from its power source by the SPVD.

Table 9. Battery identification

Battery Number	Manufacturer	Description
1	Union Carbide	Alkaline "D" Cell
2	Union Carbide	Alkaline "D" Cell
3	Union Carbide	Alkaline "D" Cell
4	Ray-O-Vac	Alkaline "D" Cell
5	Ray-O-Vac	Alkaline "D" Cell
6	Ray-O-Vac	Alkaline "D" Cell
7	Mallory	Alkaline "D" Cell
8	Mallory	Alkaline "D" Cell
9	Mallory	Alkaline "D" Cell
10	Mallory	Lithium Cell
11	Mallory	Lithium Cell
12	Union Carbide	Heavy Duty LeClanche Lantern
13	Union Carbide	Heavy Duty LeClanche Lantern
14	Union Carbide	Heavy Duty LeClanche Lantern

Table 10. First data: no battery capacity removed

Temperature	Battery Number	Load Current			Load Current			Load Current		
		No-Load E	Pulse E	Pulse I	No-Load E	Pulse E	Pulse I	No-Load E	Pulse E	Pulse I
-30 F	1	1.57	1.54	35 ma	1.57	1.52	32 ma	1.57	1.53	20 ma
	2	1.53	1.47	35 ma	1.53	1.48	32 ma	1.53	1.50	20 ma
	3	1.53	1.48	35 ma	1.53	1.49	32 ma	1.53	1.50	20 ma
	4	1.58	1.53	35 ma	1.58	1.54	32 ma	1.58	1.55	20 ma
	5	1.53	1.48	35 ma	1.53	1.48	32 ma	1.53	1.50	19 ma
	6	1.53	1.48	35 ma	1.53	1.48	32 ma	1.53	1.50	20 ma
	7	1.58	1.55	35 ma	1.58	1.55	32 ma	1.58	1.57	20 ma
	8	1.52	1.48	35 ma	1.52	1.49	30 ma	1.52	1.50	19 ma
	9	1.53	1.49	35 ma	1.53	1.50	31 ma	1.53	1.50	19 ma
	10	2.60	1.94	34 ma	2.70	2.15	30 ma	2.65	2.24	15 ma
	11	2.60	1.95	35 ma	2.60	2.00	27 ma	2.60	2.17	15 ma
	12	6.45	4.10	35 ma	6.45	4.50	30 ma	6.45	5.25	19 ma
	13	6.50	4.10	33 ma	6.50	4.50	30 ma	6.50	5.28	18 ma
	14	6.30	3.90	35 ma	6.30	4.42	28 ma	6.32	5.14	16 ma
-20 F	1	1.57	1.53	35 ma	1.57	1.54	31 ma	1.57	1.55	19 ma
	2	1.58	1.53	35 ma	1.58	1.54	33 ma	1.58	1.56	20 ma
	3	1.58	1.54	35 ma	1.58	1.55	33 ma	1.58	1.56	20 ma
	4	1.58	1.54	35 ma	1.58	1.55	33 ma	1.58	1.56	20 ma
	5	1.58	1.55	35 ma	1.58	1.55	33 ma	1.58	1.57	20 ma
	6	1.58	1.55	35 ma	1.58	1.55	32 ma	1.58	1.57	20 ma
	7	1.58	1.56	35 ma	1.58	1.56	32 ma	1.58	1.57	20 ma
	8	1.58	1.55	35 ma	1.58	1.56	32 ma	1.58	1.57	20 ma
	9	1.58	1.55	35 ma	1.58	1.56	32 ma	1.58	1.57	20 ma
	10	2.76	2.15	35 ma	2.76	2.25	28 ma	2.75	2.35	17 ma
	11	2.76	2.20	35 ma	2.76	2.25	30 ma	2.76	2.35	16 ma
	12	6.50	5.70	40 ma	6.50	5.80	35 ma	6.50	6.10	20 ma
	13	6.50	5.72	40 ma	6.50	5.80	34 ma	6.50	6.10	20 ma
	14	6.40	5.60	40 ma	6.40	5.70	35 ma	6.40	6.00	20 ma
-10 F	1	1.55	1.51	35 ma	1.55	1.52	32 ma	1.55	1.53	20 ma
	2	1.55	1.51	35 ma	1.55	1.52	32 ma	1.55	1.52	20 ma
	3	1.55	1.51	35 ma	1.55	1.51	32 ma	1.55	1.52	20 ma
	4	1.54	1.50	35 ma	1.54	1.51	32 ma	1.54	1.52	20 ma
	5	1.54	1.51	35 ma	1.54	1.51	32 ma	1.54	1.52	20 ma
	6	1.54	1.51	35 ma	1.54	1.52	32 ma	1.54	1.52	20 ma
	7	1.53	1.52	35 ma	1.53	1.52	33 ma	1.53	1.52	20 ma
	8	1.53	1.51	35 ma	1.53	1.51	33 ma	1.53	1.52	20 ma
	9	1.53	1.51	35 ma	1.53	1.52	32 ma	1.53	1.52	20 ma
	10	2.76	2.18	36 ma	2.75	2.21	28 ma	2.75	2.34	20 ma
	11	2.76	2.20	36 ma	2.76	2.26	29 ma	2.76	2.38	20 ma
	12	6.60	6.14	43 ma	6.60	6.20	35 ma	6.60	6.36	21 ma
	13	6.60	6.20	43 ma	6.60	6.24	35 ma	6.60	6.38	22 ma
	14	6.50	6.06	43 ma	6.50	6.10	35 ma	6.50	6.28	21 ma
0 F	1	1.57	1.54	35 ma	1.57	1.53	31 ma	1.57	1.55	20 ma
	2	1.57	1.53	35 ma	1.57	1.54	32 ma	1.57	1.55	20 ma
	3	1.57	1.53	35 ma	1.57	1.54	33 ma	1.57	1.55	20 ma
	4	1.57	1.53	35 ma	1.57	1.54	32 ma	1.57	1.55	19 ma
	5	1.57	1.54	35 ma	1.57	1.54	32 ma	1.57	1.55	20 ma
	6	1.57	1.54	35 ma	1.57	1.54	33 ma	1.57	1.55	20 ma
	7	1.57	1.54	35 ma	1.57	1.55	33 ma	1.57	1.56	20 ma
	8	1.56	1.54	35 ma	1.56	1.55	33 ma	1.56	1.55	19 ma
	9	1.57	1.54	35 ma	1.56	1.54	34 ma	1.57	1.56	19 ma
	10	2.80	2.21	34 ma	2.80	2.30	30 ma	2.80	2.40	18 ma
	11	2.84	2.36	35 ma	2.84	2.36	30 ma	2.84	2.48	19 ma
	12	6.64	6.30	43 ma	6.64	6.36	35 ma	6.64	6.44	22 ma
	13	6.64	6.24	43 ma	6.64	6.32	35 ma	6.64	6.44	22 ma
	14	6.50	6.20	43 ma	6.50	6.20	36 ma	6.50	6.32	22 ma

Table 10. First data no battery capacity removed (continued)

Temperature	Battery Number	Load Current			Load Current			Load Current		
		No-Load E	Pulse E	Pulse I	No-Load E	Pulse E	Pulse I	No-Load E	Pulse E	Pulse I
Room Temp.	1	1.55	1.53	36 ma	1.55	1.54	33 ma	1.55	1.54	20 ma
	2	1.54	1.53	36 ma	1.54	1.53	33 ma	1.54	1.53	20 ma
	3	1.55	1.53	35 ma	1.55	1.53	33 ma	1.55	1.54	20 ma
	4	1.53	1.52	35 ma	1.53	1.52	32 ma	1.53	1.53	20 ma
	5	1.54	1.52	35 ma	1.54	1.53	33 ma	1.54	1.53	20 ma
	6	1.54	1.52	35 ma	1.54	1.53	34 ma	1.54	1.53	20 ma
	7	1.53	1.52	36 ma	1.53	1.52	33 ma	1.53	1.52	20 ma
	8	1.53	1.51	36 ma	1.53	1.52	32 ma	1.53	1.52	20 ma
	9	1.53	1.52	36 ma	1.53	1.52	32 ma	1.53	1.52	20 ma
	10	2.92	2.66	37 ma	2.92	2.70	32 ma	2.92	2.77	20 ma
	11	2.94	2.81	37 ma	2.94	2.82	33 ma	2.94	2.86	20 ma
	12	6.62	6.42	42 ma	6.62	6.46	36 ma	6.62	6.52	22 ma
	13	6.62	6.42	42 ma	6.62	6.46	36 ma	6.62	6.54	22 ma
	14	6.50	6.34	42 ma	6.50	6.34	36 ma	6.50	6.42	22 ma
+120°F	1	1.52	1.51	30 ma	1.52	1.51	27 ma	1.52	1.52	15 ma
	2	1.53	1.51	30 ma	1.53	1.52	26 ma	1.53	1.52	16 ma
	3	1.53	1.52	31 ma	1.53	1.52	28 ma	1.53	1.52	15 ma
	4	1.53	1.52	30 ma	1.53	1.52	29 ma	1.53	1.52	17 ma
	5	1.53	1.51	31 ma	1.53	1.52	29 ma	1.53	1.52	17 ma
	6	1.52	1.51	31 ma	1.53	1.52	30 ma	1.53	1.52	17 ma
	7	1.52	1.51	31 ma	1.52	1.51	29 ma	1.52	1.51	17 ma
	8	1.52	1.51	32 ma	1.52	1.51	29 ma	1.52	1.51	17 ma
	9	1.51	1.50	31 ma	1.51	1.50	29 ma	1.52	1.51	17 ma
	10	2.96	2.89	37 ma	2.95	2.90	34 ma	2.94	2.90	20 ma
	11	2.94	2.89	38 ma	2.93	2.90	34 ma	2.92	2.90	20 ma
	12	6.70	6.61	42 ma	6.70	6.62	38 ma	6.71	6.66	21 ma
	13	6.70	6.37	41 ma	6.70	6.61	36 ma	6.70	6.66	21 ma
	14	6.61	6.52	42 ma	6.61	6.53	36 ma	6.61	6.59	21 ma
+140°F	1	1.54	1.53	35 ma	1.54	1.53	34 ma	1.54	1.54	20 ma
	2	1.53	1.52	36 ma	1.53	1.52	34 ma	1.53	1.52	19 ma
	3	1.53	1.51	37 ma	1.53	1.52	34 ma	1.53	1.52	20 ma
	4	1.55	1.53	33 ma	1.55	1.53	32 ma	1.55	1.54	19 ma
	5	1.55	1.53	35 ma	1.55	1.54	32 ma	1.55	1.54	18 ma
	6	1.55	1.53	33 ma	1.55	1.53	32 ma	1.55	1.54	19 ma
	7	1.54	1.52	35 ma	1.54	1.53	32 ma	1.54	1.53	19 ma
	8	1.54	1.52	35 ma	1.53	1.52	32 ma	1.53	1.52	19 ma
	9	1.53	1.52	35 ma	1.53	1.52	32 ma	1.53	1.53	19 ma
	10	2.90	2.85	36 ma	2.90	2.88	33 ma	2.90	2.89	20 ma
	11	2.90	2.88	38 ma	2.90	2.89	35 ma	2.90	2.89	20 ma
	12	6.80	6.72	43 ma	6.80	6.74	39 ma	6.80	6.76	21 ma
	13	6.80	6.70	44 ma	6.80	6.74	38 ma	6.80	6.78	24 ma
	14	6.70	6.64	44 ma	6.70	6.68	38 ma	6.70	6.69	24 ma

Table 11. Data taken after 0.8 ampere hours discharging at 0.400 A/Hr. rate

Temperature	Battery Number	Load Current			Load Current			Load Current		
		No-Load E	Pulse E	Pulse I	No-Load E	Pulse E	Pulse I	No-Load E	Pulse E	Pulse I
-30°F	5	1.35	1.31	35 ma						
-30°F	8	1.35	1.32	35 ma	1.35	1.32	30 ma			
-30°F	13	5.75	5.55	35 ma	5.75	5.65	35 ma	5.86	5.8	20 ma
-30°F	11	2.66	1.97	35 ma	Note: 0.042 ampere-hours was removed from this cell previous to this data. Discharge rate was 500 microamperes and time was 84 hours.					

Table 12. Data taken after 1.5 ampere hours removed at 0.4 a/Hr rate

Temperature	Battery Number	Load Current			Load Current			Load Current		
		No-Load E	Pulse E	Pulse I	No-Load E	Pulse E	Pulse I	No-Load E	Pulse E	Pulse I
-30°F	2	1.4	1.38	35 ma	1.39	1.35	28 ma	No Test		
	2	1.4	1.35	35 ma	1.39	1.35	28 ma			
		After 3 minute test			After 3 minute test					
	5	1.41	1.35	35 ma	1.41	1.36	28 ma	1.41	1.39	15 ma
	5	1.40	1.31	33 ma	1.41	1.36	28 ma	1.42	1.37	15 ma
		After 3 minute test			After 3 minute test			After 3 minute test		
	8	1.42	1.36	33 ma	1.43	1.37	28 ma	1.41	1.38	15 ma
	8	1.41	1.35	33 ma	1.42	1.37	28 ma	1.42	1.39	15 ma
		After 3 minute test			After 3 minute test			After 3 minute test		
	13	5.85	5.72	40 ma	5.85	5.75	35 ma	5.82	5.7	18 ma
	13	5.80	5.65	40 ma	5.80	5.70	35 ma	5.75	5.7	18 ma
		After 3 minute test			After 3 minute test			After 3 minute test		

Table 13. Data taken after = 8.0 ampere hours removed

Temperature	Battery Number	Load Current		
		No-Load E	Pulse E	Pulse I
-20°F	3	1.275V	1.24V	35 ma
	6	1.27V	1.24V	33 ma
	9	1.27V	1.24V	33 ma
	14	5.4V	5.25V	40 ma

Table 14. Data taken during battery capacity removal

Battery Number	Hours Load "ON"	Voltage Start	Voltage Stop	Average Voltage	Load (ohms)	Average Current	Ampere Hours	Total Ampere Hours
2, 5, 8	2.0	1.31V	1.19V	1.25V	3.0	0.417A	0.834	7.296
	0.3	1.3	1.3	1.3	3.0	0.432A	0.132	
	1.4	1.143	1.13	1.134	3.0	0.38A	0.53	
	17.5	1.036	0.96	0.998	3.0	0.33A	5.8	
13	2.0	5.95	5.3	5.62	13.2	0.425A	0.850	7.082
	0.3	5.81	5.8	5.8	13.2	0.44A	0.132	
	1.4	5.167	4.924	5.045	13.2	0.381A	0.53	
	14.2	4.62	2.931	3.775	13.2	0.393A	5.57	
3, 6, 9	3.5	1.2	1.0	1.15	1.8	0.64A	2.24	8.27
	1.7	0.672	0.979	0.825	1.8	0.46A	0.78	
	2.5	1.08	0.95	1.017	1.8	0.565A	1.41	
	1.5	0.652	0.924	0.788	1.8	0.435A	0.65	
	1.3	0.978	0.929	0.953	1.8	0.530A	0.69	
	2.4	0.950	0.891	0.921	1.8	0.51A	1.23	
	1.3	0.861	0.871	0.866	1.8	0.48A	0.63	
	1.1	0.927	0.839	0.883	1.8	0.49A	0.54	
14	3.5	5.65	4.75	5.2	13.2	0.387A	1.27	6.705
	1.7	4.764	4.548	4.656	13.2	0.354A	0.60	
	2.5	5.105	4.492	4.8	13.2	0.364A	0.91	
	1.5	4.407	4.32	4.363	13.2	0.330A	0.50	
	1.5	4.792	4.639	4.715	13.2	0.36A	0.54	
	2.1	4.509	3.724	4.116	7.35	0.56A	1.175	
	1.5	3.583	3.267	3.425	7.35	0.465A	0.7	
	2.5	2.944	2.738	2.841	7.35	0.405A	1.01	

SPVD Power Source Analysis – Transmitter Current Increases

During the course of the SPVD RF Link design, two increases in the transmitter power requirements took place. The first increase was lengthening the transmitter pulse from 10 milliseconds to 30 milliseconds. In the above estimates of required battery capacity used in the lifetime tests, the transmitter pulse was assumed to be 35 milliamperes for 10 milliseconds and the total ampere-hours required was calculated to be 4.44. With the transmitter pulse duration increased to 30 milliseconds, the required capacity will be increased by 2.84 ampere-hours to a total of 7.28 ampere-hours. To compensate for the battery self-discharge losses, the fresh battery capacity required will be:

$$\text{E95} \quad \frac{7.28}{0.855} = 8.5 \text{ ampere-hours}$$

$$\text{No. 609} \quad \frac{7.28}{0.81} = 9.0 \text{ ampere-hours}$$

These estimates are conservative since the transmitter pulse current will actually decrease as the battery voltage decreases. It is also considered, based upon the demonstrated ability of the batteries to maintain their voltage level during a continuous three-minute sequence of simulated traffic, that increasing the pulse duration from 10 milliseconds to 30 milliseconds will not cause any significant voltage drop below these values previously measured.

The second increase in transmitter power requirements was an increase in current from 35 microamperes to the present value of 45 microamperes. There are two factors to be considered:

- The increase in battery capacity needed
- The effect of voltage drop during the pulse load.

The previous estimated ampere-hours required for the transmitter pulse load was 35 microampere x 40.5 hours per year = 1.42 ampere-hours. With the new load, this will be 45 microamperes x 40.5 hours per year = 1.82 ampere-hours.

The total battery capacity required for one year of operation is increased from 7.28 ampere-hours to 7.68 ampere-hours. When this is adjusted to compensate for battery internal losses in storage, a fresh alkaline cell should have a capacity of $7.68/0.855 = 9.0$ ampere-hours and a fresh lantern battery should have $7.68/0.81 = 9.5$ ampere-hours. These values are still within the estimated capacities of 12 ampere-hours for the alkaline cell and 13.5 ampere-hours for the lantern battery based upon our tests and extrapolation of the data obtained.

In regard to the voltage drop under the pulse load, the worst condition would occur at low temperature (Table 15).

Table 15. Test data at -20°F

		Voltage		
		Under Continuous Load	Under Pulse Load	Pulse Current (mA)
Alkaline Cells	Fresh Cell	1.58V	1.55V	35
	After 0.8 A-hr Removed (-30°F)	1.35	1.32	35
	After 8.0 A-hr Removed	1.27	1.24	33
Lantern Battery	Fresh Battery	6.47	5.67	40
	After 0.8 A-hr Removed (-30°F)	5.75	5.55	35
	After 8.0 A-hr Removed	5.40	5.25	40

Assuming that the internal resistance of the battery does not change, the increased pulse load would cause a further drop in battery voltage of about the following magnitudes:

	<u>Additional Voltage Drop (Volt)</u>
Alkaline Cell	.01
Lantern Battery - Fresh	.10
Lantern Battery - Used	.02

These changes will have an insignificant effect on operation and on battery capacity available to the minimum voltage level.

In the accelerated battery discharge life test described in Appendix A, the discharge was taken beyond the 5.0 ampere-hour estimated requirement at that time to 8.17 ampere-hours for the E95 and 6.7 ampere-hours for the No. 609. At that point in the battery life, it was still above the minimum required voltage (1.2 volts per cell). By plotting the operating voltage versus the ampere-hours discharged from the battery, and extrapolating to the 1.2 volts per cell level, it appears that a fresh E95 should be capable of delivering about 12 ampere-hours and a fresh No. 609 about 13.5 ampere-hours under the type of loading applied in the SPVD. It is therefore, concluded that both of these batteries are still appropriate for use as the SPVD power source.

APPENDIX B
SPVD TRANSMITTER FREQUENCY TRADEOFF ANALYSIS

Introduction

In conjunction with the experimental effort, a great deal of analysis and literature study was devoted to defining the optimum antenna combination for the SPVD. Semeingly conflicting analysis of buried antennas may be found in the literature. This stems from the complexity of the analytical solution, which requires simplifying assumptions that are valid only for a particular set of conditions. For example, the relationship between conductivity of the surrounding medium (σ), its dielectric constant (ϵ), and the transmission frequency ($\omega = 2\pi f$) is often taken to be $\sigma \gg \omega \epsilon$ in buried-antenna calculations. The converse is true, however, for typical soils and roadway materials at frequencies above 30 MHz.

Antenna Efficiency

If the antenna is electrically small, its radiation power factor is proportional to the cube of the frequency. This radiation power factor, defined as the radiation resistance of the antenna divided by its reactance, can be converted to efficiency by multiplying the circuit Q. In free space, the circuit Q could conceivably be made very high. The radiation resistance of a small loop can be calculated from

$$R_R = 3.12 \times 10^{+4} N^2 \left(\frac{A}{\lambda^2} \right)^2 \quad (\text{Eq. 1})$$

where:

- N = Number of loop turns
- A = Loop's area
- λ = Operating wavelength⁵

The loss resistance in the antenna and the associated external circuit used to tune out its reactance and match it to the transmitter is given by

$$R_L = \frac{X}{Q} \quad (\text{Eq. 2})$$

where:

- X = Antenna reactance

⁵ F. E. Ferman, Radio Engineers Handbook,

We are assuming that the antenna is electrically very small and that the radiation resistance is a negligible fraction of the total circuit resistance.

Predicted free-space radiation efficiencies for antennas enclosed in a three-inch diameter, six-inch long container are very low; on the order of 0.01 percent at 10 MHz even with a circuit Q of 1000. This value does not include the effect of the electronics and batteries within the container, which would further reduce the radiation resistance and increase the circuit losses. A buried magnetic dipole (loop) antenna can have a Q on the order of 100 or less, depending upon the loop size and the properties of the surrounding medium. (Measurements made by Honeywell on loops inserted in the asphalt and concrete test holes show Q's on the order of 100. We have used this value in our calculations.) The reactance of the loop is proportional to the square of the number of turns, but the Q of a buried loop is not affected by N. Thus, the circuit losses and the radiation resistance are both proportional to N². The antenna efficiency, η , given by the ratio R_R/R_L , is independent of N.

For example, suppose we use a one-turn, four-inch square loop with Q = 100, as the basis for a radiation efficiency calculation. This loop has a measured inductance of 0.45 microhenry. Using Eq. 2 we find the loss resistance to be

$$R_L = \frac{2\pi fL}{Q} = \frac{X}{Q} \tag{Eq. 3}$$

$$= \frac{2\pi \times 30 \times 10^6 \times 0.45 \times 10^{-6}}{100}$$

$$R_L = 0.84 \text{ ohm.}$$

Eq. 1, in turn, yields a radiation resistance of

$$R_R = 3.12 \times 10^4 \times (1)^2 \times \frac{4 \times 4 \times .0254 \times .0254}{10^2}^2$$

$$R_R = 3.22 \times 10^{-4} \text{ ohms}$$

where:

A and λ are in units of meters.

Now, since antenna efficiency, η , is the ratio of radiated power to total antenna power, we get

$$P_{\text{rad}} = i^2 R_R \text{ and} \tag{Eq. 4}$$

$$P_{\text{total}} = i^2 (R_R + R_L) \quad (\text{Eq. 5})$$

$$\eta = \frac{P_{\text{rad}}}{P_{\text{total}}} = \frac{i^2 R_R}{i^2 (R_R + R_L)} \quad (\text{Eq. 6})$$

$$\eta = \frac{R_R}{R_R + R_L} .$$

But in our example, $R_L \gg R_R$. Therefore

$$\eta \approx \frac{R_R}{R_L} = \frac{3.32 \times 10^{-4}}{0.84} \quad (\text{Eq. 7})$$

$$\eta \approx 3.84 \times 10^{-4}$$

At UHF, the dimensions of the antenna are comparable to one-half wavelength and the free-space radiation efficiency could approach 100 percent. However, when buried in a lossy medium, the antenna efficiency will be substantially reduced. We have not made a direct calculation of the efficiency of a buried half-wave antenna and the literature references which are applicable to the SPVD environment do not present calculations from which the antenna efficiency can be readily extracted. A very liberal estimate of efficiency for a buried UHF dipole is 50 percent.

Burial Factor

Electromagnetic waves are attenuated exponentially in propagating through a lossy medium. Because of the shallow burial depths of the SPVD antenna, this factor is not significant at frequencies up to 30 MHz. It becomes quite large at UHF if the dielectric constant and loss tangent of the roadway medium are high.

The burial loss in nepers per meter is obtained by calculating the real part of the propagation constant:

$$R_e [\gamma \omega (\epsilon^* \mu^*)^{1/2}] \quad (\text{Eq. 8})$$

which can be written as

$$R_e \left[j \frac{2\pi}{\lambda_0} (\epsilon_g)^{1/2} (1 - j \tan \delta)^{1/2} \right]^{(2)} \quad (\text{Eq. 9})$$

when

$$\mu^* = \mu_0^{*(2)} \quad (\text{Eq. 10})$$

in which ϵ_g is the relative permittivity of the ground and $\tan \delta$ is its loss tangent. Multiplying by $8.69d$ (d = burial depth) gives the attenuation in dB. Except for the computational procedure, in which we considered only the attenuation term and neglected the phase factor, we used the same burial correction as the Biggs and Swarm burial factor.⁶ The expression is often written in other ways, but this formulation is convenient to use at frequencies above 10^6 Hz, where the relative dielectric constant (ϵ_g) and loss tangent ($\tan \delta$) of typical dielectric materials remain relatively constant with frequency⁷. It should be noted that a completely different answer is obtained if the propagation constant is calculated with the assumption of constant conductivity of (σ). With the highest anticipated values for ϵ_g and $\tan \delta$ ($\epsilon_g = 20$, $\tan \delta = 1$), the attenuation at 450 MHz is 19 nepers/meter = 165 decibels/meter. The burial factor at 0.1 meter is then 16.5 decibels.

There is one significant difference between our calculation and those in the Sylvania report, in that they apparently assumed a conductivity σ which was independent of frequency, whereas for most engineering materials at frequencies between one MHz and one GHz, the quantity

$$\tan \delta = \frac{\sigma}{\omega \epsilon} \quad (\text{Eq. 11})$$

is approximately constant. We used $\epsilon_g = 20$, $\tan \delta = 1$ as the anticipated highest values of dielectric constant and loss tangent for asphalt or concrete.

In a low-loss medium, an electrical dipole has a higher theoretical efficiency than a magnetic loop. However, the electric dipole antenna will be subject to detuning effects due to changes in the dielectric constant of the surrounding medium.

⁶ Sylvania Report FHWA-RD-72-11, Appendix B.

⁷ Von Hippel, A. R., Dielectric Materials and Applications, Wiley, New York, 1954.

Impedance measurements on magnetic loop antennas inserted in core holes verify that the reactance and loss terms are not significantly different from the free-space values. As anticipated, the electric dipole antennas undergo reactance changes greater than a factor of two, with a severe increase in loss when installed in concrete or bituminous surfaces. Published data on electrical properties of asphalt and concrete have been obtained for use in establishing ground-wave propagation parameters. The extremes in dielectric constant and conductivity vary from $\epsilon = 3$, $\sigma = 10^{-9}$ mhos/meter for very dry samples to $\epsilon = 15$, $\sigma = 10^{-2}$ for samples with high moisture content. These values can be used to estimate the amount of antenna detuning caused by the surrounding medium.

Horizontal electric or magnetic dipoles may both be used as buried transmitting antennas. Some analyses reject the vertical electric dipole, but they may not apply in the SPVD environment. A vertical magnetic dipole is an ineffective surface-wave antenna.

When the antenna dimensions are a small fraction of the free-space wavelength (λ_0), the electric fields in the vicinity of an electric dipole result in large losses if the antenna is filled with, or surrounded by, a lossy dielectric. This has been pointed out by Galejs⁸ and by Row⁹. For larger antennas, however, the electric dipole is superior to the magnetic dipole. Within the size constraints of the SPVD, the magnetic dipole offers better radiation efficiency at frequencies below about 150 MHz. The "loop" is also virtually immune to detuning effects caused by changes in the dielectric properties of the roadway medium. In contrast, the impedance of a small electric dipole is strongly affected by the surrounding medium, and some form of "autotune" circuit would be a virtual necessity. A vertically polarized electric-field vector dominates in groundwave radio-frequency propagation. Thus, the receiving antenna should be a vertical electric or horizontal magnetic dipole. A vertical electric-field dipole is omnidirectional and simple in construction, making it the preferred choice for an above-ground antenna.

⁸ Galejs, J., "Small Electric and Magnetic Antennas with Cores of a Lossy Dielectric," J. Research National Bureau of Standards 67D, p. 445, July-August 1963.

⁹ Row, R. V., "Radiation Efficiency of Electric and Magnetic Dipole Antennas Surrounded by a Small Spherical Shell of Lossy Dielectric," IEEE Trans. Antennas and Propagation, AP-12, p. 646, September 1964.

Propagation Loss

Norton's equations¹⁰

$$E_{su}^{mh} = ik \frac{e^{i(kR-wt)}}{R} \left\{ \cos \phi (1-R_v) F \left[\cos \psi \left(1 + \frac{\sin^2 \psi}{2} \right) k + \right. \right. \quad (\text{Eq. 12}) \\ \left. \left. u \sqrt{1 - u^2 \cos^2 \psi} r \right] + \sin \phi \frac{\sqrt{1 - u^2 \cos^2 \psi}}{u} (1 + R_h) G_\phi \right\}$$

were used to calculate the groundwave propagation loss between points at 10 meters and 150 meters from the transmitter, over the frequency range of 1 MHz to 100 MHz. These points are plotted in Figure 43 for three soil conditions ranging from very high conductivity to very low conductivity. The curves of path loss are bounded by lines representing losses proportional to $1/R$ and $1/R^2$. Measure values of path loss, obtained over an unobstructed path in the bituminous-surfaced parking lot, are also plotted in Figure 43. Using the relative path loss between 10 meters and 150 meters avoids the near-field region. It also removes the uncertainty in transmitter power which exists because of the difficulty in measuring the antenna power in the buried, self-contained transmitter.

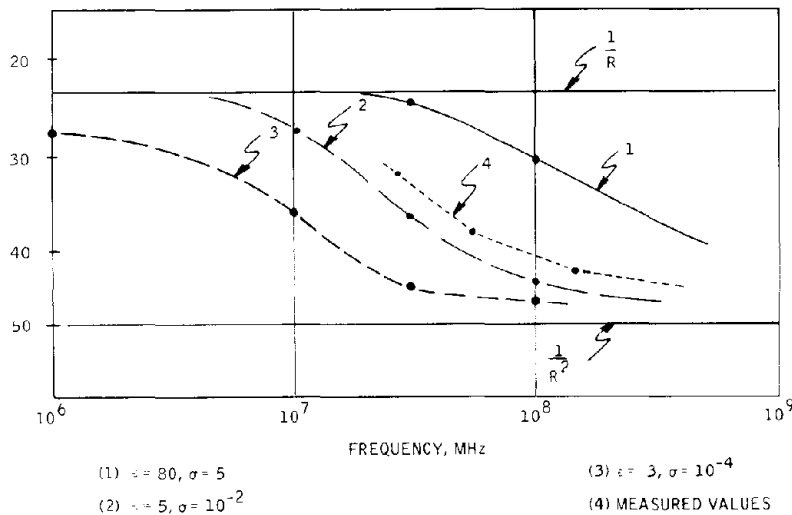


Figure 43. Groundwave propagation losses

¹⁰Norton, K. A., "The Physical Reality of Space and Surface Waves in the Radiation of Radio Antennas," Proc. IRE 25, p. 1192, September 1937.

A difference of about 7 db was noted in path loss measurements made at 420 MHz on vertical and horizontal dipole antennas. (The vertical dipole antenna had a lower measured path loss.) The average of these two measurements was used in extending the curve drawn through the experimental points obtained at 27, 54 and 146 MHz. This curve parallels the calculated curve for $\epsilon = 10$, $\sigma = 10^{-2}$. The increased propagation loss at higher frequencies partially offsets the improvement in antenna radiation efficiency.

D-C to R-F Conversion Efficiency

In present-day commercial communication equipment, the overall transmitter efficiency is nearly 70 percent in the 30 to 50 MHz range, but drops to 20 to 30 percent in the UHF range because of lower device efficiencies and the need for several multiplier stages.

Ambient Noise

Our measurements of impulse noise showed little variation in noise field intensity between 10 and 200 MHz. In a recent survey paper on metropolitan noise, Skomal¹¹ presents sets of data which show both increasing and decreasing noise intensity with frequency in the UHF range. He cites data which show a peak in automotive ignition noise between 350 and 600 MHz, attributable to resonances in ignition wires. Extensive traffic noise data taken in the Washington, D.C.¹² area do not show a pronounced difference in noise at 50, 150 and 450 MHz when the received noise is corrected for the antenna factor.

Radio-frequency noise measurements in the 2 to 200 MHz range were conducted at two urban locations. Both receiving sites were in industrial areas and within 300 feet of a major roadway. Below 10 MHz, the major noise sources were power-line operated equipment. At higher frequencies, noise impulses from automobile ignition systems were dominant. Peak noise impulses observed in a two-minute interval were generally between 20 and 30 db above one microvolt per meter per KHz. We chose the peak impulse measurement technique because it is directly applicable to detection probability calculations for pulsed r-f transmission. Published data are usually given in terms of "average" or "quasi-peak" field intensities. The difference in measurement technique, and the broadband

¹¹ Skomal, E. N., "An Analysis of Metropolitan Incidental Radio Noise Data," IEEE Trans. Electromagnetic Compatibility, EMC-15, p. 45, May 1973.
¹² Dietz et al, "Man-Made Noise," Report to FCC Technical Committee of the Advisory Committee for Land Mobile Radio Services, June 1966.

nature of the noise sources which dominated our measurements account for the apparent disagreement with published data. On the basis of the available data, we conclude that although vehicular noise is a very important factor in the communication link design, it does not have a strong influence on the selection of operating frequency.

Bandwidth

Because of frequency-stability limitations, the minimum receiver pre-detection bandwidth increases linearly with frequency. In an ideal detector, the output signal-to-noise ratio is determined by the post-detection bandwidth (B_2) and is independent of the predetection bandwidth (B_1). For a non-coherent detector, such as an envelope detector or f-m discriminator operating with very low input carrier-to-noise ratios, the noise bandwidth is approximated by $(B_1 B_2)^{1/2}$. Thus, the input signal power must be increased as $(B_1)^{1/2}$ for constant output signal-to-noise ratio.

Blockage and Multipath Effects

Our 27 MHz data shows that a vehicle directly over the sensor can produce a signal null as great as 20 db. However, at this frequency, the nulls do not occur at a position where the transmitter would be activated. Experiments at 146 MHz also show nulls of approximately 20 db. The major difference is that the null pattern is more complex at shorter wavelengths, and several nulls are observed during the passage of an average-size automobile. Thus, there is a greater probability that the null will occur at the position where the transmitter is keyed by the magnetometer.

Experimental Verifications

A preliminary propagation experiment was conducted with a 10 MHz transmitter installed in an existing core hole in the I-35W test location. Through the cooperation of the Minnesota Highway Department, a test site was made available for propagation measurements from a reinforced concrete roadway. The test location was an unopened section of Interstate 35W adjacent to the Honeywell Stinson/Ridgway plant. Propagation tests on transmitters buried in a bituminous-surfaced roadway were conducted on Honeywell property. The test units were packaged in three-inch ID, one-eighth-inch wall containers, which fit in the hole produced by a three-inch core drill. Batteries and a pulse keyer were contained in the same package. The test transmitter had a peak power input of 100 milliwatts. Pulse operation was provided with selectable 10-millisecond and 100-millisecond "on" time and a 10-percent duty cycle. Quantitative signal-to-noise measurements were not completed, but the pulsed signals were clearly audible in a battery-powered receiver 500 feet away with 100 mw of transmitter input power.

Propagation measurements were also made at 2, 9 and 27 MHz using self-contained 100-milliwatt transmitters with magnetic dipole antennas. The transmitters were installed in 4.25-inch diameter core holes in bituminous and reinforced concrete surfaces. Preliminary measurements were also made with a 27 MHz electric dipole antenna.

As expected, radiation efficiency increases rapidly with increasing frequency. Soil attenuation is still not a strong influence at 27 MHz because the burial depth is small compared to the penetration depth for electro-magnetic waves in the medium. The received signal strength at 27 MHz changes less than 6 db when the transmitter is lowered from the surface into the core hole, even in steel reinforced concrete. These results were observed with magnetic dipole antennas with no retuning after installation in the holes. An electric dipole antenna, tested at 27 MHz, proved to be considerably less effective when installed in the core hole. This may have been partially due to improper impedance matching.

Antenna efficiency at two MHz was found to be too low for reliable communication at 500 feet with 100 mw input power. At nine MHz, the signal-to-noise ratio (with 100 mw input power) is acceptable during daytime conditions on a "quiet" frequency. However, spectrum occupancy is extremely heavy in this region.

Signal-to-noise ratios of 20+ db were obtained with buried 27 MHz transmitters at ranges in excess of 500 feet. The wavelength (11 meters) is short enough so that an average size vehicle is approximately one-half wavelength long. Under certain conditions, the presence of a vehicle produced large variations in signal strength. A sharp null was observed when the test vehicle (Ford station wagon) was approximately centered over the transmitter and traveling directly toward the receiver. The electric dipole antenna also showed a signal null, but at a different vehicle position. At nine MHz, the vehicle produces an enhancement of the signal rather than a null. Antenna efficiency and spectrum occupancy considerations strongly favor frequencies above 25 MHz. Therefore, a considerable amount of experimental effort was devoted to studying this "multipath" effect at frequencies in the neighborhood of 30 MHz.

Experiments were also aimed at determining the influence of vehicle size, position and direction of travel on the received signal. These results were compared with the magnetometer data to determine the probability of failure in the communication link at vehicle positions where "enter" or "exit" pulses are generated.

In Table 16 we present values of the tradeoff factors described above for frequencies of 30, 50 and 450 MHz. When all of the factors are taken into account and normalized to 30 MHz, it is found that there is not an extremely large variation in communication link performance over this entire frequency range. There is an indicated preference for frequencies between 30 and 50 MHz. Factors such as circuit cost and complexity, channel spacing requirements, and multipath/blockage effects were not included in the comparison table because we cannot readily assign a numerical weighting value. However, these factors all favor operation at the low frequency end of the range.

Table 16. Summary of frequency tradeoffs

	30 MHz (db) (Decibels)	50 MHz (db) (Decibels)	450 MHz (db) (Decibels)
Antenna Efficiency (0 db = 100 percent)	-34.0	-27.5	- 3.0
Measured Path Loss, 10 to 150 meters	-33.0	-37.5	-43.5
Burial Factor (0.1 meters, $\epsilon = 20$, $\tan \delta = 1$)	- 1.0	- 2.0	-16.5
(Prediction Bandwidth) ^{1/2} (referred to 30 MHz)	0	- 1.0	- 6.0
D-C to R-F Conversion Efficiency	- 1.5	- 1.5	- 5.0
Merit Factor, relative to 30 MHz	0	0	- 4.5

Twenty-Seven MHz Propagation Study -- Figure 44 is a recording of field strength versus distance made with a Hewlett-Packard spectrum analyzer, operating as a fixed-tuned receiver, in conjunction with a calibrated vertical receiving dipole. The receiving dipole was mounted with its center approximately two meters above ground on a trailer towed behind the equipment van. A continuous record of field strength was made while the van was driven at constant speed away from the transmitter. The transmitter consisted of a six-volt battery-powered, 27 MHz crystal oscillator/r-f amplifier combination with 100 mw total d-c input power. Because the two-turn, four-inch-square loop was matched directly to the collector of the r-f amplifier transistor, an in-plane r-f power measurement was not attempted. However, the estimated 50 mw delivered to the loop, based upon a 50 percent efficiency estimate, is probably accurate with +1, -3 db.

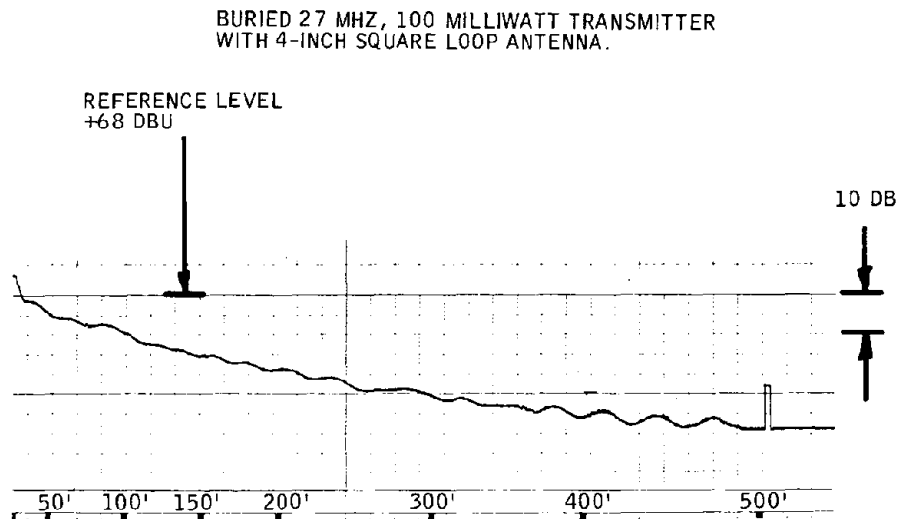


Figure 44. Field strength versus distance
26.6 MHz, 4"x4" loop in asphalt, 5 db/div.

The field strength at 500 feet was 34 db above one microvolt per meter. In view of the antenna size and the -13 db W power level, this field intensity compares favorably with the 49 db above one microvolt per meter measured in Sylvania's tests with one watt to a half-wave dipole¹³.

¹³ Sylvania Report FHWA-RD-72-11, Figure 5-1.

Using the same receiving equipment, null patterns and signal-to-noise ratios were obtained with orthogonal, time-shared loops at 27 MHz. Figures 45 through 47 show representative results. The transmitting loops were oriented with their axes horizontal. Figure 48 is a sketch defining the experimental layout and the notations used. All measurements were made with the receiving van at approximately the same elevation as the roadway surface. The noise level, shown in Figure 47 was recorded with an IF bandwidth of three kHz and a video filter bandwidth of 100 Hz.

This gives a close approximation to the predetection and post-detection bandwidths which would be used in a simple amplitude-modulated, tone-code system. Signal-to-noise ratio remain above 20 db even in the most severe nulls.

In many situations, orthogonal time-shared antennas will offer a significant reduction in the null problem. They also remove the antenna orientation problem which would be present with a single horizontal electric or magnetic transmitting dipole.

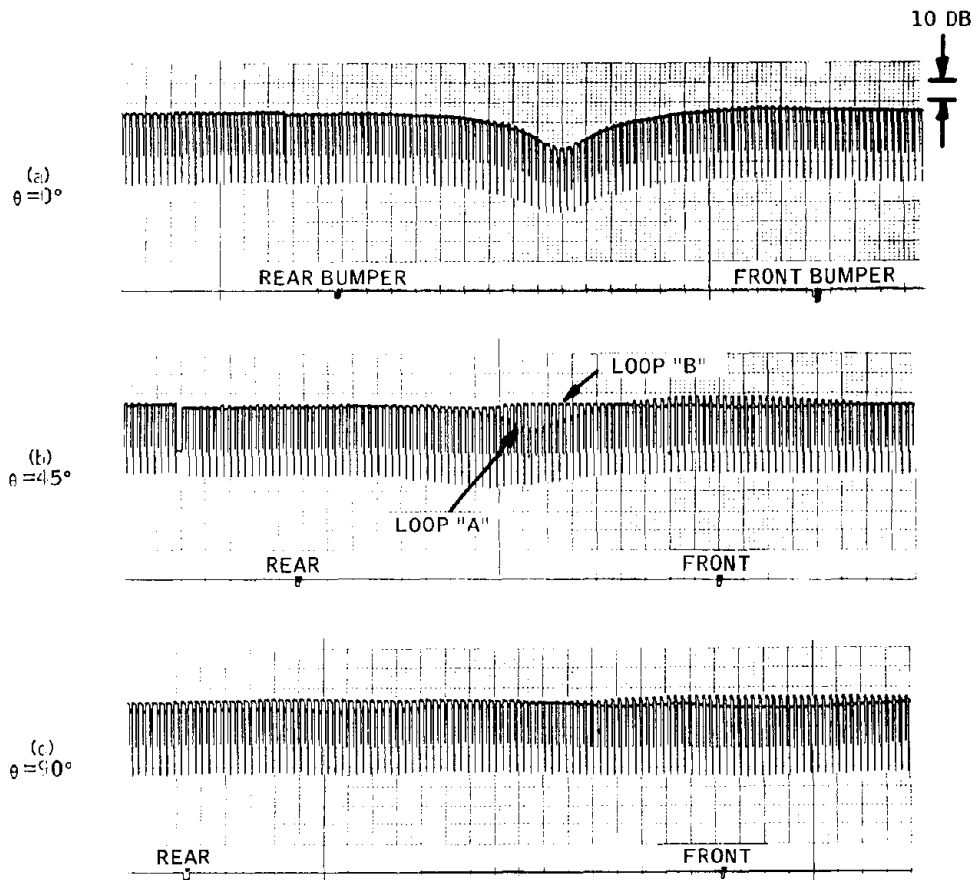


Figure 45. Near-field vehicle nulls, range = 200 ft, orthogonal 26.6 MHz loops, asphalt roadway, ford station wagon, 10 db/div.

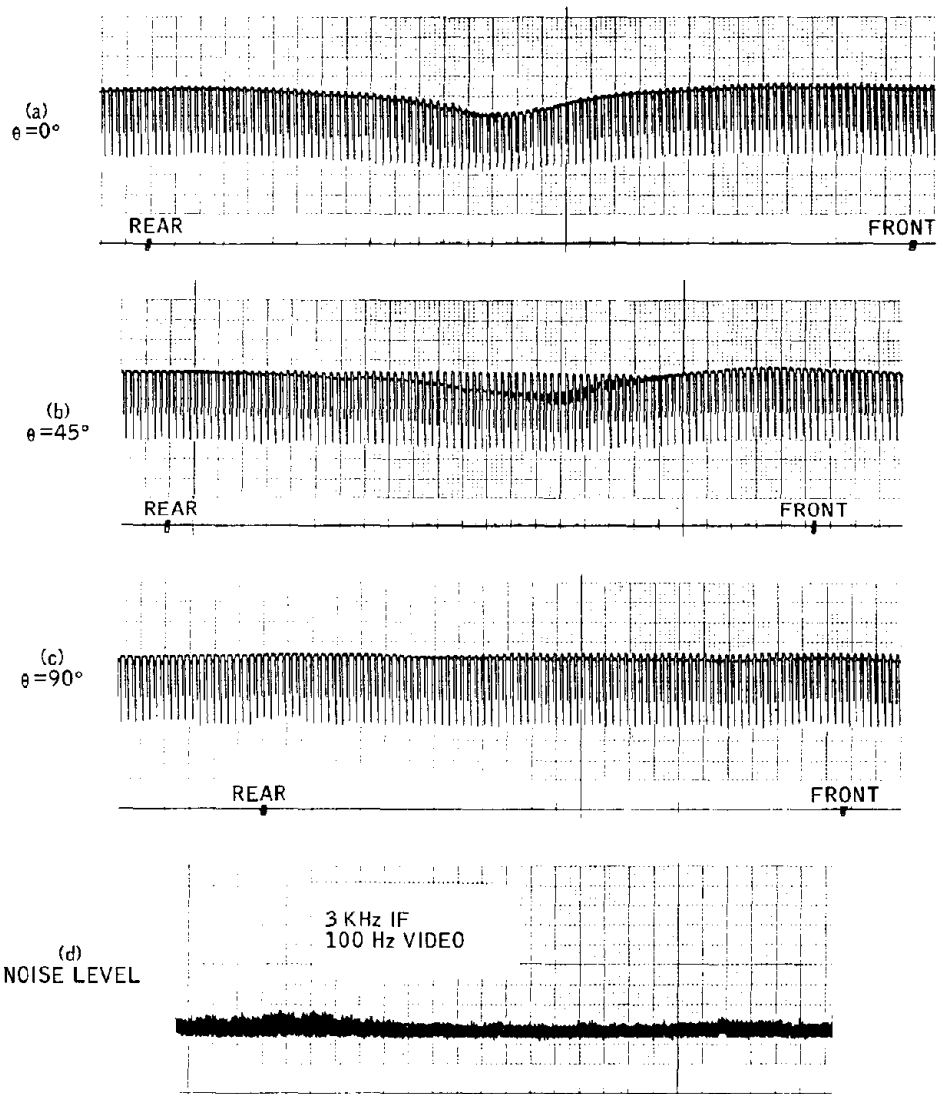


Figure 46. Near-field vehicle nulls, range = 500 ft, asphalt roadway, 10 db/div.

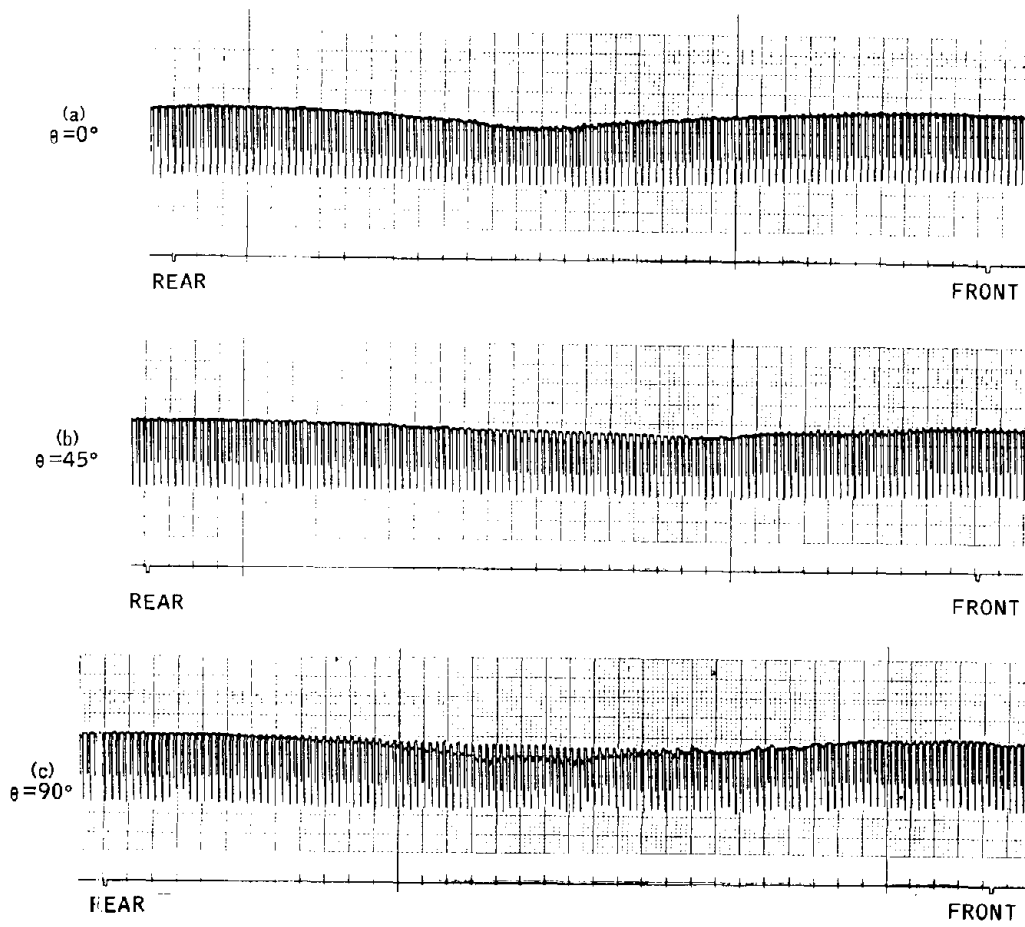


Figure 47. Near-field vehicle nulls, range = 495 ft, reinforced concrete, 10 db/div.

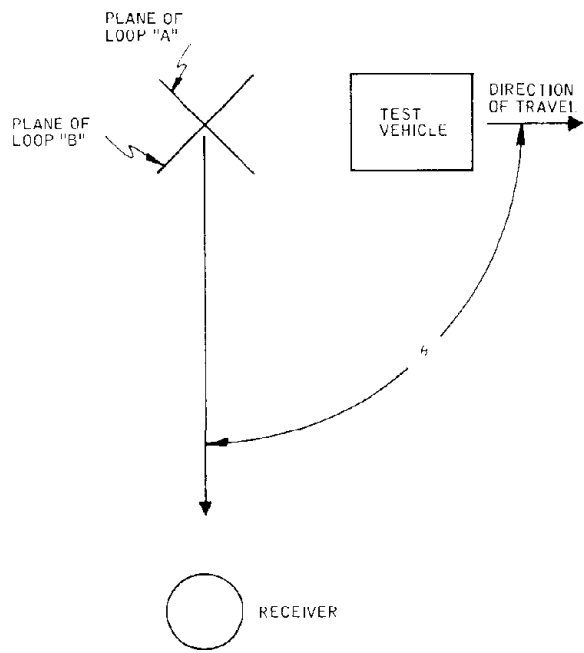


Figure 48. Experimental layout

APPENDIX C
PASSIVE VEHICLE DETECTOR ANALYSIS

The Concept

Briefly, the concept which was considered was as follows (see Figure 49).

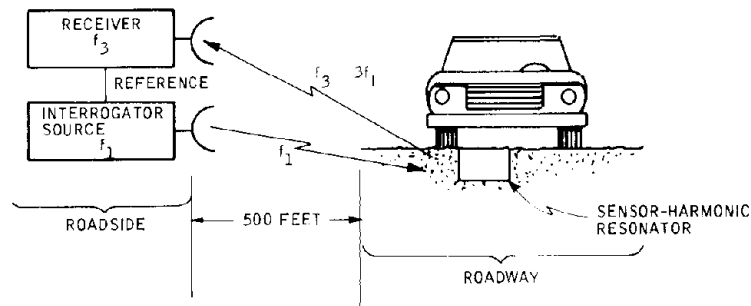


Figure 49. Harmonic resonator sensing concept

In this concept, an interrogating source illuminates the roadway sensor with energy at frequency f_1 . The sensor itself consists of a passive resonant circuit incorporating a nonlinear conduction element, such as a diode, in conjunction with an antenna which serves as a receiving/radiation element. The sensor circuit considered was as shown in Figure 50. The incident energy from the roadside interrogator serves to excite the sensor tank circuit which is designed to have its fundamental resonance nominally at frequency f_1 . The existence of nonlinear conduction element in the sensor

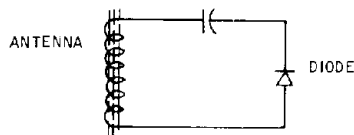


Figure 50. Passive roadway unit - Sensor Circuit (simplified schematic)

circuit gives rise to a significant amount of third harmonic current at frequency $f_3 = 3f_1$ in the circuit. This third harmonic energy is then re-radiated from the antenna to the roadside and received by a very sensitive narrowband receiver which uses synchronous detection, the reference for which is derived from the transmitted frequency f_1 .

In actual use, the interrogator output would be swept over a finite frequency range $f_0 \pm \Delta f$. This frequency range would encompass the natural resonant frequency f_1 of the roadway sensor element, i. e., $(f_0 - \Delta f) < f_1 < (f_0 + \Delta f)$. When the interrogator sweeps across frequency f_1 , a response will be received at frequency $3f_1$.

When a metallic vehicle is positioned over the roadway sensor, the inductance of the antenna element will be changed, thereby changing the resonant frequency of the sensor circuit to some value $f_1 + \delta f$. Now when the sensor is interrogated under these conditions, the re-radiated response will occur at frequency $3(f_1 + \delta f)$ and the system will recognize the presence of the vehicle. Since the interrogation cycle will be continuously repeated at a rapid rate commensurate with the transmitted frequency, the time duration of vehicle presence can be easily obtained. By dividing the interrogation sweep frequency range, $2\Delta f$, into several channels, a number of roadway sensors placed at several locations on an intersection could be addressed using a single interrogate/receive system.

The advantages of such a system would include:

- Elimination of power requirements at the roadway sensor by transferring all energy requirements to the roadside where power is readily available
- Capability for multiple sensor operation
- Incorporation of both sensing and telemetry function into a single, simple, and potentially inexpensive circuit element
- Potentially high reliability of non-active elements
- Low maintenance requirements.

Analysis

The two critical parameters determining passive sensor feasibility are the round trip transmission losses incurred between the transponder antenna in the roadway and the roadside unit, and the power conversion efficiency of the passive transponder.

Transmission Losses

The field-strength measurements made on the active RF communication link provide a direct measure of the coupling loss between a half-wave dipole antenna at the roadside and an antenna buried in the roadway. This information is used to estimate the roadside transmitter power required for a passive communication link using a similar antenna combination.

At 27 MHz, when a 50 millivolt (± 17 dbm) signal was supplied to a roadway antenna, the power delivered to a half-wave receiving dipole 500 feet away was -64 dbm. This measurement was made over an unobstructed path with the transmitter embedded in a bituminous surface. An additional 20 db propagation loss has been measured with the transmitter embedded in a reinforced concrete roadway, and with obstructing vehicles in the near field of the transmitter. If these losses are totaled we obtain:

$$P_{\text{LOSS}} = -64 \text{ dbm} + (-20 \text{ dbm}) - 17 \text{ dbm}$$

$$P_{\text{LOSS}} = -101 \text{ dbm}$$

By reciprocity, we can assume the same coupling loss between a half-wave transmitting dipole at the roadside and a buried, passive transponder. This assumption is valid if the transponder input and output frequencies are not drastically different.

In order to determine the transponder antenna power required to overcome receiver noise, we note that the average noise level in an urban environment at 30 MHz is approximately 30 db above the theoretical noise limit set by thermal noise (kt_0B). If coherent detection is used in conjunction with a passive transponder, the receiver bandwidth can then be limited to the minimum information bandwidth. Also, to detect the presence and speed of vehicles traveling at freeway speeds, the required bandwidth is approximately 10 Hz.

The equivalent noise power seen at the receiver input is, therefore, 4×10^{-17} watts = -134 dbm. For the input signal to be 10 db above the noise, the signal power must be -124 dbm. Then, with a coupling loss of 101 db, the passive transponder antenna input power must be -23 dbm = 50 microwatts.

Conversion Efficiency

We have measured the conversion efficiency of a varactor multiplier operating at low input power levels. These measurements were made at a relatively low input frequency (2 MHz) and with circuit Q's in excess of

200. (Attainable conversion efficiencies in a buried transponder would be considerably lower because of increase circuit losses and detuning problems). The measured data points are shown in Figure 51.

Note:

Second-harmonic conversion efficiencies have been measured for passive multipliers using a hot-carrier diode and a varactor (voltage-variable capacitor) as the non-linear elements. At very low input power levels the hot-carrier diode and varactor given approximately the same results; with 1 microwatt input a 2 MHz, the second-harmonic component is 20 db down (1 percent conversion efficiency). Efficiency increases substantially at higher input levels. At 0.8 milliwatts input, the conversion efficiency is 50 percent for the varactor and about 12 percent for the hot-carrier diode.

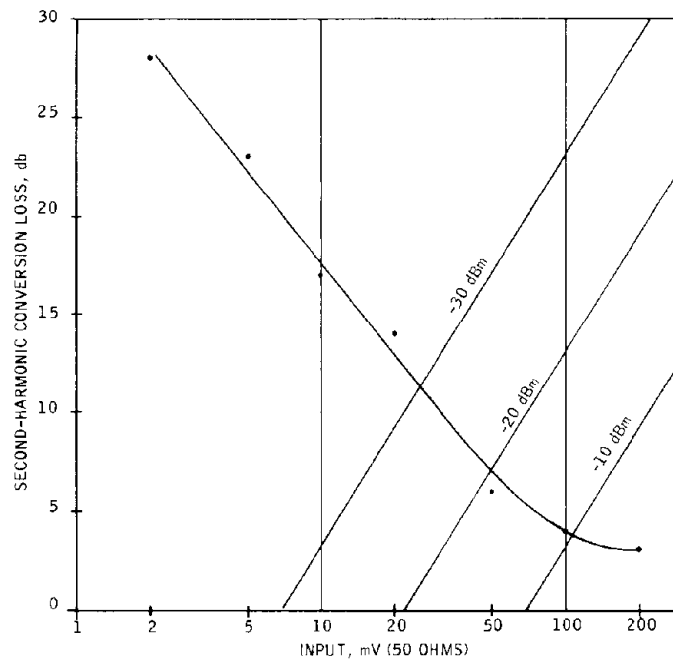


Figure 51. Second harmonic conversion efficiency

It was possible to attain a conversion efficiency of -3db at input power levels below on milliwatt by optimizing the tuning and impedance matching. At a second-harmonic power level of -23 dbm, as noted above, the conversion loss was about 8 db, requiring an input power of -15 dbm.

Transmitter Power Requirements

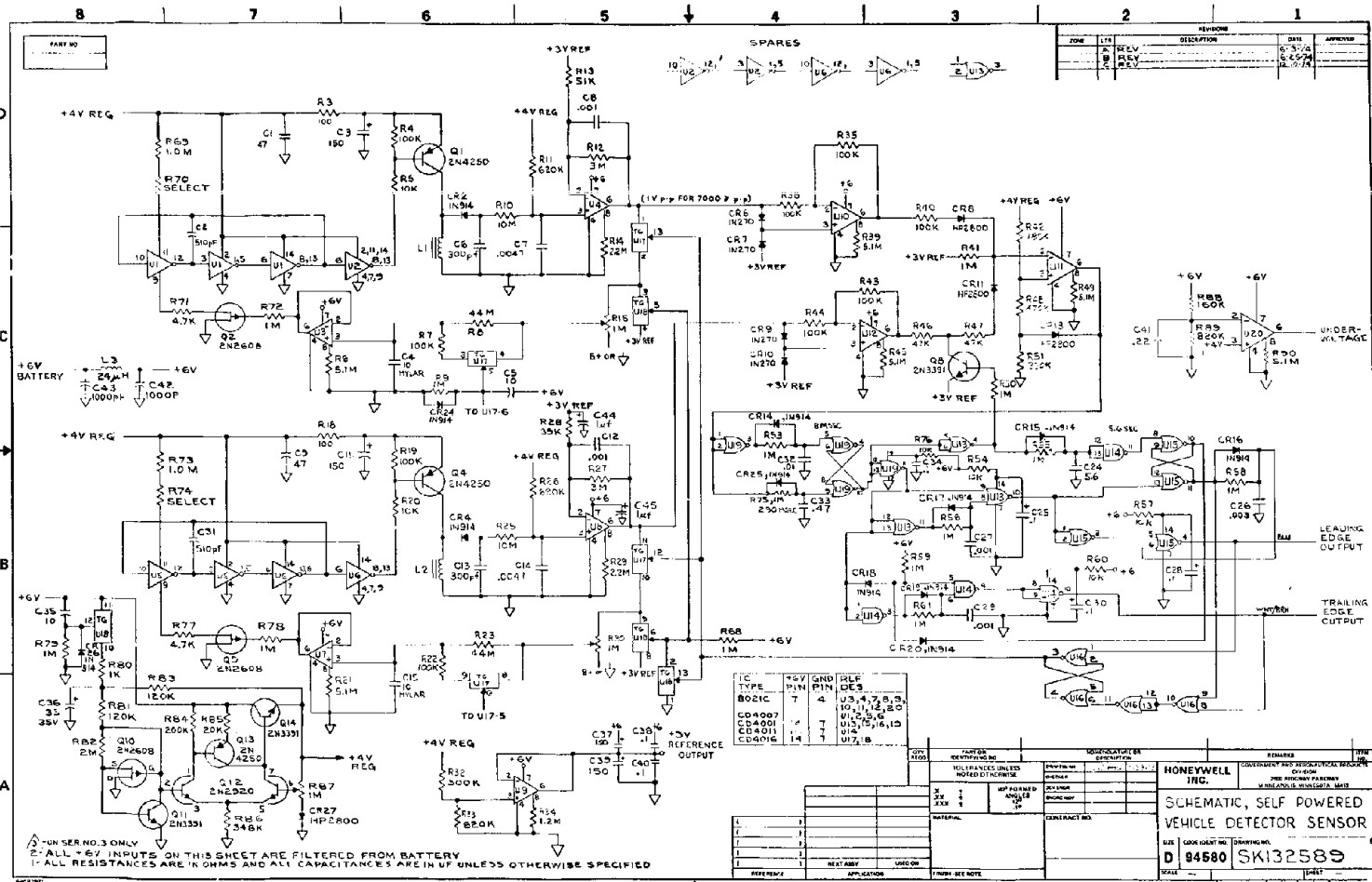
To provide a -15 dbm signal level in the transponder receiving antenna, the roadside transmitter would have to deliver $101 \text{ dbm} - 15 \text{ dbm} = +86 \text{ dbm}$ to a half-wave dipole. This corresponds to 400 kilowatts of c-w power.

Pulse operation with high peak power levels could improve the radiation efficiency by as much as 5 db. Because almost the entire package volume of a passive roadway unit could be used for antennas, the radiation and receiving efficiency would both be approximately three times better than for the 4 x 4 inch loop used in the above field-strength measurement. Combined with pulse operation, this could reduce the average power requirement to about 12.5 kilowatts.

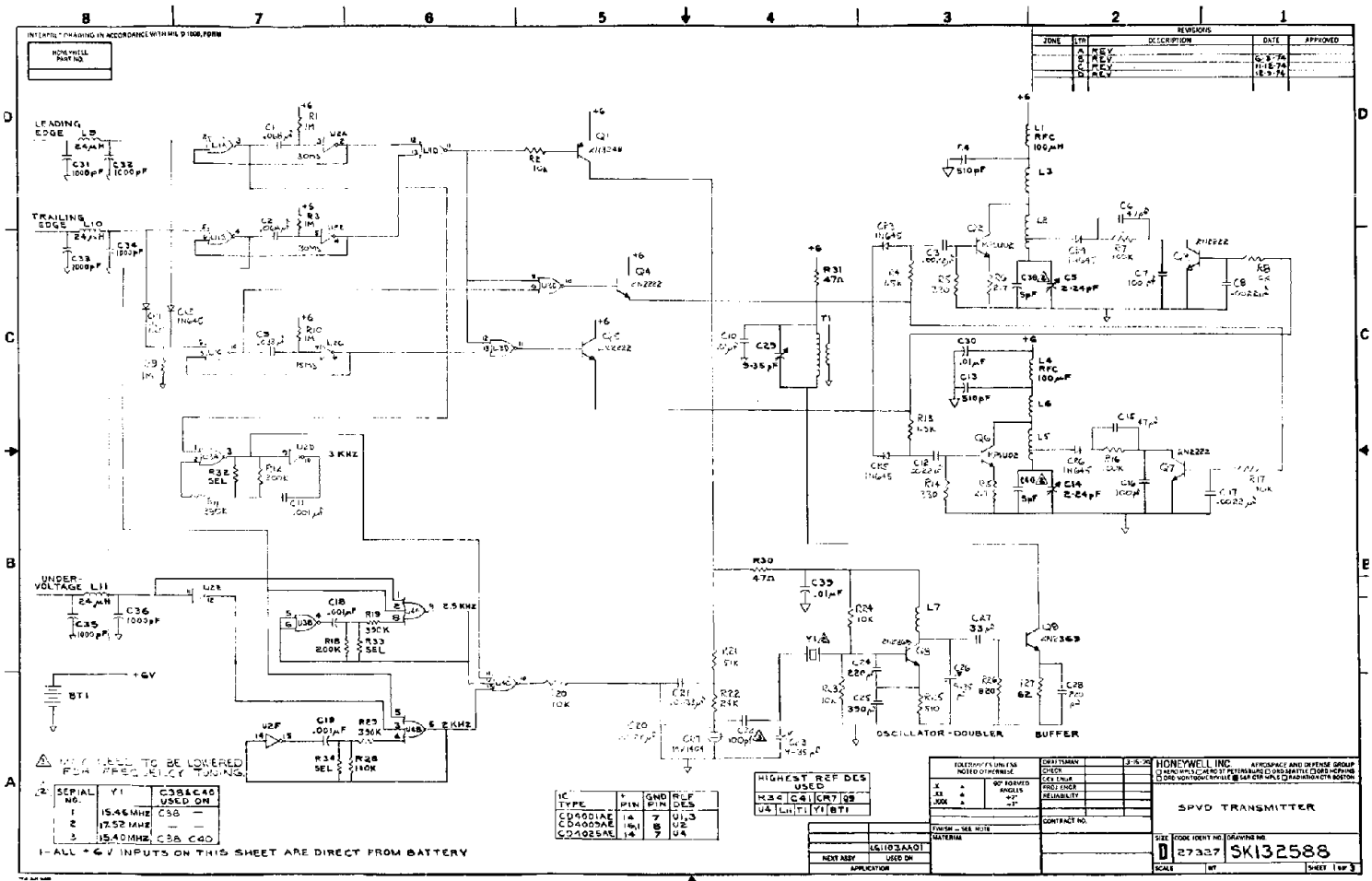
Conclusion

Although our analysis shows that a harmonic resonator sensing concept is indeed feasible, the high power level transmissions required to make this concept workable, make it rather impractical to implement for the following reasons: The 12.5 kw transmitter would, of course, require an FCC license. In addition, a 12.5 kw transmitter at every intersection would probably result in a great deal of r-f spectrum clutter. In light of these reasons and the promise of lower power communication ($\leq 100 \text{ mw}$) with the Self Powered Vehicle Detector, the harmonic resonator concept was not developed any further.

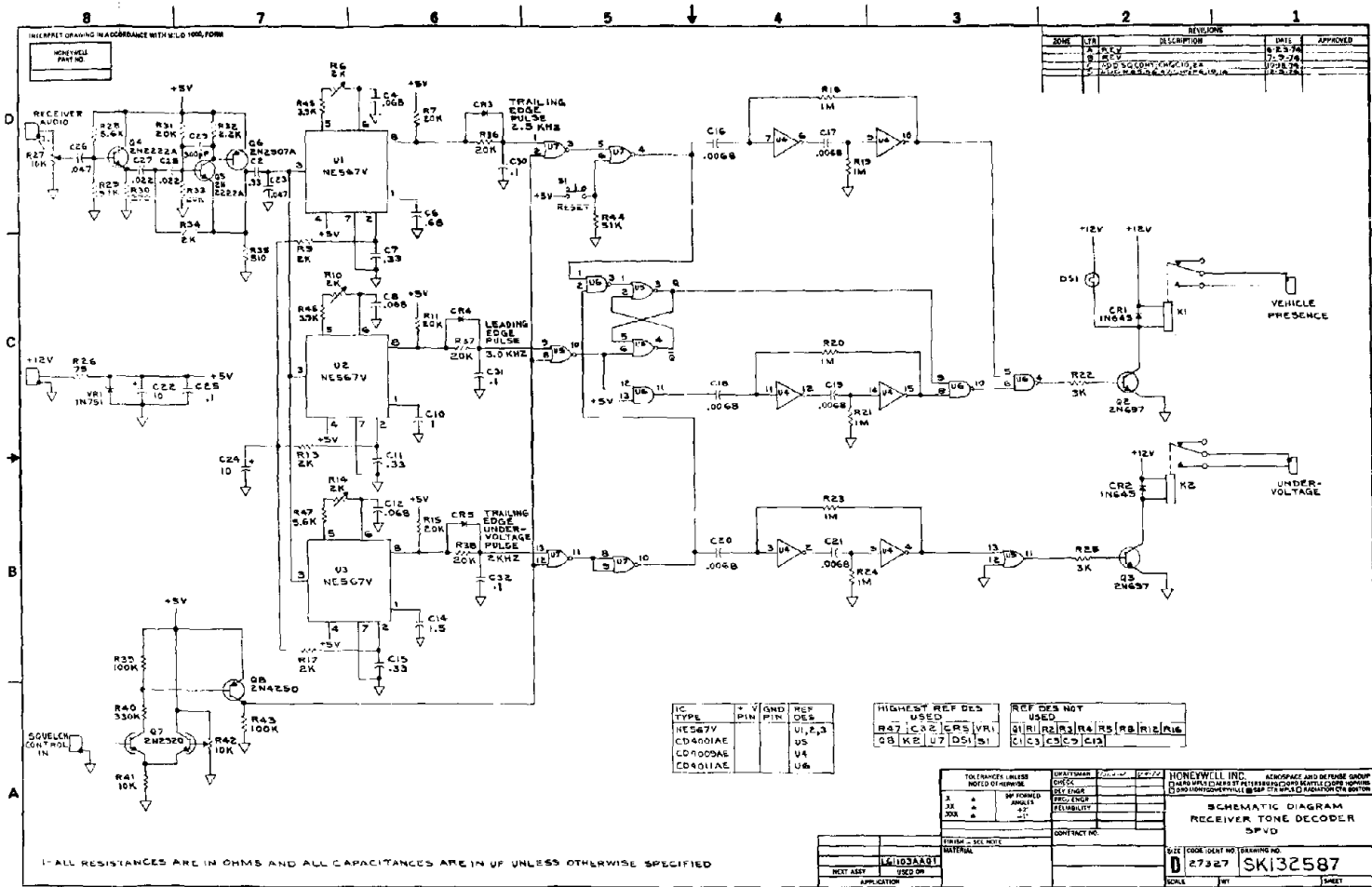
APPENDIX D
SPVD PRODUCTION DRAWINGS



B



Preceding page blank



REVIEWS			
DATE	BY	DESCRIPTION	APPROVED
8-23-74
9-7-74
10-28-74

IC TYPE	V	V GND	REF DES
NE567V	1	7	V1, P, 3
CD4009AE	1	14	U4
CD4011AE	1	14	U6

HIGHEST REF DES USED	REF DES NOT USED
R27, C22, C25, V1	U1, R2, R3, R4, R5, R6, R7, R8, R9, R10, R11, R12, R13, R14, R15, R16, R17, R18, R19, R20, R21, R22, R23, R24, R25, R26, R28, R29, R30, R31, R32, R33, R34, R35, R36, R37, R38, R39, R40, R41, R42, R43, R44, R45, R46, R47, R48, R49, R50, R51, R52, R53, R54, R55, R56, R57, R58, R59, R60, R61, R62, R63, R64, R65, R66, R67, R68, R69, R70, R71, R72, R73, R74, R75, R76, R77, R78, R79, R80, R81, R82, R83, R84, R85, R86, R87, R88, R89, R90, R91, R92, R93, R94, R95, R96, R97, R98, R99, R100

TOLERANCES UNLESS NOTED OTHERWISE	RESISTORS	0.1% 1% 5% 10%	0.1% 1% 5% 10%
1	BY FORMER ANALYST	DESIGN	FEASIBILITY
2	BY ANALYST	DESIGN	FEASIBILITY
3	BY ANALYST	DESIGN	FEASIBILITY
4	BY ANALYST	DESIGN	FEASIBILITY
5	BY ANALYST	DESIGN	FEASIBILITY
6	BY ANALYST	DESIGN	FEASIBILITY
7	BY ANALYST	DESIGN	FEASIBILITY
8	BY ANALYST	DESIGN	FEASIBILITY
9	BY ANALYST	DESIGN	FEASIBILITY
10	BY ANALYST	DESIGN	FEASIBILITY
11	BY ANALYST	DESIGN	FEASIBILITY
12	BY ANALYST	DESIGN	FEASIBILITY
13	BY ANALYST	DESIGN	FEASIBILITY
14	BY ANALYST	DESIGN	FEASIBILITY
15	BY ANALYST	DESIGN	FEASIBILITY
16	BY ANALYST	DESIGN	FEASIBILITY
17	BY ANALYST	DESIGN	FEASIBILITY
18	BY ANALYST	DESIGN	FEASIBILITY
19	BY ANALYST	DESIGN	FEASIBILITY
20	BY ANALYST	DESIGN	FEASIBILITY
21	BY ANALYST	DESIGN	FEASIBILITY
22	BY ANALYST	DESIGN	FEASIBILITY
23	BY ANALYST	DESIGN	FEASIBILITY
24	BY ANALYST	DESIGN	FEASIBILITY
25	BY ANALYST	DESIGN	FEASIBILITY
26	BY ANALYST	DESIGN	FEASIBILITY
27	BY ANALYST	DESIGN	FEASIBILITY
28	BY ANALYST	DESIGN	FEASIBILITY
29	BY ANALYST	DESIGN	FEASIBILITY
30	BY ANALYST	DESIGN	FEASIBILITY
31	BY ANALYST	DESIGN	FEASIBILITY
32	BY ANALYST	DESIGN	FEASIBILITY
33	BY ANALYST	DESIGN	FEASIBILITY
34	BY ANALYST	DESIGN	FEASIBILITY
35	BY ANALYST	DESIGN	FEASIBILITY
36	BY ANALYST	DESIGN	FEASIBILITY
37	BY ANALYST	DESIGN	FEASIBILITY
38	BY ANALYST	DESIGN	FEASIBILITY
39	BY ANALYST	DESIGN	FEASIBILITY
40	BY ANALYST	DESIGN	FEASIBILITY
41	BY ANALYST	DESIGN	FEASIBILITY
42	BY ANALYST	DESIGN	FEASIBILITY
43	BY ANALYST	DESIGN	FEASIBILITY
44	BY ANALYST	DESIGN	FEASIBILITY
45	BY ANALYST	DESIGN	FEASIBILITY
46	BY ANALYST	DESIGN	FEASIBILITY
47	BY ANALYST	DESIGN	FEASIBILITY
48	BY ANALYST	DESIGN	FEASIBILITY
49	BY ANALYST	DESIGN	FEASIBILITY
50	BY ANALYST	DESIGN	FEASIBILITY
51	BY ANALYST	DESIGN	FEASIBILITY
52	BY ANALYST	DESIGN	FEASIBILITY
53	BY ANALYST	DESIGN	FEASIBILITY
54	BY ANALYST	DESIGN	FEASIBILITY
55	BY ANALYST	DESIGN	FEASIBILITY
56	BY ANALYST	DESIGN	FEASIBILITY
57	BY ANALYST	DESIGN	FEASIBILITY
58	BY ANALYST	DESIGN	FEASIBILITY
59	BY ANALYST	DESIGN	FEASIBILITY
60	BY ANALYST	DESIGN	FEASIBILITY
61	BY ANALYST	DESIGN	FEASIBILITY
62	BY ANALYST	DESIGN	FEASIBILITY
63	BY ANALYST	DESIGN	FEASIBILITY
64	BY ANALYST	DESIGN	FEASIBILITY
65	BY ANALYST	DESIGN	FEASIBILITY
66	BY ANALYST	DESIGN	FEASIBILITY
67	BY ANALYST	DESIGN	FEASIBILITY
68	BY ANALYST	DESIGN	FEASIBILITY
69	BY ANALYST	DESIGN	FEASIBILITY
70	BY ANALYST	DESIGN	FEASIBILITY
71	BY ANALYST	DESIGN	FEASIBILITY
72	BY ANALYST	DESIGN	FEASIBILITY
73	BY ANALYST	DESIGN	FEASIBILITY
74	BY ANALYST	DESIGN	FEASIBILITY
75	BY ANALYST	DESIGN	FEASIBILITY
76	BY ANALYST	DESIGN	FEASIBILITY
77	BY ANALYST	DESIGN	FEASIBILITY
78	BY ANALYST	DESIGN	FEASIBILITY
79	BY ANALYST	DESIGN	FEASIBILITY
80	BY ANALYST	DESIGN	FEASIBILITY
81	BY ANALYST	DESIGN	FEASIBILITY
82	BY ANALYST	DESIGN	FEASIBILITY
83	BY ANALYST	DESIGN	FEASIBILITY
84	BY ANALYST	DESIGN	FEASIBILITY
85	BY ANALYST	DESIGN	FEASIBILITY
86	BY ANALYST	DESIGN	FEASIBILITY
87	BY ANALYST	DESIGN	FEASIBILITY
88	BY ANALYST	DESIGN	FEASIBILITY
89	BY ANALYST	DESIGN	FEASIBILITY
90	BY ANALYST	DESIGN	FEASIBILITY
91	BY ANALYST	DESIGN	FEASIBILITY
92	BY ANALYST	DESIGN	FEASIBILITY
93	BY ANALYST	DESIGN	FEASIBILITY
94	BY ANALYST	DESIGN	FEASIBILITY
95	BY ANALYST	DESIGN	FEASIBILITY
96	BY ANALYST	DESIGN	FEASIBILITY
97	BY ANALYST	DESIGN	FEASIBILITY
98	BY ANALYST	DESIGN	FEASIBILITY
99	BY ANALYST	DESIGN	FEASIBILITY
100	BY ANALYST	DESIGN	FEASIBILITY

Preceding page blank

